Aus dem Center for Regenerative Therapies Dresden

Direktor: Prof. Dr. Ezio Bonifazio

Characterization of non-coding transcripts involved in the development of the cerebral cortex

DISSERTATIONSSCHRIFT

zur Erlangung des akademischen Grades

Doctor of Philosophy (Ph.D.)

vorgelegt

der Medizinischen Fakultät Carl Gustav Carus

der Technischen Universität Dresden

von

Daniel Cavalli

Biotechnologist

aus Reggio Emilia, Italien

geboren am 05.09.1990 in Reggio Emilia, Italien

Dresden 2018

1. Gutachter: Prof. Dr. Frank Buchholz

                  Biotechnology Center TU Dresden

2. Gutachter: Prof. Dr. Marius Ader

                  Center for Regenerative Therapies Dresden

Tag der mündlichen Prüfung: 06.05.2019

                        gez.: _____

                              Vorsitzender der Promotionskommission

SUMMARY

The mammalian cortex is the brain area fundamental for high cognitive functions such as learning, memory, attention and complex thinking. Cortical development is orchestrated by neural progenitor cells, which proliferate rapidly to expand their pool, before switching to differentiative divisions to generate all neurons that compose the mature six-layered neocortex. The progressive switch from self-renewal to neurogenesis is a timely regulated process whose failures cause severe life-lasting cognitive disorders. For this reason, it is crucial to understand which factors govern neural progenitors fate decision.

In the last two decades, several studies highlighted the importance of non-coding RNAs, such as long non-coding and micro RNAs, for that timely regulation. Through the generation of a combinatorial RFP/GFP reporter mouse line, which allows the isolation of proliferative and differentiative progenitors, and newborn neurons, the long non-coding RNA Miat was reported as a regulator of neural progenitors fate via splicing.

This work of thesis shows that Miat overexpression delays neural progenitors switch from proliferative to neurogenic division and establishes a system to unravel Miat-spliced targets at single-population level during corticogenesis. Moreover, the double-reporter mouse line was used to generate a comprehensive and complete catalog of microRNAs expressed in neural progenitors and neurons. This led to the identification of miR-486-5p as a novel regulator of neural progenitors fate decision.

ZUSAMMENFASSUNG

Der Cortex von Säugetieren ist der Hirnbereich, der fundamental für höhere kognitive Funktionen wie Lernen, Gedächtnis, Aufmerksamkeit und komplexes Denken ist. Die Entwicklung des Cortex wird von neuralen Vorläuferzellen gesteuert, die schnell proliferieren, um ihren Pool zu expandieren, bevor sie zu differenzierenden Zellteilungen wechseln, um alle Neuronen zu generieren, aus denen der reife sechs schichtige Neokortex besteht. Der schrittweise Wechsel von Selbsterneuerung zu Neurogenese ist ein zeitlich regulierter Prozess, dessen Fehler schwere lebenslange kognitive Erkrankungen verursachen können. Aus diesem Grund ist es enorm wichtig zu verstehen, welche Faktoren die Schicksalsentscheidung der neuralen Vorläuferzellen regulieren.

In den letzten zwei Jahrzehnten haben mehrere Studien die Wichtigkeit von nicht-kodierenden RNAs, wie lange nicht-kodierende und micro RNAs, für diese zeitliche Regulierung hervorgehoben. Mithilfe der Generierung einer kombinatorischen RFP/GFP Reporter Mauslinie, die die Isolierung von proliferierenden und differenzierenden Vorläuferzellen und neugeborenen Neuronen erlaubt, wurde berichtet, dass die lange nicht-kodierende RNA Miat als ein Regulator des neuralen Vorläuferzellen-Schicksals mittels Spleißen fungiert.

Die Arbeit dieser Thesis zeigt, dass die Überexpression von Miat den Wechsel der neuralen Vorläuferzellen von proliferierenden zu neurogenen Zellteilungen verzögert und etabliert eine Strategie, um Miat-gespleißte Ziele auf

Einzelpopulationslevel während der Corticogenese zu entdecken. Außerdem wurde die doppelte Reporter Mauslinie genutzt, um einen umfassenden und kompletten Katalog von micro RNAs, die in neuralen Vorläuferzellen und Neuronen exprimiert sind, zu erstellen. Dies führte zur Identifizierung von miR-486-5p als ein neuer Regulator der neuralen Vorläuferzellen-Schicksalsentscheidung.

Übersetzt von Simon Hertlein

CONTENTS

Contents

FIGURES

LIST OF TABLES

ABBREVIATIONS

AP	Apical progenitor
BFP	Blue fluorescent protein
BP	Basal progenitor
BrdU	5-bromo-2'-deoxyuridine
Celf3	CUGBP Elav-Like Family Member 3
CNS	Central nervous system
CP	Cortical plate
DAPI	4',6-diamidino-2-phenylindole
DNA	Deoxyribonucleic acid
DP	Differentiative progenitor
E	Embryonic day
EdU	5-ethynyl-2-'deoxyuridine
FACS	Fluorescence activated cell sorter
GFP	Green fluorescent protein
ISH	*In situ* hybridization
IUE	*In utero* electroporation
IZ	Intermediate zone
LNA	Locked nucleic acid
lncRNA	Long non-coding RNA
MHP	Medial hinge point
miR	micro RNA
miRNA	micro RNA
mRNA	Messenger RNA
MZ	Marginal zone

N	Neuron
N2a	Neuro2a cell line
NEC	Neuroepithelial cells
NLS	Nuclear localization signal
nt	Nucleotide
piRNA	Piwi-interacting RNA
PP	Proliferative progenitor
RFP	Red fluorescent protein
RISC	RNA-induced silencing complex
RNA	Ribonucleic acid
SD	Standard deviation
SF1	Splicing factor 1
siRNA	small-interfering RNA
SP	Subplate
sRNA	Small non-coding RNA
SVZ	Subventricular zone
TGF-β	Transforming Growth Factor-β
UTR	Untranslated region
VZ	Ventricular zone

CHAPTER 1

INTRODUCTION

The nervous system is a very sophisticated structure present in almost all multicellular animals. In simple terms, we could imagine the nervous system as the air traffic control center of an airport: it receives information from the environment (i.e. air traffic, weather conditions, etc.), elaborates them and coordinates all procedures of landing and takeoff. The same way, the nervous system receives environmental stimuli, elaborates them and coordinates the maintenance and functions of all other tissues. In vertebrates, the nervous system is composed of central and peripheral nervous systems.

The central nervous system (CNS) develops from the most distal embryonic layer, the ectoderm, in a remarkably conserved fashion from reptiles to fishes, amphibians, birds and mammals. Briefly, the neural part of the ectoderm invaginates to form the neural tube, which further specializes into all CNS structures upon to the combined action of different morphogens (Gilbert, 2000). Among all CNS regions, the cerebral cortex gained particular attention due to its remarkable expansion (relative to body size) during evolution and its key roles in high cognitive functions. The cortex develops from neural tube stem cells of the dorsal telencephalon, which undergo several rounds of proliferative divisions followed by consecutive waves of neurogenesis. Newly generated

neurons migrate and eventually form the highly specialized mature six-layered neocortex (Gilbert, 2000).

Decades of research identified dozens of proteins, such as transcription factors, morphogens and so on, regulating neural stem cells proliferation and differentiation, as well as neuronal specification and migration (Paridaen and Huttner, 2014). Although, more recently it became clear that other cellular products, such as non-coding RNAs play major regulatory roles during cortical development (Aprea and Calegari, 2015; Rajman and Schratt, 2017). As the name suggests, those RNAs do not constitute a template for protein synthesis, but rather exert specific functions through their structure. Non-coding RNAs can be grossly classified in long- and small-non-coding RNAs, based on the length of their sequence. On the one hand, long non-coding RNAs (lncRNAs) may regulate any cellular function thanks to the interactions mediated by their complex secondary structure. On the other hand, small non-coding RNAs (sRNAs) have rather defined roles ranging from housekeeping functions to post-transcriptional regulation.

The complexity and critical functions of the cerebral cortex make it scientifically important and intriguing to fully characterize its developmental mechanisms.

1.1 NEURAL TUBE: THE PRECURSOR OF THE CNS

Neurulation: formation of the neural tube

The series of events that leads to the formation of the neural tube is termed neurulation. Neurulation takes place as a two-step process: a) primary neurulation gives rise to the cranial part of the neural tube and b) secondary neurulation forms the posterior part of it. Primary neurulation is triggered by the notochord, which induces the medial hinge point (MHP) cells of the neural plate to rearrange their cytoskeleton and bend the plate caudally, forming a pit: the neural groove (Smith and Schoenwolf, 1989; van Straaten et al., 1988) (Fig. 1.1). As a consequence, pushed by the cells of the dorsolateral hinge points, the lateral edges of the neural plate elevate and become neural folds. Neural folds begin to converge and their extremities, the neural crests, eventually approach each other and fuse. This event gives rise to the neural tube that progressively detaches from the non-neural ectoderm above, which generates the skin (Fig. 1.1). Some cells of the neural crests do not give rise to the CNS either, but rather migrate away and differentiate into components of the peripheral nervous system (Erickson and Weston, 1983). In mammals, the neural tube closes at several distinct sites along the anterior-posterior axis (Golden and Chernoff, 1993), resulting in a hollow tube with cranial and caudal openings (neuropores). Secondary neurulation is species-specific and occurs posteriorly to the caudal neuropore. In mice, for instance, cells of the caudal cell mass are simply added to the caudal part of the neural tube formed by primary neurulation (Nievelstein et al., 1993).
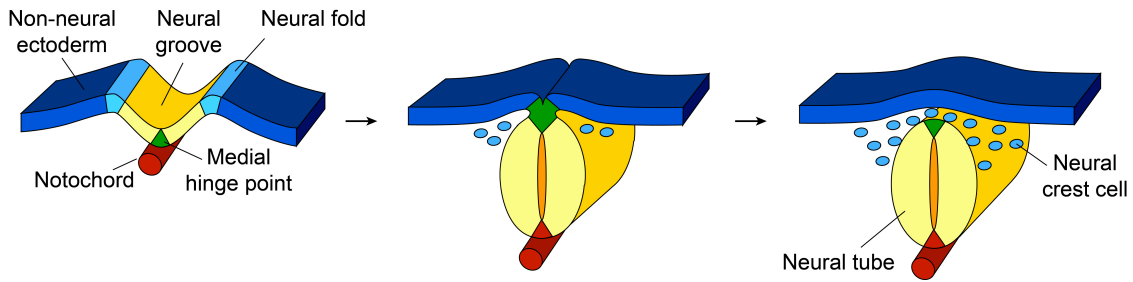
Fig. 1.1 Neural tube development

The notochord (red) primes the neural plate (blue) to bend caudally and form the neural groove (yellow). Neural folds (light blue) rise and approach each other. Eventually the neural tube (yellow, right panel) detaches from the non-neural ectoderm and some neural crest cells (light blue, right panel) migrate away. (Adapted from Liu and Niswander, 2005).

Patterning of the neural tube

While secondary neurulation takes place, the anterior part of the neural tube begins to pattern along the anterior-posterior axis by blossoming into the three primary vesicles: prosencephalon (forebrain), mesencephalon (midbrain) and rhombencephalon (hindbrain) (Fig. 1.2a). As neural tube patterning continues, the three primary become five secondary vesicles (Gilbert, 2000). Specifically, prosencephalon enlarges into two new vesicles: the telencephalon and the diencephalon. The former gives rise to cerebrum and hippocampus, whereas the latter develops into important brain structures like thalamus and hypothalamus. Moreover, the optic cup branches out of the diencephalon and differentiates into the neural part of the retina (Gilbert, 2000). While the mesencephalon swells and remains largely unchanged in morphology, the rhombencephalon grows into two vesicles: the metencephalon and the myelencephalon. Those vesicles give rise to pons and cerebellum, and medulla oblongata, respectively (Fig. 1.2a). While the brain develops from the anterior neural tube, the spinal cord is generated by the posterior neural tube. Despite slightly different in origin, the spinal cord also develops as an elongated hollow tube (Gilbert, 2000).

The neural tube does not only pattern in anterior-posterior direction, but also along the dorsal-ventral axis. On the ventral side, the main inductor of neural tube specification is sonic hedgehog (Shh), a morphogen initially secreted by the notochord. Shh uptake by the MHP cells prompts the formation of the floor plate, whose cells also start releasing Shh (Fig. 1.2b). Consequently, the neural tube cells closer to the floor plate receive higher concentrations of Shh and become ventral neurons, whereas the cells receiving progressively less Shh mature into motor neurons and interneurons (Roelink et al., 1995). Likewise, on the dorsal side, the non-neural epithelium secretes members of the Transforming Growth Factor-β (TGF-β) family, such as Bmp4 and Bmp7. Those growth factors induce the formation of the roof plate, whose cells also begin to express waves of other TGF-β factors like dorsalin, activin and BMP4/7 themselves (Fig. 1.2b). The gradient of TGF-β and the distance from the roof plate induce the expression of different transcription factors in different cells, ultimately influencing their fate (Liem et al., 1995).
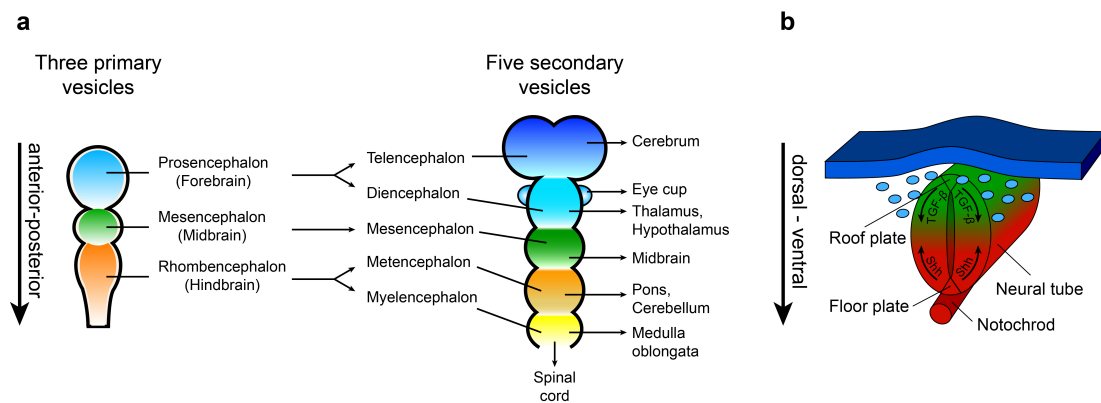
Fig. 1.2 Patterning of the neural tube

a. Patterning along the anterior-posterior axis: during primary neurulation, the neural tube balloons into the three primary vesicles, which, upon secondary neurulation, form the five secondary vesicles. **b.** Patterning along the dorsal-ventral axis: neural tube cells identity is established by gradual expression of sonic hedgehog (Shh) in the floor plate and TGF-β in the roof plate. (Adapted from OpenStax, 2013 and Liu and Niswander, 2005).

1.2 DEVELOPMENT OF THE MAMMALIAN CORTEX

Neural stem and progenitor cells

The neural plate is composed of a single layer of neuroepithelial cells (NECs) (His W., 1889), which are regarded as neural stem cells, as they show two key features: high self-renewal capacity and multipotency through differentiation into all types of neurons and macroglia (astrocytes and oligodendrocytes). NECs also show epithelial characteristics, such as apical-basal polarity and tight and adherens junctions at the apical end of the plasma membrane (Aaku-Saraste et al., 1996; Manabe et al., 2002; Zhadanov et al., 1999). The neural tube is also a monolayer of NECs connected to the lumen and the basal lamina, but appears multilayered and it is thereby considered a pseudostratified epithelium (Fig. 1.3a). This is due to the fact that NECs nuclei scatter at different "heights", following the so called interkinetic nuclear migration (Sauer, 1935). Basically, during the G1 phase of the cell cycle, the nucleus moves towards the basal lamina and remains at the basal side throughout the S phase. Then, during the G2 phase, the nucleus migrates back towards the lumen and the M phase takes place at the apical side (Sauer and Walker, 1959) (Fig. 1.3b). Although the developmental reasons underlying interkinetic nuclear migration are not entirely known, it is believed that shuttling the nucleus along the apical-basal axis exposes it to gradients of morphogens such as Notch (Del Bene et al., 2008).

After neural tube closure, NECs rapidly proliferate and form a densely packed layer called ventricular zone (VZ) (Boulder Committee, 1970). In mice, around embryonic day (E) 10, two important events take place in the VZ: a) NECs give rise to the first wave of neurons and b) NECs undergo a series of changes that

progressively convert them into another type of neural progenitors: radial glial cells (RGC) (Fig. 1.3b). RGCs down-regulate tight junctions (Aaku-Saraste et al., 1996) and connect with the endothelial cells of the developing vascular system (Takahashi et al., 1990). Moreover, they display glial properties such as glycogen storage granules (Gadisseux and Evrard, 1985) and expression of an array of glial markers: GLAST (glutamate transporter), vimentin, RC2 epitope, Fabp7 (brain lipid-binding protein) (Feng et al., 1994; Kamei et al., 1998; Misson et al., 1988) and, in some species, GFAP (fibrillary protein) and S100 (calcium-binding protein) (Levitt et al., 1981). Although, RGCs also retain NECs features like apical-basal polarity and adheres junctions (Götz and Huttner, 2005). Despite progressive thickening of the cortical tissue, RGCs maintain a short pedicle connecting to the apical membrane and extend a long process to the basal lamina. RGCs nuclei reside in VZ and undergo interkinetic nuclear migration within the VZ itself (Fig. 1.3b). In the dorsal telencephalon, the transition from NEC to RGC is completed by E 12 (Noctor et al., 2002).
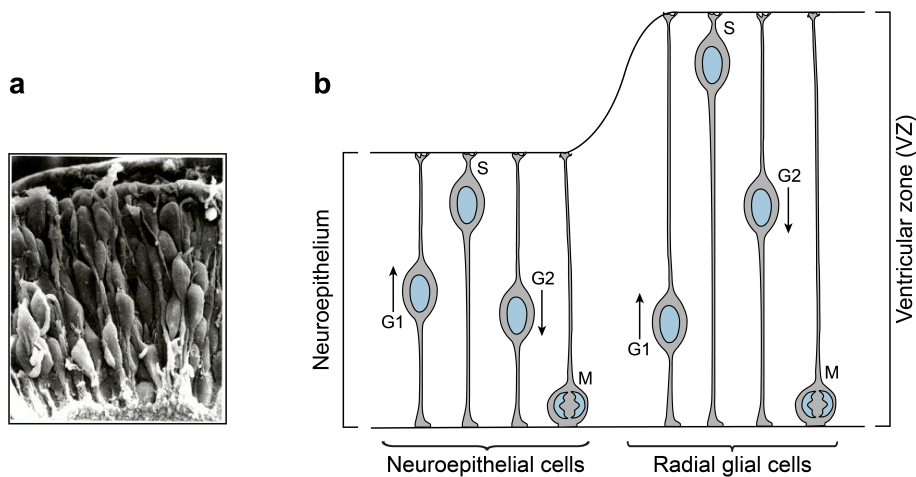
Fig. 1.3 Interkinetic nuclear migration

a. Electron microscopy picture of pseudostratified chick neuroepithelium. (Gilbert, 2000).

b. Representation of mouse neuroepithelial and radial glial cells undergoing interkinetic nuclear migration within the neruoepithelium and ventricular zone, respectively.

NECs and RGCs, also referred to as apical progenitors (AP), are the direct or indirect source of most neuronal types throughout the CNS. In mouse dorsal telencephalon, between E 9-12, APs greatly expand their pool by symmetric proliferative divisions. Following cytokinesis, the apical membrane is inherited by both daughter cells, whereas the basal process is either split or retained by one daughter and the other extends a new process (Miyata et al., 2001). When neurogenesis begins, APs increasingly switch to asymmetric divisions generating one AP and either a neuron or another progenitor type termed intermediate progenitor (Miyata et al., 2004; Noctor et al., 2004) (Fig. 1.4). Intermediate progenitors, initially intermingled with APs (Noctor et al., 2007), delaminate and migrate basally, forming a new cortical layer around E 13: the subventricular zone (SVZ) (Haubensak et al., 2004; Miyata et al., 2004). Intermediate progenitors are multipolar and do not display interkinetic nuclear migration, but rather divide at the basal side of the VZ or in the SVZ and are therefore termed basal progenitors (BP). Contrary to APs, BPs do not express glial markers, down-regulate proliferating factors like Pax6 and Hes, and up-regulate the transcription factors CUX1, CUX2 and SATB2 (Götz and Huttner, 2005). Above all, BPs transiently express the transcription factor Tbr2 (also called Eomes), which is considered the main marker to identify them (Englund et al., 2005). Few BPs even express neuronal genes such as Tubb3 and NeuN (Englund et al., 2005; Miyata et al., 2004). Despite the SVZ was already regarded as a proliferative layer by Magini J. more than 100 years ago, the BPs populating it were suggested to undergo neurogenic divisions only from the 1970's (Smart, 1973). This hypothesis was later confirmed by a series of studies that established BPs as the main source of cortical neurons in mammals (Haubensak et al., 2004; Noctor et al., 2004). In fact, in rodents more than 90% of BPs divides symmetrically to generate two neurons, which migrate through

the intermediate zone (IZ) and eventually settle down in the cortical plate (CP) (Fig. 1.4). The remaining 10% of BPs also divides symmetrically but gives rise to two BPs (Haubensak et al., 2004; Noctor et al., 2004).

For decades lissencephalic animal models such as mice and rats were used for studying corticogenesis, thereby overlooking one additional type of BPs which is typical of gyrencephalic species: basal RGCs. These intermediate progenitors are generated by asymmetric divisions of APs, resulting in the retention of the basal process by only one daughter cell, which becomes a basal RGC (LaMonica et al., 2013; Shitamukai et al., 2011) (Fig. 1.4). Basal RGCs are the only type of BPs connected to the basal lamina and form an additional cortical layer: the outer SVZ (Smart et al., 2002). In mice, basal RGC are extremely underrepresented and divide mainly asymmetrically, generating one basal RGC and one neuron (Shitamukai et al., 2011). On the contrary, in gyrencephalic species basal RGCs are abundant and divide symmetrically to form two basal RGCs, thus largely expanding the SVZ area (Fietz et al., 2012; Smart et al., 2002). Consequently, basal RGCs are believed to produce the enormous amount of additional neurons found in gyrencephalic species and possibly induce cortical surface folding (Kriegstein et al., 2006). In support of this theory, expansion of basal RGCs in mice was shown to induce folding of the otherwise lissencephalic cortex (Nonaka-Kinoshita et al., 2013; Stahl et al., 2013).
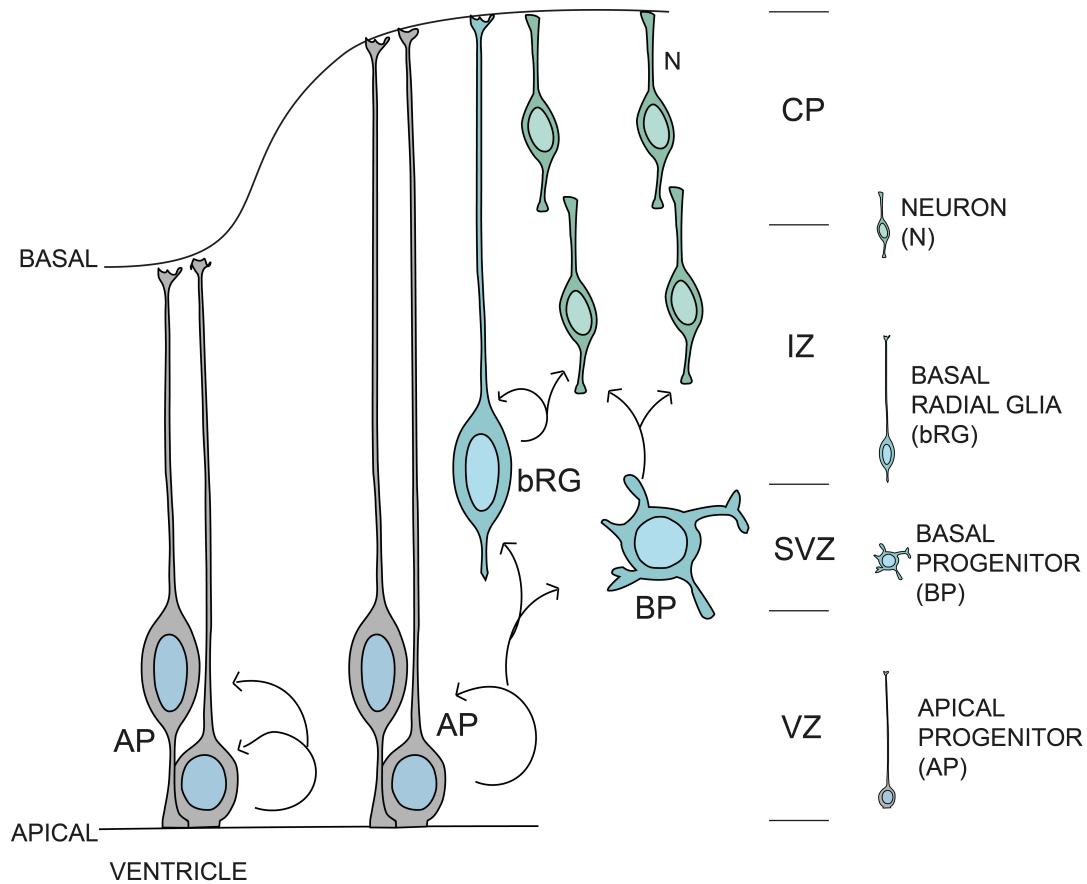
Fig. 1.4 Neural stem and progenitor cells

Schematic representation of the developing mammalian cortex: apical progenitors (AP) self-renew (left) or divide asymmetrically (right) generating one AP and one intermediate progenitor. Intermediate progenitors, composed of basal progenitors (BP) and basal radial glial cells (bRG) produce neurons (N), which migrate across the intermediate zone (IZ) and form the cortical plate (CP). (Adapted from Aprea, 2014).

Neurogenesis in the dorsal telencephalon

In mammals, the cerebral cortex is the brain area fundamental for high cognitive functions such as learning, memory and complex thinking. The cortex is generated from neural stem and progenitor cells of the dorsal telencephalon, which produce a terrific amount of neurons distributing in six histologically different layers. Although those neurons are specialized in a number of different functions, they can be classified into two main neuronal types: interneurons and

projection neurons. Interneurons are inhibitory GABAergic neurons born in the ventral telencephalon that migrate into the cortex and establish local connections. Instead, projection neurons are excitatory glutamatergic neurons, which are generated in the dorsal telencephalon starting from E 10 and connect to distant areas of the brain. A third type of neurons, Cajal–Retzius cells, generated in the cortical hem, eventually migrate into the marginal zone (MZ) of the developing cortex and secrete reelin, a glycoprotein important for proper migration of later-born neurons (O'Leary et al., 2007).

As neurogenesis begins, early-born neurons migrate away from the VZ and establish the preplate. The following waves of neurons, first split the preplate into MZ and subplate (SP), then squeeze between MZ and SP forming the CP. Notably, the CP in mammals is formed in an "inside-out" fashion: deep layers are generated first, followed by superficial layers (Rakic, 1974). Specifically, neurogenic events in the VZ mainly produce the neurons populating layers VI and V, whereas BPs of the SVZ produce the vast majority of neurons of layers IV, III and II (Fig. 1.5). As progenitors proliferate and new neurons are deposited onto the CP, newly born neurons must migrate a longer way across IZ and CP to reach their final place. In a series of studies from the 1970's, Rakic and colleagues clarified the fascinating mechanism of neuronal migration. Basically, a newborn neuron and a RGC interact and "recognize" each other, then the neuron hooks onto the basal process of the RGC and uses it as a rail to climb across the cortex and reach its final destination (Rakic, 1972, 1971) (Fig. 1.5). In mice, the last neurons are generated around E 17.5, contextually with the beginning of the process of gliogenesis. Eventually, most RGCs lose apical contact and terminally differentiate into astrocytes. Only a small percentage of

RGCs persists in the lateral wall of the ventricle and gives rise to new neurons throughout adulthood (Kriegstein and Alvarez-Buylla, 2009).
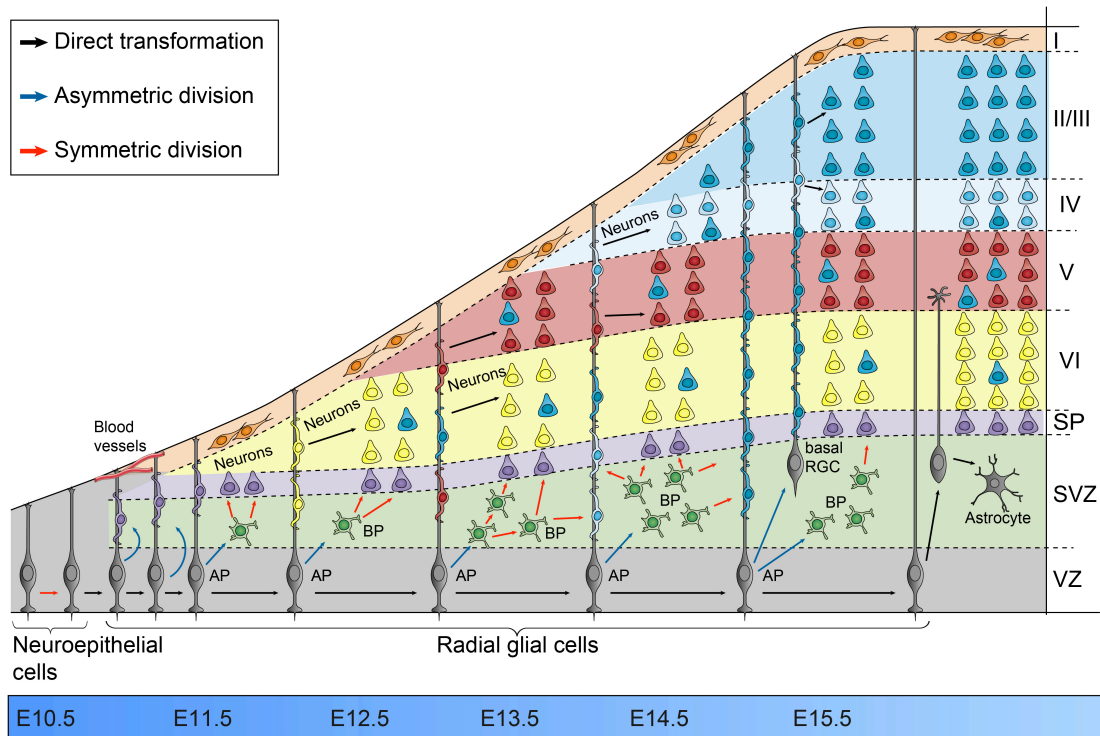
Fig. 1.5 Neurogenesis in the dorsal telencephalon

Neuroepithelial and radial glial cells give rise directly or indirectly (through intermediate progenitors) to all neurons. Neurons migrate radially on radial glial cells processes and form the six-layered cortex in an inside-out fashion. AP: apical progenitor. BP: basal progenitor. RGC: radial glial cell. VZ: ventricular zone. SVZ: subventricular zone. SP: subplate. (Adapted from Custo Greig et al., 2013 and Kriegstein and Alvarez-Buylla, 2009).

1.3 NEURAL PROGENITORS FATE DECISION: PROLIFERATION versus DIFFERENTIATION

Neurogenesis in the dorsal telencephalon is a sophisticated process that relies on the timely regulation of neural progenitors expansion, followed by their progressive differentiation. For decades, scientists tried to answer an intriguing question: what decides whether a neural progenitor cell should proliferate or differentiate? Dozens of studies pointed out aspects ranging from extracellular signaling molecules, to intrinsic factors, epigenetic modifications and even alternative splicing (for detailed reviews see: Hirabayashi and Gotoh, 2010; Martynoga et al., 2012; Norris and Calarco, 2012). However, a comprehensive answer to that basic question has not been found yet, partially due to the inability to study pure populations of neural progenitors during their developmental process.

Btg2 as a marker of differentiative divisions

Taking one-step back from the factors controlling progenitors fate, another key question is: how can we define a neural progenitor as proliferative or differentiative? As described in section 1.2, both APs and BPs can undergo symmetric divisions where the two daughter cells continue proliferating, or asymmetric divisions in which one of the daughters becomes a committed progenitor or a neuron. The answer came almost 20 years ago, in an elegant piece of work from Iacopetti et al., who described Btg2 (also termed Tis21) as an anti-proliferative marker expressed by neural progenitors committed to lineage differentiation. Interestingly, Btg2 messenger RNA (mRNA) is expressed during the G1 phase of the cell cycle and degraded during the S phase.

However, the protein persists in the cell throughout the cell cycle and is inherited by the daughter cells. Based on Btg2 positivity, we can now distinguish between proliferative progenitors (PP, Btg2□) and differentiative progenitors (DP, Btg2+). In the scenario of mouse cortical development, PPs are the APs that keep dividing symmetrically and the few BPs that proliferate and give rise to two BPs. Instead, DPs are the APs dividing asymmetrically and the vast majority of BPs producing neurons by symmetric division (Fig. 1.6a). Specifically, at the peak of neurogenesis (E 14.5 in mice), roughly 60% of APs are PPs and the remaining 40% are DPs, whereas only 15% of BPs are PPs and the other 85% are DPs.

In order to characterize the behavior of PP, DP and newborn neurons, several transgenic mouse lines were generated expressing a reporter protein, typically a green fluorescent protein (GFP), under control of progenitor- or neuronal-specific promoters. Among others, GFP was driven by Btg2 (Haubensak et al., 2004), Tbr2 (Kwon and Hadjantonakis, 2007) or the neuronal marker Tubb3 (Attardo et al., 2008). However, despite the mRNA of GFP (along with the one of Btg2 and Tbr2) is degraded after DP differentiation, the protein persists in newborn neurons, thereby limiting the application of those lines to in-tissue morphological and immunophenotypical studies.

Btg$^{\text{RFP}}$/Tubb3$^{\text{GFP}}$ mouse line: a versatile tool to study corticogenesis

To overcome previous limitations, Calegari's group recently generated a double-reporter mouse line that expresses: a) red fluorescent protein (RFP) under control of Btg2 and b) GFP under control of Tubb3 (Aprea et al., 2013). The Btg2$^{\text{RFP}}$/Tubb3$^{\text{GFP}}$ mouse line was used to isolate PP, DP and neurons (N) at the peak of neurogenesis (E 14.5), when the lateral cortex is populated almost

exclusively by those three cell types. Isolation was performed by fluorescent-activated cell sorter (FACS), based on endogenous fluorescence: PP (RFP⁻/GFP⁻), DP (RFP+/GFP⁻), N (GFP+) (Fig. 1.6a). As a proof-of-principle, deep-sequencing transcriptome analyses revealed that PPs were enriched in genes expressed in APs (Nestin, Glast, Vimentin, Fabp7, Pax6) as well as in widely known proliferation markers (Notch1, Noggin, Nanog, Sox2) (Fig. 1.6b). Likewise, DPs showed high levels of BP-specific genes including Btg2, Tbr2, Insm1, Neurog2, Emx1 and N expressed well-characterized neuronal markers such as Tubb3, Tbr1, Dcx (Aprea et al., 2013) (Fig. 1.6b).
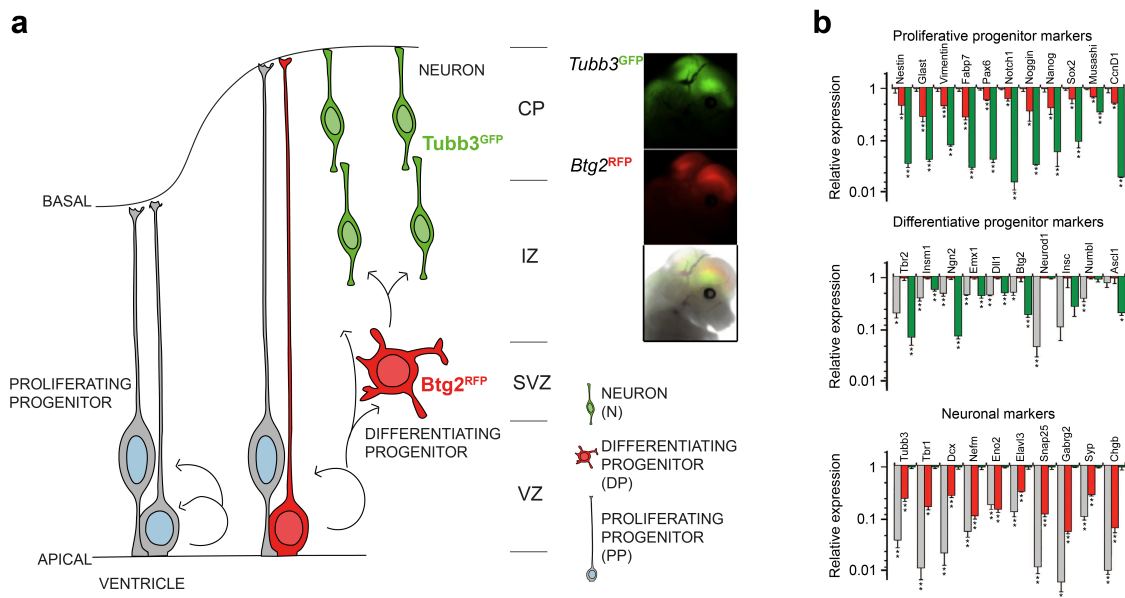
Fig. 1.6 Btg2^{RFP}/Tubb3^{GFP} mouse line

a. Representation of mouse lateral cortex development and markers used to generate the Btg2^{RFP}/Tubb3^{GFP} line: proliferative progenitors (PP) do not express Btg2 (RFP-/GFP-), differentiative progenitors (DP) express Btg2 (RFP+/GFP-) and newborn neurons (N) are positive for Tubb3 (GFP+). **b.** Cell-specific markers expressed by PP (grey), DP (red) and neurons (green). Error bars = SD. * p<0.05 ; ** p<0.01. (Adapted from Aprea, 2014; Aprea et al., 2013).

Switch genes regulate cortical development

Genome-wide comparisons of PP, DP and N expression profiles revealed an interesting class of transcripts termed "switch" genes, displaying a peculiar up- or down-regulation in the transient population of DPs. Specifically, on-switch genes were up-regulated from PP to DP and down-regulated from DP to N, whereas off-switch genes showed the opposite trend (Fig. 1.7a). Not only switch genes were, enriched in markers of DP known to be regulators of neurogenesis, but also in completely uncharacterized transcripts and lncRNAs. Switch genes identify the signature of neurogenic commitment and provide a pool of novel candidates possibly regulating cortical development (Aprea et al., 2013).

The first evidence of the power of switch genes came from their manipulation by *in utero* electroporation (IUE). IUE consists in injecting an expression vector in the ventricle of developing mouse embryos, followed by electroporation of the APs lining the ventricle of the dorsal telencephalon. Typically, the vector overexpresses (or knocks down) a gene of interest and carries a fluorescent reporter protein to mark electroporated cells (method in Fig. 2.1). The gain (or loss)-of-function affects electroporated APs and their progeny. Ultimately, if the gene controls progenitors proliferation or fate, as well as neuronal migration or survival, cell distribution across cortical layers appears abnormal.

Initially, four genes were chosen for *in vivo* manipulation based on the only criterion that they were not linked with brain development. Among them, three were on-switch: the predicted protein-coding 9630028B13Rik and the lncRNAs Gm17566 and Miat, whereas one was off-switch: the protein-coding Schip1. Upon overexpression for 48 hours in E 13.5 embryos by IUE, they all displayed dramatic phenotypes as compared to control (Fig. 1.7b). Later, as a second

evidence of the regulatory roles of switch genes, Artegiani et al., reported the off-switch transcription factor Tox as an inducer of neural progenitors commitment and neuronal process outgrowth.
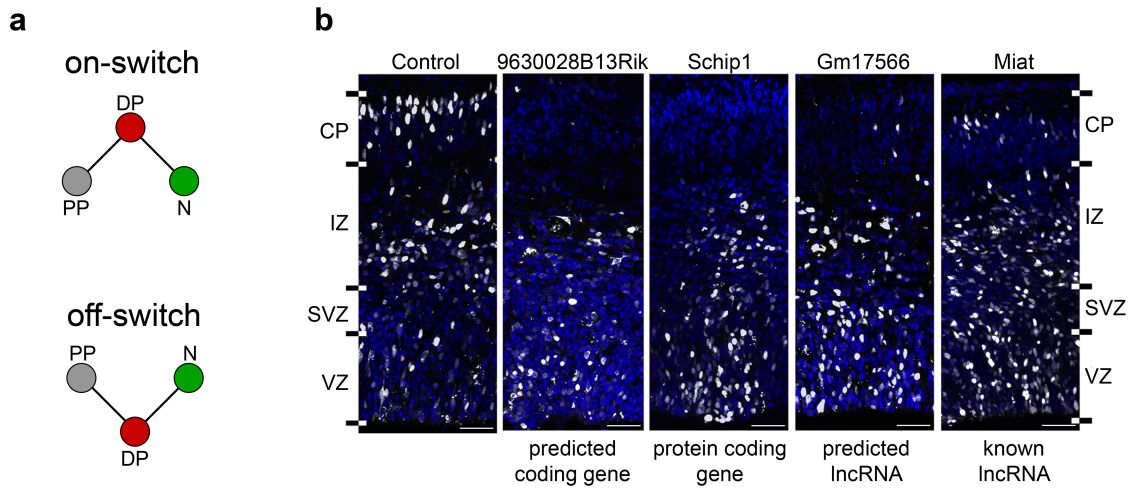
Fig. 1.7 Switch genes regulate cortical development

a. Representation of on-switch genes (top) up-regulated from PP-DP and down-regulated from DP-N, and off-switch genes (bottom) showing the opposite pattern. **b.** Coronal sections of mouse cortex displaying the distribution of electroporated cells (white) across cortical layers. Control, on-switch (9630028B13Rik, Gm17566, Miat) and off-switch (Schip1) genes were overexpressed for 48 hours in E 13.5 embryos by IUE. (Adapted from Aprea et al., 2013).

Those examples were just the "tip of the iceberg" of the contribution that the Btg2^{RFP}/Tubb3^{GFP} mouse line gave the field of cortical developmental studies. In fact, at RNA-level, it was also used for novel lncRNAs discovery (Aprea et al., 2015) and for pioneering the field of circular RNAs (Dori et al., In revision), whereas at DNA-level, it allowed the description of epigenetic modifications (methylation and hydroxy-methylation) taking place during lineage commitment (Noack et al., In revision). Clearly, the possible applications of this versatile tool go beyond what was just described. In fact, it can be exploited for understanding the contributions of histone modifications, alternative splicing, sRNA, as well as mRNA methylation on neural progenitors fate regulation.

1.4 THE DARK MATTER OF THE GENOME: NON-CODING RNAs AS REGULATORY MOLECULES

" The Central Dogma. This states that once 'information' has passed into protein it cannot get out again. In more detail, the transfer of information from nucleic acid to nucleic acid, or from nucleic acid to protein may be possible, but transfer from protein to protein, or from protein to nucleic acid is impossible. "
- Francis Crick, 1958 -

Francis Crick's central dogma of biology was reformulated a few years later by James Watson, who stated that the DNA is transcribed into RNA and RNA is translated into protein (Watson, 1965). Besides the known roles of ribosomal and transfer RNAs in translation, the latter quote tagged the RNA just as a template for protein synthesis. If, on the one hand, Crick's dogma still holds true nowadays, as proteins do not carry genetic information across generations, on the other hand Watson's statement was dismantled in the last 30 years. The era of "-omic" technologies and next generation sequencing revealed that 60-80% of the genome of mice and humans is transcribed and only about 2% of it is translated into proteins (Djebali et al., 2012; ENCODE Project Consortium, 2012). All those transcripts of uknown function were regarded as the "dark matter" of the genome and cosist of thousands of non-coding RNAs. This led to the prediction that in the genome there might be as many protein-coding as non-coding genes (Rinn and Chang, 2012).

Generally, non-coding RNAs were classified in housekeeping and regulatory (Pauli et al., 2011). The former class includes (among others) ribosomal,

transfer, small nuclear and small nucleolar RNAs, which are involved in cell-maintenance mechanisms such as ribosome assembly, protein synthesis, RNA modification and splicing, respectively (Alberts et al., 2014). The latter class was subjected to an arbitrary size cut-off of 200 nucleotides (nt) to define long and small non-coding RNAs (Pauli et al., 2011). The following chapters will focus on regulatory non-coding RNAs, with particular attention to their functions during cortical development.

lncRNAs are versatile regulatory molecules

Molecular biology textbooks define lncRNAs as transcripts longer than 200 nt lacking coding potential, as assessed by various bioinformatics tools (Ilott and Ponting, 2013; Rinn and Chang, 2012; Ulitsky and Bartel, 2013). Despite the simple definition, lncRNAs are a quite complex class of transcripts, which display remarkable similarities with mRNAs, but also sharp differences. On the one hand, alike protein-coding genes, the vast majority of lncRNAs are transcribed by RNA polymerase II, thereby featuring 5'-m^{7}GpppN cap, 3'-poly(A) tail and exon-exon splicing (Shoemaker and Green, 2012). Interestingly, a peculiar type of splicing termed head-to-tail splicing (or back-splicing) occurs on a subset of lncRNAs, producing covalently-bound circular RNAs lacking the poly(A) tail (Memczak et al., 2013). On the other hand, bioinformatics comparisons between lncRNA and protein-coding genes identified some important differences. lncRNA genes are generally shorter, on average composed of only 2-3 exons, spliced with a low efficiency and displaying low median expression (Cabili et al., 2011; Pauli et al., 2012). On top of that, their sequence is overall poorly conserved: only about 12% of mouse lncRNAs have homologs in humans and vice versa (Cabili et al., 2011; Church et al., 2009). As low expression and poor conservation are typically considered two hints of a

lack of biological function, initially some concern rose upon whether lncRNAs might be products of RNA polymerase II spurious transcription (Ebisuya et al., 2008; Kowalczyk et al., 2012; Struhl, 2007). However, as literature flourished more and more with papers showing clear functions and regulatory mechanisms involving lncRNAs, now there is general agreement on the fact that some lncRNAs are non-functional, whereas many others are (Kowalczyk et al., 2012).

A key feature of lncRNAs is their secondary structure, which confers them significant versatility in terms of interacting with DNA, RNA and proteins, as well as folding into complex 3D arrangements and bridging DNA-protein complexes (Geisler and Coller, 2013). This versatility implies that lncRNAs do not have a unique function as a class, but rather participate in any biological process within the cell. Depending on their subcellular localization, lncRNAs might play a role at transcriptional or post-transcriptional level. Supporting that, John Rinn's group showed that lncRNA tissue distribution ranges from nuclear foci, to diffused nuclear localization with or without foci, to cytoplasmic and nuclear, to mainly cytoplasmic (Cabili et al., 2015).

One of the most characterized functions of nuclear lncRNAs is transcriptional regulation via interaction with chromatin-remodeling complexes. This mechanism was well described for one of the first lncRNAs identified: the X-inactive specific transcript (Xist). Xist mediates the so-called dosage compensation, which consists in the inactivation of one of the two X chromosomes in female mammalian cells. Expressed by the X chromosome that will be inactivated, Xist coats the whole chromosome and recruits the Polycomb repressive complex 2 (PRC2), which catalyzes histone 3 lysine 27 trimethylation (H3K27me3), a repressive epigenetic modification that leads to chromosome

condensation and inactivation (reviewed in Wutz, 2011) (Fig. 1.8a). Nuclear lncRNAs were also shown to modulate transcription by other means such as sequestering the RNA polymerase II, or directly dragging the polymerase itself or transcriptional activators/repressors onto genomic loci (extensively reviewed by Geisler and Coller, 2013) (Fig. 1.8b). Two examples of those regulatory mechanisms are PAX6 upstream antisense RNA (Paupar) and Rhabdomyosarcoma 2 associated transcript (Rmst). Paupar is a critical regulator of Pax6, one of the main transcription factors maintaining neural progenitors stemness (Martynoga et al., 2012). Thorough its secondary structure, Paupar directs Pax6 and a transcriptional co-activator onto the genomic loci of target genes (Vance et al., 2014). On the other hand, Rmst drags Sox2 on the promoter of pro-neural genes, thereby promoting neural progenitors differentiation (Ng et al., 2013).

Both nuclear and cytoplasmic lncRNAs might play a role in post-transcriptional regulation. In this regard, a subset of nuclear lncRNAs that includes Nuclear paraspeckle assembly transcript 1/2 (NEAT1/2) and Miocardial infarction associated transcript (Miat) were shown to modulate the kinetics of several splicing factors (Romero-Barrios et al., 2018) (Fig. 1.8c). This type of regulation becomes extremely fascinating in the context of brain development. In fact, the mammalian brain seems to be the organ expressing most of the tissue-specific lncRNAs (Derrien et al., 2012) and alternative splicing is a prominent event during brain development (Li et al., 2007; Raj and Blencowe, 2015; Vuong et al., 2016). Often overlooked (partially due to technical limitations), alternative splicing increases gene complexity and/or specificity independently of up- or down-regulation and might significantly contribute to the complexity of the mammalian cortex. Other post-transcriptional regulatory mechanisms are

exerted mostly by cytoplasmic lncRNAs, which may act on mRNAs as enhancers of translation or, on the contrary, mediators of decay (Fig. 1.8d-e). Moreover, lncRNAs can protect mRNA 3'-untranslated regions (UTR) from microRNA-induced silencing or even sponge microRNAs preventing them from inhibiting their target genes (extensive review by Geisler and Coller, 2013) (Fig. 1.8f-g).
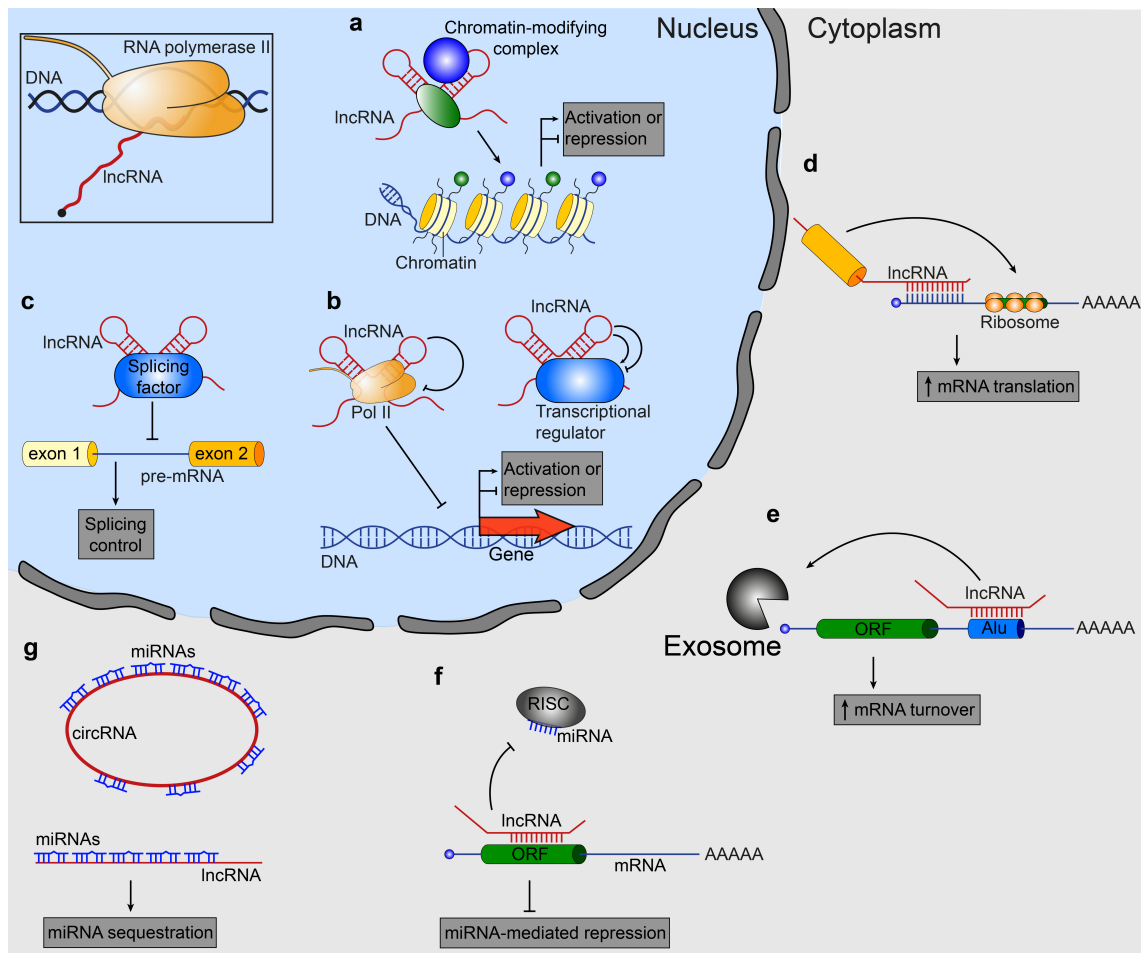
Fig. 1.8 lncRNA regulatory mechanisms

lncRNAs are transcribed by RNA polymerase II and regulate gene expression at transcriptional or post-transcriptional levels. In the nucleus, lncRNAs may interact with chromatin remodeling complexes (**a**), promote/inhibit transcription (**b**) and regulate splicing (**c**). In the cytoplasm, lncRNAs might enhance mRNA translation (**d**) or degradation (**e**), as well as inhibit miRNAs by covering their binding sites (**f**) or by sequestering them (**g**). (Adapted from Geisler and Coller, 2013).

The lncRNA Miat regulates corticogenesis via splicing

Miat was first described as an abundantly expressed lncRNA in the developing mouse retina (Blackshaw et al., 2004; Sone et al., 2007). Although, Miat is not only expressed in retina, but also in the nervous system of mouse embryos from E 8.5 throughout development (Sone et al., 2007). At E 14.5, in the developing lateral cortex, Miat is enriched in BPs of the VZ and SVZ (Fig. 1.9 and Fig. 1.10a), whereas in the adult brain, its expression persists in a subset of neurons in the cortex and hippocampus (Sone et al., 2007). MIAT gene was identified as an intergenic predicted lncRNAs exquisitely conserved between mice and humans. In mice, Miat is a 9 Kb-long transcript with at lest 10 isoforms (Sone et al., 2007), whereas in humans it is 10 Kb-long and has a minimum of 4 spliced variants (Ishii et al., 2006). In both species, Miat transcripts were predicted to be lncRNAs containing just few short open reading frames possibly producing peptides without homology with any known protein sequence (Ishii et al., 2006; Sone et al., 2007). Eventually, Miat was validated as a lncRNAs when the human transcript was subjected to *in vitro* translation and did not produce any peptide (Ishii et al., 2006).

Ever since its discovery, Miat studies focused on two main branches: pathologies and development. On the one hand, Miat was found to carry a single nucleotide polymorphism correlated with myocardial infarction in the Japanese population (Ishii et al., 2006). Following that, a few other reports associated Miat with pathological conditions such as atherosclerosis (Arslan et al., 2017; Zhong et al., 2018), vascular dysfunction (Jiang et al., 2016; Yan et al., 2015), leukemia (Sattari et al., 2016) and schizophrenia (Barry et al., 2014). On the other hand, Miat was linked with the regulation of several developmental processes. For

instance, Miat ablation was found to promote retinal progenitors differentiation towards amacrine and Müller glia cells (Rapicavoli et al., 2010), as well as loss of pluripotency of embryonic stem cells and acquisition of trophoblastic-like morphology (Sheik Mohamed et al., 2010).

A hint towards understanding the molecular mechanism underlying Miat function came from the analysis of Miat homologs across species. In particular, chicken, xenopus, mouse and human Miat, despite being overall different in transcript length and primary sequence, displayed tandem repeats of the nucleotides TACTAAC in their last exon at the 3'-end side (Rapicavoli et al., 2010; Tsuiji et al., 2011). This motif is the critical consensus sequence for exon removal in the buddying yeast *Saccharomyces cerevisiae* (Langford et al., 1984) and was shown to be bound by the splicing factor 1 (SF1) in mice (Tsuiji et al., 2011). Those findings raised the hypothesis that Miat might be involved in the regulation of splicing, a speculation corroborated by the fact that a) Miat interacts with other splicing factors such as the Quaking homolog (QKI) (Barry et al., 2014) and the CUGBP Elav-Like Family Member 3 (Celf3) (Ishizuka et al., 2014) and b) Miat shows a peculiar nuclear distribution with foci not overlapping know nuclear bodies (Sone et al., 2007) (Fig. 1.9b). As Miat interacts only with a fraction of the nuclear pool of SF1 and Celf3, it is currently believed that Miat affects the kinetic of splicing via sequestering that fraction of those splicing factors.
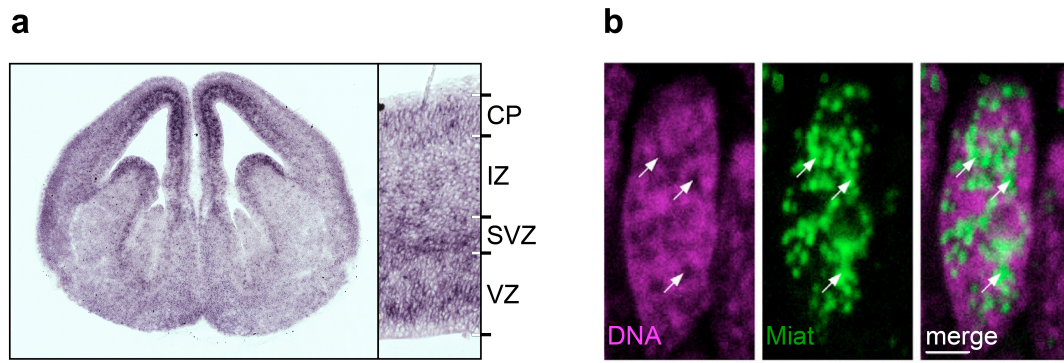
Fig. 1.9 Miat expression and cellular localization

a. *In situ* hybridization of E 14.5 mouse brain showing Miat distribution. Magnification of the lateral cortex is shown to appreciate Miat enrichment in SVZ and some cells (BPs) of the VZ. **b.** Fluorescent *in situ* hybridization of E 14.5 mouse retina showing Miat (green), mainly localizing in nuclear regions with weak DNA (magenta) signal. (Adapted from Sone et al., 2007).

An interesting validation of Miat role as a regulator of developmental processes via splicing came from Calegari's group. Upon transcriptome sequencing of the three cell types of the developing mouse cortex (PP, DP, N), Miat was identified as an on-switch gene enriched in DP (Aprea et al., 2013) (Fig. 1.10a). *In vivo* manipulation of Miat by IUE resulted in a peculiar phenotype characterized by an increase in progenitors and a decrease in neurons (Fig. 1.10b). The loss of neurons was partially due to apoptosis in the IZ (Fig. 1.10c), but mostly to a shift in progenitors fate: more BPs were generated in the VZ but they remained proliferative rather than switching to neurogenic divisions (Aprea et al., 2013). Whether that switch was postponed (thus delaying neurogenesis) or impeded (thus partially blocking neurogenesis), it has not been investigated yet. Mechanistically, a differential isoform usage of the cell-fate determinant Wnt7b was found as a possible reason for the observed phenotype (Aprea et al., 2013). Although reasonable to assume that other genes were differentially spliced upon Miat manipulation, an extensive characterization of

them was not carried out. Interestingly, since Miat seems to play different roles in different cell types, as it affects progenitors fate as well as neuronal survival, the subset of genes that Miat influences the splicing of may also vary along with lineage differentiation.
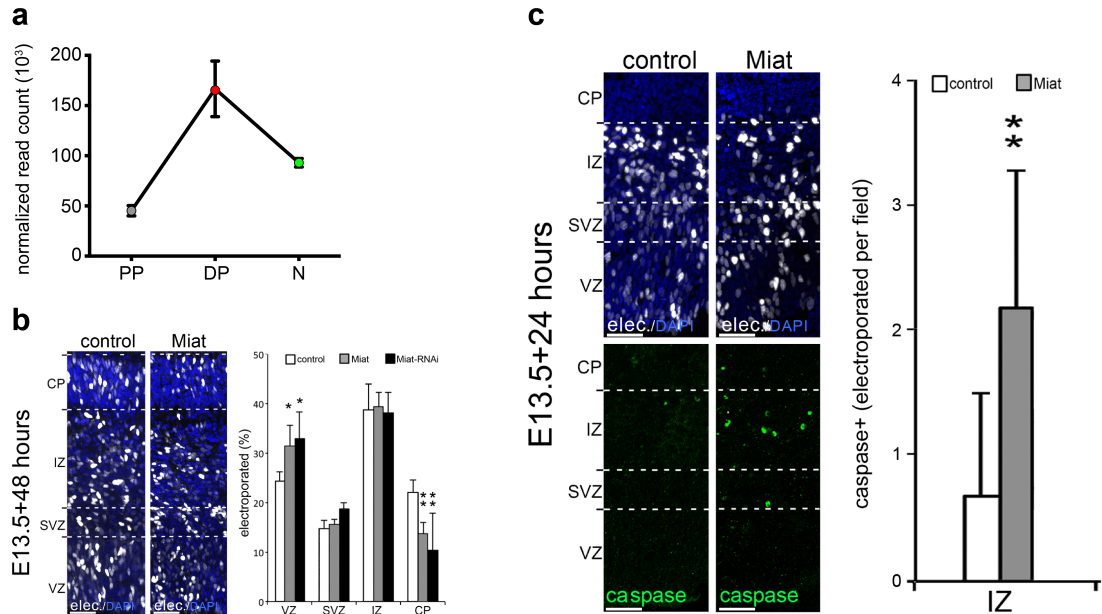
Fig. 1.10 Miat regulates corticogenesis

a. Miat expression in PP, DP and N measured by deep sequencing. **b-c.** Coronal sections of mouse lateral cortex 48 (**b**) and 24 (**c**) hours after Miat manipulation by IUE. Bar graphs shows the proportion of electroporated cells (white) across cortical layers (**b**) and the number of apoptotic cells (caspase3+) normalized per area in the IZ (**c**). Error bars = SD. * $p<0.05$; ** $p<0.01$. (Adapted from Aprea et al., 2013).

miRNAs as post-transcriptional regulators

Small regulatory non-coding RNAs are short (20-30 nt) RNAs that regulate gene expression at various levels ranging from chromatin structure to chromosomes segregation, RNA transcription, processing and translation (Grewal and Elgin, 2007; Humphreys et al., 2005; Maroney et al., 2006; Moazed, 2009; Petersen et al., 2006). Given that the general effect of sRNAs on gene expression is inhibitory, their regulatory activity is referred to as RNA-induced silencing (Carthew and Sontheimer, 2009). There are three main classes of sRNA: microRNA (miRNA), small-interfering RNA (siRNA) and Piwi-interacting RNA (piRNAs). piRNAs are specifically expressed in the germline from clusters of transposable elements, they interact with the piwi-subfamily of Argonaute proteins and suppress transposon activity, thus preserving genome integrity (Malone and Hannon, 2009). siRNAs are processed from double stranded RNAs of exogenous (e.g. viral or experimentally introduced RNAs) or endogenous (e.g. repeat-associated transcripts or pseudogenes duplexes) origin, whereas miRNAs are derived from different genomic sources. siRNAs and miRNAs are processed similarly and eventually destabilize or cleave complementary mRNAs (target mRNAs), thereby inhibiting their translation (Bartel, 2004).

Among those three classes, miRNAs were best characterized because of their importance for proper development of several tissues as well as because of their frequent alteration in pathological conditions (Sayed and Abdellatif, 2011). The discovery of miRNAs dates back to 1993 when it was observed that the gene *lin-4* in C. *elegans* does not give rise to a mRNA, but rather to a pair of non-coding RNAs (Lee et al., 1993). The longer of the two (61nt) folds into a stem-loop structure and is processed into the mature 21-nt *lin-4* miRNA (Lee et

al., 1993). Few months later, *lin-4* was shown to down-regulate the abundance of LIN-14 protein by antisense-pairing with the 3'-UTR of *lin-14* mRNA, preventing its translation and timing the developmental transition from first to second larval stage (Wightman et al., 1993). Following that, a second miRNA was identified as a regulator of the transition between larval and adult stages: that 21-nt-long miRNA was termed let-7 and it down-regulates the translation of *lin-41* mRNA (Reinhart et al., 2000; Slack et al., 2000). The number of miRNAs grew from 2 to over one hundred in a few years with several groups cloning sRNAs from flies, worms, mouse and human cells (Lagos-Quintana et al., 2003, 2002, 2001; Lau et al., 2001; Lee and Ambros, 2001). Nowadays, miRBase, the reference database for miRNA sequences, includes around 2000 miRNAs in both mice and humans (Kozomara and Griffiths-Jones, 2014).

Canonical miRNA biogenesis is a 2-step process that begins with the transcription of a miRNA-containing gene mostly by the RNA polymerase II. The transcript then folds to form a double-stranded primary miRNA (pri-miRNA) (Cai et al., 2004; Lee et al., 2004), which is processed in the nucleus by the RNase III Drosha together with the cofactor Dgcr8 (Han et al., 2006; Kim, 2005) (Fig. 1.11). This first maturation step produces a double-stranded stem loop RNA with a staggered cut (5'-phophate and 2-nt-overhang at the 3'-end side), termed precursor-miRNA (pre-miRNA) (Han et al., 2006; Kim, 2005) (Fig. 1.11). The pre-miRNA is exported by Exportin-5 and undergoes the second maturation step into the cytoplasm (Kim, 2005). Therein, the RNase III Dicer recognizes the staggered cut of the pre-miRNA and cleaves away the loop, ultimately releasing a short double-stranded RNA with staggered ends (Kim, 2005) (Fig. 1.11). That RNA is quickly unwound and one of the two strands is loaded into the Ago protein, whereas the other one is degraded (Kim,

2005) (Fig. 1.11). The strand associated with Ago was initially termed "guide strand" and the other one "passenger strand" (or miRNA*). This is due to the fact that the pre-miRNA was believed to give rise to only one functional miRNA. However, later it was shown that two functional miRNAs might originate from a single pre-miRNA, thereby the official nomenclature became 5p- and 3p- for the miRNAs derived from the 5'- and the 3'-end sides of the pre-miRNA, respectively (Ambros et al., 2003).

Lately, some miRNAs that skip one of the two maturation steps were identified. These non-canonical miRNAs are divided in two main classes: Drosha-independent (Berezikov et al., 2007; Cheloufi et al., 2010; Okamura et al., 2007) and Dicer-independent (Cifuentes et al., 2010; Yang et al., 2010). The former class contains those miRNAs originating from introns or exons of longer genes. After splicing, the intron/exon folds to form a pre-miRNA, which is exported and eventually processed by Dicer (Berezikov et al., 2007; Cheloufi et al., 2010; Okamura et al., 2007). Instead, the miRNAs belonging to the latter class might or might not be cut by Drosha and are further processed in the cytoplasm by Dicer-independent mechanisms not yet fully understood (Cifuentes et al., 2010; Yang et al., 2010).
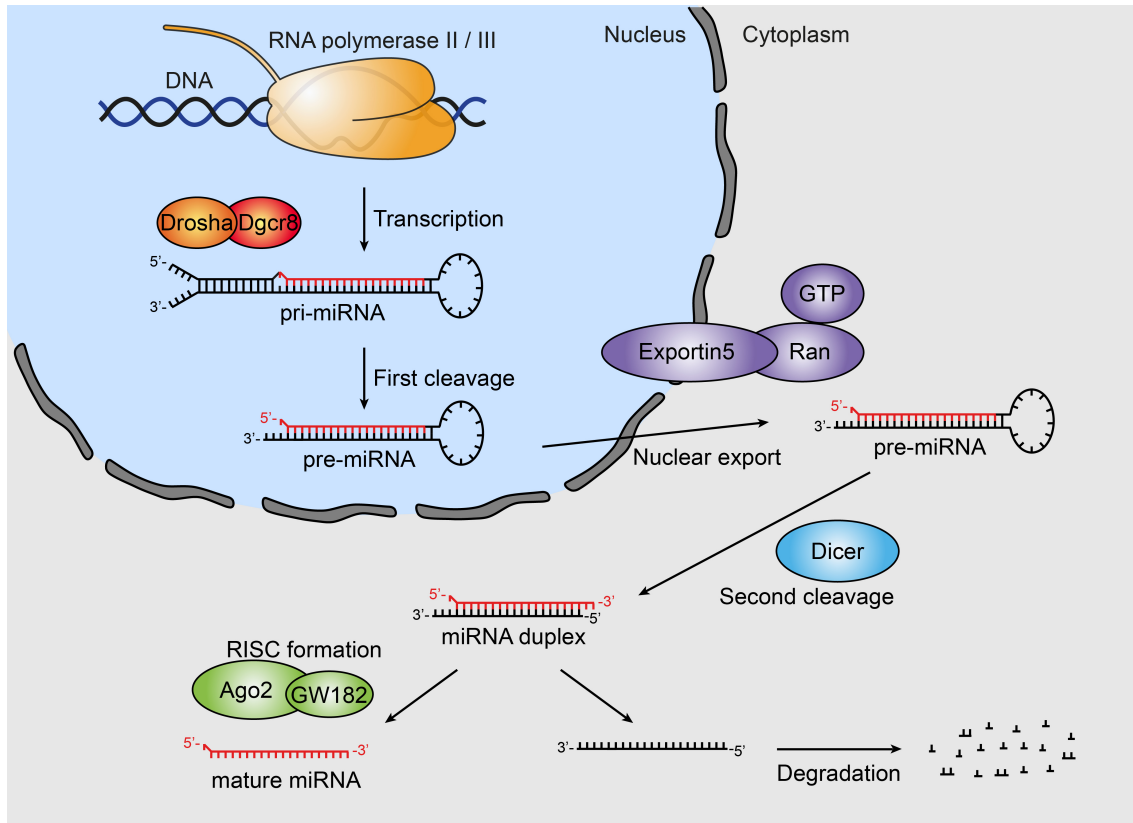
Fig. 1.11 miRNA biogenesis and processing

A miRNA gene is transcribed into a pri-miRNA by RNA polymerase II or III, followed by processing by Drosha/Dgcr8 and Exportin5-mediated export into the cytoplasm. Here, the pre-miRNA is further processed by Dicer and the mature miRNA strand is loaded intro the RISC complex, whereas the other strand is generally degraded. (Adapted from Winter et al., 2009).

Independently of the maturation steps undertaken, the mature miRNA is finally loaded into a complex composed of Ago2 and GW182 proteins, to form the so-called RNA-induced silencing complex (RISC) (Liu et al., 2005; Meister et al., 2005) (Fig. 1.11). The miRNA-RISC complex is the final effector of miRNA-mediated post-transcriptional regulation of target genes. The key feature of target recognition is base pairing of miRNA nucleotides 2-8 (seed sequence) with the target mRNA. This binding was initially thought to occur only on the 3'-UTR of target mRNAs (Wightman et al., 1993), but it is emerging that miRNAs can efficiently bind also the 5'-UTR (Lytle et al., 2007) and the coding

sequence (Forman et al., 2008; Schnall-Levin et al., 2010) of target mRNAs. An extensive complementarity beyond the miRNA seed sequence is believed to induce degradation of the mRNA (Bagga et al., 2005; Behm-Ansmant et al., 2006; Giraldez et al., 2006; Lim et al., 2005; Wu et al., 2006). The mechanisms by which the miRNA-RISC complex prevents mRNA translation are still under debate. Petersen et al., proposed that RISC induces ribosome drop-off, thereby stopping translation elongation. Instead, other studies pointed at a RISC-mediated inhibition of translation initiation by a) competing with eIF4E for 5'-cap binding (Kiriakidou et al., 2007; Mathonnet et al., 2007; Thermann and Hentze, 2007) or b) inducing deadenylation of the mRNA tail (Behm-Ansmant et al., 2006; Giraldez et al., 2006; Wu et al., 2006) or c) blocking the association of the two ribosomal subunits (Chendrimada et al., 2007; Wang et al., 2008).

The fact that only 7 nucleotides of the miRNA are necessary and sufficient for driving miRNA-target binding implies that a single miRNA may act on hundreds of target genes, thereby regulating different pathways (Bartel, 2004). Several miRNA target prediction programs were developed, most of which score candidates binding-sites by interspecies conservation and/or complementarity extending the seed sequence (Riffo-Campos et al., 2016). However, all algorithms yield hundreds of putative targets for a single miRNA, most of which are false positives or biologically irrelevant (Pinzón et al., 2016). Selecting biologically relevant miRNA-targets still remains one of the major challenges in the miRNA field, which limits the understanding of their regulatory roles during developmental processes.

miRNAs regulate brain development

miRNA-mediated regulation is far more than a simple adjustment of tissue protein levels, but rather an essential developmental mechanism. In fact, all mouse lines mutant for miRNA-processing enzymes died prenatally (Bernstein et al., 2003; Chong et al., 2008; Morita et al., 2007; Wang et al., 2007). The next generation of mouse lines, allowing conditional knockout of Dicer or Dgcr8 at different developmental times, highlighted a markedly severe effect during brain development. In particular, ablation of Dicer in NECs or RGCs of the dorsal telencephalon led to RGCs malfunction, expansion of BPs and defects in neuronal migration (Nowakowski et al., 2011). Cortical layering was disrupted with an excess of deep layer neurons and lack of superficial neurons (Saurat et al., 2013), ultimately resulting in thinner cortices and postnatal mouse death (Kawase-Koga et al., 2009). Dgcr8 conditional ablation showed a similar phenotype characterized by neural progenitors early differentiation and apoptosis (Marinaro et al., 2017). miRNA biogenesis is not only required for neural progenitors functioning, but also for neuronal survival. In fact, conditional knockouts of Dicer and Dgcr8 in post-mitotic neurons induced neuronal apoptosis, loss of neuronal branches, microcephaly and fatal outcome (Babiarz et al., 2011; Davis et al., 2008). From those studies it emerged that investigating the physiological expression pattern (i.e. the abundance) of miRNAs in the different cell types of the developing cortex is crucial to gain insights into the pathways underlying the timely regulation of progenitors proliferation and differentiation, as well as neuronal specification and survival.

In this regard, several miRNA-target loops were described as critical tuners of cortical development. For instance, the miRNA cluster 17-92 was shown to include miRNAs important for maintaining neural progenitors in an

undifferentiated state. Two of those, namely miR-17 and miR-92, target the BMP receptor 2 and Tbr2 respectively, thus favoring progenitors proliferation (Bian et al., 2013; Fei et al., 2014; Mao et al., 2014). Another well-established regulatory loop is the synergistic effect of miR-9 and let-7b in inducing neural progenitors differentiation by targeting the Tlx nuclear receptor (Nr2e1), a crucial transcription factor for maintaining neural progenitors self-renewal (Zhao et al., 2010, 2009) In addition, miR-9 down-regulates Hes1, another transcription factor required for neural progenitor cells maintenance (Tan et al., 2012), whereas let-7b targets CyclinD1, thereby inducing cell-cycle exit (Zhao et al., 2010). Interestingly, miR-9 does not only facilitate neural progenitors differentiation, but also promotes neuronal specification. In fact, in neurons miR-9 joins forces with the neuron-enriched miR-124 to target the RE-1 Silencing Transcription factor (REST), a strong inhibitor of pro-neural genes (Conaco et al., 2006; Laneve et al., 2010; Visvanathan et al., 2007). Moreover, miR-124 targets the phosphatase SCP1, which also takes part in the pathway of REST and the nuclear ribonucleoprotein PTBP1 that represses neuron-specific alternative splicing (Makeyev et al., 2007; Visvanathan et al., 2007).

In general, years of research revealed dozens of miRNAs indispensable for proper brain development (Barca-Mayo and De Pietri Tonelli, 2014; Rajman and Schratt, 2017). On the one hand, high-throughput technologies like microarrays and, more recently, sRNA deep sequencing led to a great increase in the number of miRNAs detected in the brain (Krichevsky et al., 2003; Ling et al., 2011; Miska et al., 2004; Nielsen et al., 2009; Sempere et al., 2004). Moreover, the detection power was improved by the development of algorithms like miRDeep, which predicts novel miRNAs from deep sequencing experiments (Friedländer et al., 2014, 2008). On the other hand though, the resolution of all

those studies was limited by the variety of probes printed on the microarray chip or by the coexistence in time and space of different cell types in the developing brain. Even the FANTOM5 and the ENCODE projects, which aimed at fully characterizing the transcribed regions of the genome including their promoters and regulatory elements, annotated miRNAs expressed in the whole brain or bulk parts of it (telencephalon, cerebellum, etc.), thus again lacking single-population resolution (de Rie et al., 2017; ENCODE Project Consortium, 2012). This is not only due to the lack of efficient methods to separate cell types, but also to the fact that single-cell sequencing has not reached a decent coverage for sRNAs yet (Faridani et al., 2016). Consequently, a catalog of miRNAs expressed in cortical progenitor subpopulations and neurons has not been generated yet.

1.5 AIM OF THE PROJECT

The cerebral cortex plays key roles in high cognitive functions such as learning, memory, attention and complex thinking. This sophisticated structure is composed of millions of neurons generated by relatively few neural progenitors. During corticogenesis, those progenitors rapidly proliferate to expand their pool then they progressively switch to differentiative divisions, giving rise to consecutive waves of neurons. The regulation of that switch is a very complex developmental process, whose failures cause severe life-lasting cognitive disorders.

Through the generation of a double-reporter mouse line, Calegari's group contributed to the identification of factors controlling that switch by describing epigenetic modifications as well as novel genes regulating corticogenesis. Intriguingly, those studies pointed at non-coding RNAs as an underestimated class of transcripts playing leading roles in neural progenitors fate decision.

The aim of this work of thesis was to extend the current knowledge of non-coding RNAs as regulators of cortical development. As both long and small non-coding RNAs are important gene regulators, first I aimed at dissecting the crosstalk between the lncRNA Miat and the splicing machinery in regulating neural progenitors fate. Second, I wanted to comprehensively characterize global miRNA expression in neural progenitors and newborn neurons and finally to identify novel miRNAs functionally involved in the regulation of neural progenitors proliferation and differentiation.

CHAPTER 2

MATERIALS AND METHODS

2.1 MATERIALS

2.1.1 Bacteria, cell and mouse strains

Bacteria, cell or mouse line	Supplier
One Shot^{TM} Top10 E. coli	Thermo Fisher Scientific
Neuro-2a	Gift from Huttner W. lab
C57BL/6JOlaHsd	Biomedical Services (BMS) of the MPI-CBG
	Janvier Labs
Btg2^{RFP}/Tubb3^{GFP}	Biomedical Services (BMS) of the MPI-CBG

Table 2.1. Bacteria, cell and mouse strains

2.1.2 Plasmids

Plasmid	Source
pDSV-mRFPnls	(Lange et al., 2009)
mTagBFP2-pBAD	Addgene
pSilencer^{TM}2.1-U6-Neo	Thermo Fisher Scientific
psiCHECK2^{TM}-2 PTEN 3'UTR	Addgene

Table 2.2 Plasmids

2.1.3 Primers and oligonucleotides

All listed primers and unmodified oligonucleotides were ordered from Biomers and Eurofins Genomics. LNA oligonucleotides were purchased from Exiqon.

Primers

Restriction sites underlined. Designed mutations in bold.

Target	Sequence	Name
Miat	5'-ATTA<u>ACGCGT</u>CCCTTTGTGAGGCGCGGGAGAGAT-3'	Miat-Fwd
	5'-TTACC<u>ACGCGT</u>TCCAGTGTGTGTCGGTTTTAATATTGAAATGGC-3'	Miat-Rev
	5'-AAGTACGACAATGCATCACTACAGC-3'	Miat-qPCR-Fwd
	5'-TCTTCAGGGAGACAGGTTGCTC-3'	Miat-qPCR-Rev
BFPnls	5'-ATCC<u>ACCGGT</u>CGCCACCATGGTGTCTAAGGGCGAA-3'	BFP-Fwd
	5'-GGGG<u>ACTAGT</u>TATCTATACCTTTCTCTTCTTTTTTGGATCTACCTTTCTCTTCTTTTTTGGATCTACCTTTCTCTTCTTTTTTGGATCATTAAGCTTGTGCCCCAGTTTGC-3'	BFPnls-Rev
miR-486a	5'-ATCG<u>GGATCC</u>TACGCAACGAAGATCTTCAGCAG-3'	miR-486a-Fwd
	5'-TGCC<u>AAGCTT</u>TTCAAAAAGAAGGGGCAATAACCCAGTTAG-3'	miR-486a-Rev
Pten 3'-UTR	5'-GGTT<u>CTCGAG</u>CTCCCGTGTTTCTGGAATGC-3'	Pten-Fwd
	5'-ATTC<u>GCGGCCGC</u>TCATGTAACATTAAGACTCC-3'	Pten-Rev
	5'-GATACACAAATATGACGTGT**TGT**GGATAATGCCTCATACCAATCAGATGTCCATTTGTTA-3'	Pten-mut-Fwd
	5'-TAACAAATGGACATCTGATTGGTATGAGGCATTATCC**ACA**ACACGTCATATTTGTGTATC-3'	Pten-mut-Rev
Foxo1 3'-UTR	5'-GGTT<u>CTCGAG</u>AGGCTACATTTAAAAGTCCTTC-3'	Foxo1-Fwd
	5'-ATTA<u>GCGGCCGC</u>ACAAAGAACATCACCTTAG-3'	Foxo1-Rev
	5'-GATTAAGTGCCAGCTTTGT**TGT**GGTCTTTTTCTATTGTTTTTGTTGTTGTTTATTTTGTT-3'	Foxo1-mut-Fwd
	5'-AACAAAATAAACAACAACAAAAACAATAGAAAAAGACC**ACA**ACAAAGCTGGCACTTAATC-3'	Foxo1-mut-Rev
Eef1a1	5'-ACAAGCGAACCATCGAAAAG-3'	Eef1a1-qPCR-Fwd
	5'-GTCTCGAATTTCCACAGGGA-3'	Eef1a1-qPCR-Rev

Table 2.3 Primers

Oligonucleotides

Target	Sequence	Name
Control	5'-TAACACGTCTATACGCCA-3'	LNA-Control
	5'-DIG-TCACTGCATACGACGATTCT-3'	LNA-Control-DIG
miR-486a/b-5p	5'-TCGGGGCAGCTCAGTACAG-3'	LNA-486
let-7b-5p	5'-AACCACACAACCTACTACCTCA-DIG-3'	LNA-let-7b-DIG

Table 2.4 Oligonucleotides

2.1.4 Chemicals, buffers and culture media

Chemicals were purchased from Thermo Fisher Scientific, Merck or Roche.

Solution	Composition
Phosphate buffer saline (PBS)	137 mM NaCl 2.7 mM KCl 10 mM Na2HPO4 1.8 mM KH2PO4 in H_2O – pH = 7.4
PFA 4%	1.3 M formaldehyde 100 mM Na2HPO4/NaH2PO4 in H_2O – pH = 7.4
Sucrose solution	30% w/v sucrose in PBS
Tris-borate-EDTA (TBE) (10X)	0.89 mM Tris base 0.89 mM boric acid 20 mM EDTA in H_2O – pH = 8.0
SSC (20X)	3 M NaCl 0.3 M sodium citrate in H_2O-DEPC
Denhardt solution (50X)	1% w/v ficoll 400 1% w/v polyvinylpyrrolidone 1% w/v bovine serum albumin in H_2O

Table 2.5 Buffers for general use

For immunohistochemistry

Solution	Composition
Citrate buffer	4 mM sodium citrate 6 mM citric acid in H_2O – pH = 6.0
Quenching solution	0.1 M glycine in PBS – pH = 7.4
Blocking buffer	10 % donkey serum 0.3 % triton-X 100 in PBS
Incubation solution	3 % donkey serum 0.3 % triton-X 100 in PBS
DNA denaturalization solution	2 M HCl in H_2O
DAPI (1000X)	0.1 w/v DAPI in H_2O

Table 2.6 Immunohistochemistry buffers and solutions

For *in situ* hybridization

Solution	Composition
H$_2$O/PBS - DEPC	0.1% v/v DEPC in H$_2$O/PBS
Acetylation buffer	0.1 M triethanolamine pH = 8.0 with acetic acid 0.25% H$_2$O$_2$ in H$_2$O-DEPC
Hybridization buffer	50 % formamide 5X SSC 0.1 mg/ml Heparin 1X Denhardt solution 0.1 % CHAPS 0.2 mg/ml yeast tRNA 10 mM EDTA 0.4 % Tween-20 in H$_2$O-DEPC
Washing buffer	50 % formamide 2X SSC 0.1 % Tween-20 in H$_2$O-DEPC
Maleic acid buffer (MAB) (2X)	200 mM maleic acid 300 mM NaCl in H$_2$O-DEPC – pH = 7.8
Maleic acid buffer tween (MABT)	1X MAB 0.25% tween-20 in H$_2$O-DEPC
Blocking solution	20% goat serum 2% Boehringer Blocking Reagent in MAB
NTMT	100 mM Tris-HCl pH=9.5 100 mM NaCl 50 mM MgCl$_2$ 0.1 % Tween-20 in H$_2$O-DEPC

Table 2.7 Buffers for *in situ* hybridization

For Northern blot

Solution	Composition
Formamide Loading buffer (2X)	95% formamide 18 mM EDTA 0.025% bromphenolblue 0.025% xylenxyanol 0.025% SDS in H_2O
Hybridization buffer	5X SSC 20 mM Na_2HPO4 pH=7.2 7% SDS 2X Denhardt's solution 40 µg/mL salmon sperm DNA in H_2O
Non-stringent wash solution	3X SSC 25 mM NaH_2PO4 pH=7.5 5% SDS 10X Denhardt solution in H_2O
Stringent wash solution	1X SSC 1% SDS in H_2O
Stripping solution	0.1% SDS 5 mM EDTA

Table 2.8 Buffers for Northern blot

Culture media

Medium	Composition
LB medium (CRTD media kitchen)	1% w/v tryptone 0.5% w/v yeast extract 171 mM NaCl in H2O – pH = 7.0
LB agar	1.5% agar in LB medium
SOC medium	2% w/v tryptone 0.5% w/v yeast extract 8.56 mM NaCl 2.5 mM KCl 10 mM MgCl$_2$ 20 mM glucose in H2O – pH = 7.0
Cell culture medium	DMEM (Gibco) 10% Fetal bovine serum 100 U/ml penicillin-streptomycin

Table 2.9 Culture media

2.1.5 Antibodies

Antigen	Species	Supplier	Catalog number	Dilution
RFP	Rat	Chromotek	5F8	1:400
RFP	Rabbit	Rockland	600-401-379	1:2000
Tbr2	Rabbit	Abcam	ab183991	1:500
BrdU	Rat	Abcam	Ab6326	1:250
Caspase 3	Rabbit	BD Biosciences	559565	1:300
DIG-AP	Sheep	Roche	11093274910	1:2000

Table 2.10 Primary antibodies

Secondary antibodies

IgG raised in donkey (against rabbit and rat) and DyLight-conjugated (Cy2, Cy3 or Cy5) were used as secondary antibodies, all purchased from Jackson ImmunoResearch and used at a dilution of 1:500.

2.1.6 Kits and enzymes

Kit/enzyme	Provider	Catalog
Phusion high-fidelity DNA polymerase	NEB	M0530S
iQ^{TM} SYBR$^{®}$ Green Supermix	Bio-Rad	170-8880
Restriction enzymes	NEB	
DNaseI	NEB	M0303S
SuperScript^{TM} III Reverse Transcriptase	Invitrogen	18080-093
Antarctic Phosphatase	NEB	M0289S
T4 DNA ligase	NEB	M0202S
Quick RNA Mini Prep^{TM}	Zymo Research	R1054
QIAprep Spin Miniprep Kit	Qiagen	27106
EndoFree Plasmid Maxi Kit	Qiagen	12362
Invisorb Fragment CleanUP	STRATEC Biomedical	1020300200
Neural Tissue Dissociation Kit with Papain (P)	Miltenyi Biotec	130-092-628
7-AAD	BD Pharmigen	559925
NEB Next Small RNA Library Prep Kit	NEB	E7330S
SMARTer$^{®}$ Stranded Total RNA-Seq Kit - Pico Input Mammalian	Takara	635006
Click-iT Edu Alexa Fluor 647 Imaging Kit	ThermoFisher Scientific	C10340
Click-iT Edu Alexa Fluor 488 Imaging Kit	ThermoFisher Scientific	C10337
Dual Luciferase Reporter Assay System	Promega	E1910

Table 2.11 Kits and enzymes

2.2 METHODS

2.2.1 Animal experiments

Animals and embryos dissection

Mice were housed into the Biomedical Services Facility (BMS) of the MPI-CBG under standard conditions (12-hour light-dark cycle, $22 \pm 2\,^\circ$C temperature, 55 ± 10 % humidity, food and water supplied *ab litium*). All experimental procedures were performed according to local regulations and approved by the "Landesdirektion Sachsen" under the licenses 11-1-2011-41 and TVV 16-2018. $\text{Btg2}^{\text{RFP}}/\text{Tubb3}^{\text{GFP}}$ males were time-mated with C57BL/6J females, which were marked as E 0.5 the morning that a spermatic plug was observed. Pregnant females were anesthetized using Isoflurane (Baxter) and sacrificed by cervical dislocation at E 14.5 or E 15.5. Brains of RFP/GFP double-positive embryos were collected and lateral cortices isolated after removal of meninges and ganglionic eminences. Plugged C57BL/6J females for IUE or RNA extraction for Northern blot were purchased from Janvier Labs. Mice were sacrificed at E 14.5, E 15.5 or E 18.5 and embryo brains and cortices were dissected as above.

Cell dissociation and FAC-sorting

Lateral cortices were dissociated using Papain-based Neural Tissue Dissociation Kit (Miltenyi Biotech) according to the manufacturer's protocol. Cells were resuspended in 500 µl - 1 ml of ice-cold PBS and 7-AAD (BD Pharmingen, 1:100) or DAPI (1:1000) were added for dead cells discrimination. Sorting was

performed by BD FACSAria^{TM} III (BD Biosciences) with previously described gating (Aprea et al., 2013). For deep sequencing or RT-qPCR of Miat-manipulated brains, cells were sorted in lysis buffer of Quick RNA Mini Prep^{TM} kit (Zymo Research). For miRNA deep sequencing, a minimum of 1 x 10^6 cells per sample was collected in PBS and centrifuged (300 g, 10 min at 4 °C) before RNA extraction.

In utero electroporation

For IUE, plasmid DNA was purified using EndoFree Plasmid Maxi Kit (Qiagen), following the manufacturer's protocol and resuspended in sterile PBS. DNA solutions for IUE contained either 1-4 µg/µl of plasmid DNA or 10µM LNA + 2 µg/µl of reporter plasmid DNA. IUE was performed as previously described (Artegiani et al., 2012; Lange et al., 2009). C57BL/6J or Btg2^{RFP}/Tubb3^{GFP} E 13.5 pregnant mice received pain treatment by subcutaneous injection of 100 µl of Carprofen (dosage of 5 mg/kg) one hour prior to surgery. Animals were then anesthetized with Isoflurane, the uterus was exposed and 1 µl of DNA solution was injected into the embryo left ventricle, followed by the application of 6 electric pulses (30V and 50 ms each at 1 s intervals) through platinum electrodes using a BTX-830 electroporator (Genetronics) (Fig. 2.1). Then, the uterus was reembedded and the surgical incision was closed in two ways: absorbable suture (Vicryl Plus Ethicon) to close the inner muscle layer and surgical clips to close the outer skin layer. The wound was carefully cleaned with an antiseptic 10% iodine solution (Betadine). When applicable, pain treatment was reapplied 24 and 48 hours after surgery. When appropriate, pregnant females received intraperitoneal injections of 5-bromo-2'-deoxyuridine (BrdU) or 5-ethynyl-2-'deoxyuridine (EdU) (1 mg BrdU or 0.1 mg EdU in 100 µl of PBS).
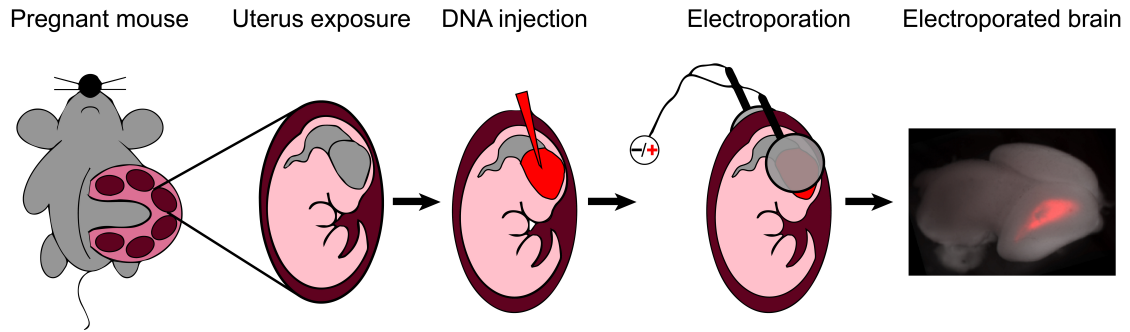
Fig. 2.1 Schematic representation of *in utero* electroporation

2.2.2 Molecular biology

RNA extraction

For deep sequencing and RT-qPCR, total RNA was isolated using Quick RNA Mini Prep kit (Zymo Research) from cells sorted as described above. RNA quality and integrity were assessed by Bioanalyzer (Agilent Genomics). RNA integrity values (RIN) were above 8.0. For Northern blot, total RNA was isolated by TRI Reagent (Sigma-Aldrich). Briefly, lateral cortices of all E 14.5 embryos of one litter were pooled and lysed in 1 ml of TRI Reagent. Samples were added 200 µl of chloroform, mixed and left at RT for 15 min before centrifugation at 12,000 g for 30 min at 4 °C. Aqueous phases were transferred to new tubes and RNAs were precipitated by adding 500 µl of 2-propanol. RNA pellets were washed with 1 ml of 75 % ethanol and eventually resuspended in 50 µl of nuclease-free water.

Library preparation and deep sequencing

Miat sequencing. Library preparation was performed on 5 ng of total RNA with SMARTer® Stranded Total RNA-Seq Kit - Pico Input Mammalian (Takara).

All cDNA libraries were prepared according to the manufacturer's specifications, including adapter ligation, first-strand cDNA synthesis and PCR enrichment. Samples were sequenced on Illumina HISeq 2500 and paired-end 75-bp reads were obtained.

<u>miRNA sequencing.</u> Library preparation was performed on 1 µg of total RNA with NEB Next Small RNA Library Prep Kit. All cDNA libraries were prepared according to the manufacturer's specifications, including adapter ligation, first-strand cDNA synthesis, PCR enrichment and size selection. cDNA purity and concentration after gel extraction were measured by qPCR. Samples were sequenced on Illumina HISeq 2500 and single-end 75-bp reads were obtained.

RT-qPCR

RT-qPCR was used to quantify Miat overexpression. After IUE, FAC-sorting of electroporated cells and RNA extraction as previously described, 20 ng of total RNA were DNase-treated (NEB) and retrotranscribed using SuperScript^{TM} III Reverse Transcriptase (Invitrogen) according to the manufacturers' protocols. iQ^{TM} SYBR$^{®}$ Green Supermix (Bio-RAD)-based quantitative PCRs were carried out using Miat-qPCR- (for Miat) or Eef1a1-qPCR- (for the housekeeping gene Eef1a1) primer pairs on a Stratagene MX 3005P machine. Results were analyzed using the $2^{-\Delta\Delta Ct}$ method (Livak and Schmittgen, 2001).

Cloning

For all constructs, PCR products were run on a 1-2% agarose gel, followed by excision of the band corresponding to the expected size and purification using Invisorb Fragment CleanUp kit (STRATEC Biomedical). Fragments were

subsequently digested using NEB restriction enzymes (enzyme sequences included in the primers used for PCR) and reactions cleaned up with Invisorb Fragment CleanUp kit. Likewise, vectors backbones were digested using the appropriate restriction enzymes (NEB), deposhporilated and gel purified. Ligations were carried out using T4 DNA ligase (NEB) with a 3:1 insert:vector molar ratio at 16°C overnight. 2-4 µl of ligation mix were transformed into Top10 E. coli competent cells (Thermo Fisher Scientific) according to the manufacturer's protocol and plated overnight on LB agar plates containing ampicillin. On average, 5 colonies were inoculated in 5 mL LB Buffer supplemented with ampicillin and cultured overnight. Plasmid DNA was then purified using QIAprep Spin Miniprep Kit and an aliquot of it sent for sequencing to Eurofins Genomics to confirm the correct insertion/orientation of the fragment and the presence/absence of mutations.

Blue fluorescent protein (BFP): to generate a vector expressing a nuclear-localized BFP (BFPnls), the BFP coding sequence was amplified from the mTagBFP2-pBAD using the primer pair: BFP-Fwd & BFPnls-Rev. The reverse primer included the nuclear localization signal (nls). AgeI and SpeI restriction enzymes were used to excise the RFPnls from the pDSV-mRFPnls backbone and to replace it with the BFPnls. The resulting vector was termed pDSV-BFPnls (Fig. 2.2b).

Miat: Miat was amplified from E 14.5 cortical cDNA using the primer pair Miat-Fwd & Miat-Rev. The amplicon was then cloned into the multiple cloning site of both pDSV-mRFPnls and pDSV-BFPnls using MluI as a restriction enzyme. The final constructs were named pDSV-Miat-mRFPnls and pDSV-Miat-BFPnls, respectively (Fig. 2.2a-b).

miR-486: the generation of a vector expressing pre-miR-486a under control of a U6 promoter and RFPnls under control of a SV40 promoter was done in two steps. First, the whole RFPnls cassette (SV40 promoter, RFP coding sequence, nls and poly(A) signal) was excised from the pDSV-mRFPnls plasmid using SspI restriction enzyme (NEB) and cloned into the pSilencer^{TM}2.1-U6-Neo vector (replacing the Neomycin cassette). pre-miR-486a (miRBase accession number: MI0003493) plus 50 bp flanking each side were PCR-amplified from mouse genomic DNA (kindly provided by Sara Zocher, Kempermann G. lab) using miR-486a-Fwd & miR-486a-Rev primer pair and cloned downstream of the U6 promoter using BamHI and HindIII restriction sites (Fig. 2.2c).

Luciferase constructs: psiCHECK-2 double luciferase vector containing human Pten 3'-UTR flanked by XhoI and NotI restriction sites was purchased from Addgene. Human Pten 3'-UTR was replaced by parts of mouse Foxo1 or Pten 3'-UTRs (containing miR-486-5p binding site), which were PCR-amplified from mouse genomic DNA (kindly provided by Sara Zocher, Kempermann G. lab) and inserted into the psiCHECK-2 vector downstream of Renilla Luciferase using XhoI and NotI restriction sites.

For Pten, the 3'-UTR region between nucleotides 2558 – 3865 was amplified using the following primer pair: Pten-Fwd & Pten-Rev (Fig. 2.2d).

For Foxo1, the 3'-UTR region between nucleotides 12 – 1281 was amplified using the primer pair: Foxo1-Fwd & Foxo1-Rev (Fig. 2.2e).

Mutants of both constructs carrying a 3-nt-mutation in miR-486a-5p binding site were generated in two steps. First, each cloned 3'-UTR was amplified in two different (but overlapping) fragments carrying the mutation (using Pten and Foxo1 mutated primers listed in Table 2.3). Then, the fragments were pooled, re-amplified using the cloning primer pairs listed above and cloned into

the psiCHECK-2 vector using XhoI and NotI as restriction enzymes (Fig. 2.2d-e).
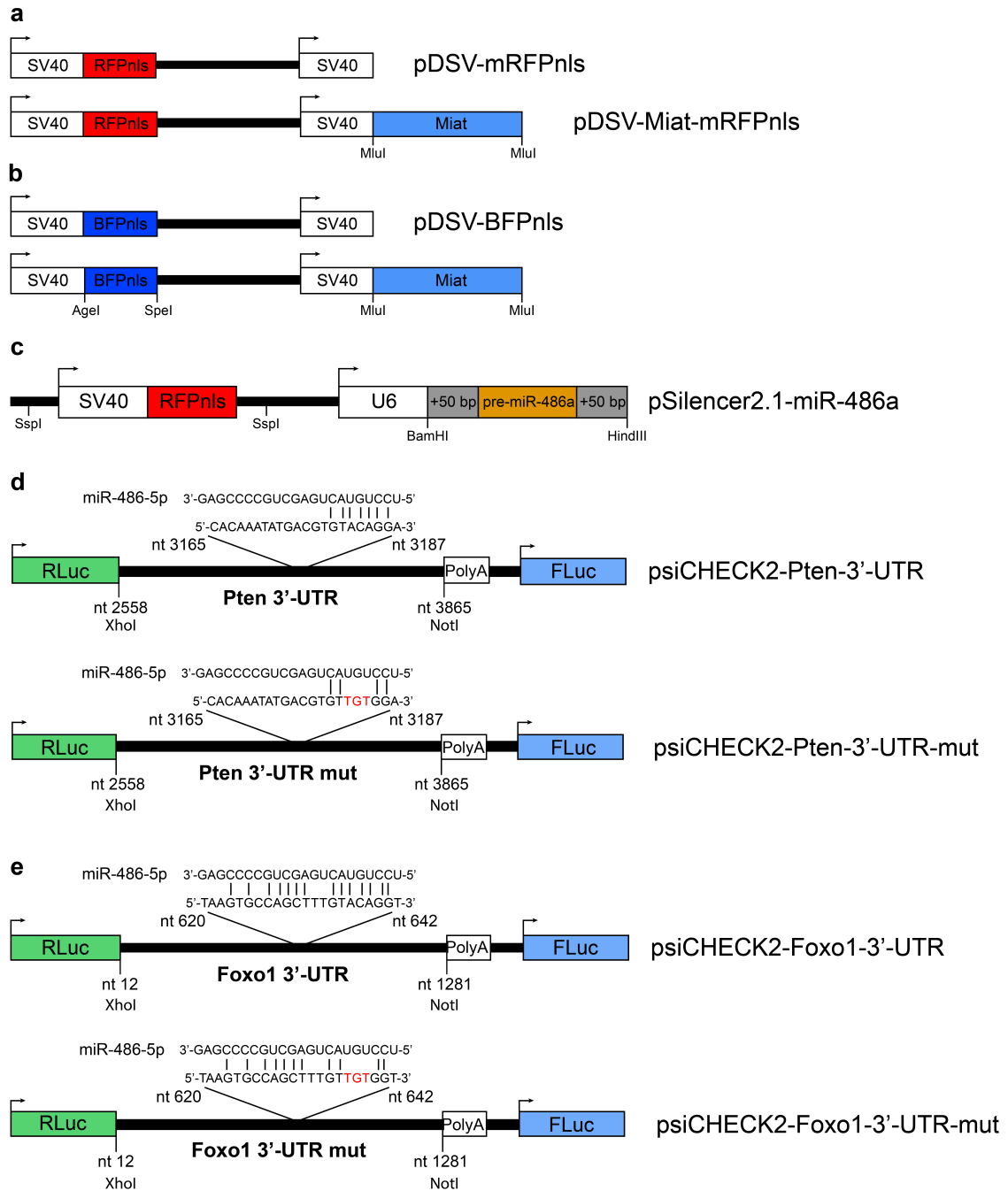
Fig. 2.2 Cloned expression vectors

Schematic representation of the constructs used. Vectors not in scale.

In situ hybridization

In situ hybridization (ISH) was performed as previously described (Laguesse et al., 2015), using digoxigenin (DIG)-labeled LNA probes purchased from Exiqon. Cryosections were fixed in 4% PFA for 10 min and acetylated for 15 min constantly rocking at RT. Pre-hybridization was carried out in hybridization buffer (HB) for 1 h at 53 °C. Hybridization was performed in HB containing 50 nM LNA probes (previously denatured at 75 °C for 5 min) overnight at 53 °C. Sections were washed first in washing buffer for 90 min at 53 °C, then in 2X SSC for 1 h at 53 °C and eventually in MABT for 30 min at RT. Next, blocking solution was applied for 30 min at RT, followed by incubation with anti-DIG-AP antibody (1:2000 in blocking solution, Roche) overnight at 4 °C. Washings were performed in MABT for 90 min and NTMT for 1 h at RT. Labeling was developed in BM purple (Roche) overnight at 37 °C.

Northern blot

30 μg of total RNA extracted from E 14.5 mouse cortices were separated using denaturing urea 15 % PAGE gel (Mini-PROTEAN system; Bio-Rad) in 1x TBE and blotted onto a GeneScreen Plus nylon membrane (PerkinElmer) in pre-cooled 0.5x TBE. Radioactively labeled Decade marker (Ambion) was used as molecular marker. RNAs were cross-linked to the membrane by UV irradiation (1,200 mJ), followed by baking for 30 min at 80 °C. The membrane was pre-incubated in hybridization buffer for 2 h at 50 °C in constant rotation, followed by incubation overnight at 50 °C in hybridization buffer containing the denatured 32P-labeled DNA probes against the predicted novel mature miRNA sequences. Probes against miR-9-5p and miR-124-3p were used as positive controls. The membrane was washed twice for 10 min and twice for 30 min at

50 °C with non-stringent wash solution and once for 5 min at 50 °C with stringent wash solution. Signals were detected by autoradiography using the Cyclone Plus Phosphor Imager (PerkinElmer). The membrane was stripped for 1 h and re-used several times to detect additional miRNAs.

Luciferase assay

Luciferase assays were performed using Neuro2a (N2a) cells maintained in DMEM (Gibco) supplemented with 10 % FBS at $37\,°C$ and 5 % CO^2. 7 x 10^5 cells/well were seeded in 24-well plates and co-transfected with 215 ng of psiCHECK-2, 150 ng of miR-486a plasmid and 100–150 nM LNA, using polyethylenimine (PEI, Sigma Aldrich) (PEI:DNA ratio 3:1). 24 hours after transfection cells were washed with PBS, lysed and luciferase assay was performed using Dual Luciferase Reporter Assay System (Promega) on a Synergy Neo Plate Reader (BioTek). For all samples, relative luminescence was calculated as a ratio between Renilla and Firefly luciferase values, to account for differences in transfection efficiency.

2.2.3 Immunohistochemistry

After dissection, brains were fixed in 4% PFA overnight at $4\,°C$, cryoprotected in 30% sucrose and cryosectioned (10 µm thick slices). Cryosections were then permeabilized (0.5 % Triton X-100 in PBS) for 20 min, quenched for 30 min and blocked for 30 min at RT. All primary antibodies were incubated overnight at $4\,°C$, followed by washing and incubation with secondary antibodies for 2 h at RT. For Tbr2 staining, antigen-retrieval was performed in Citrate Buffer for 1 h at $70\,°C$. For BrdU staining, sections were incubated in 2M HCl for 30 min

at 37 °C. EdU detection was performed using Click-iT Edu kit (Thermo Fisher Scientific). Nuclei were counterstained with DAPI.

2.2.4 Bioinformatics, statistical analyses and image processing

<u>Miat deep sequencing</u>: sequencing data were obtained for PP, DP and N in three biological replicates. After adapter removal, reads were aligned using gsnap (Wu and Nacu, 2010) to the mouse genome (Ensembl v.81, based on mm10) integrated with the map of the plasmid encoding for Miat and the BFPnls. Eventually, a table of read counts was generated using featureCounts (v.1.5.1) (Liao et al., 2014).

<u>miRNA deep sequencing</u>: sequencing data were obtained for PP, DP and N in 3 biological replicates. After adapter removal, reads shorter than 30 bp were aligned with gsnap (Wu and Nacu, 2010) using miRBase (v.20) as a reference (Kozomara and Griffiths-Jones, 2014). Alignment was performed in 3 consecutive steps: a) on mature miRNAs, b) unmapped reads were extracted and c) aligned on pre-miRNA. During all steps, no mismatches were allowed and multi-mapped reads discarded. Eventually, a table of read counts per mature miRNA (read count >1) was assembled. For novel miRNA prediction, all unmapped reads were extracted and aligned using miRDeep2 (Friedländer et al., 2008) on mouse genome (mm10).

<u>Differential expression analysis</u>: the R package DESeq2 (Love et al., 2014) was used for normalization of the read count table and further testing of differential expression. Mean counts from replicates were used for fold change calculations:

log$_2$ fold change values ≥ 0.58 or ≤ -0.58 were considered up- or down-regulation, respectively.

Statistical analyses: for differential expression analyses, Benjamini–Hochberg procedure was applied for multiple t-test adjustment and FDR values lower than 0.05 were considered significant. For all other experiments, a minimum of 3 biological replicates was used. Statistical differences of mean values were calculated by two-tailed student t-test. Comparisons between expressions of intergenic/intragenic/other miRNAs were performed by Mann-Whitney U test. Significance of Spearman correlations were evaluated by student T-distribution test. P-values lower than 0.05 were considered significant.

Image processing: sections were imaged using an automated microscope (ApoTome; Carl Zeiss), pictures digitally assembled using Axiovision or Zen software (Carl Zeiss) and composites analyzed using Photoshop CS6 (Adobe). Cellular quantifications were normalized per RFP+ cells (electroporated population, total or per cortical layer) or per area (total population, measured with Fiji 1.49m - ImageJ).

CHAPTER 3

RESULTS

Previously, the Btg2$^{\text{RFP}}$/Tubb3$^{\text{GFP}}$ mouse line was reported as an efficient and versatile tool to unravel genes playing pivotal roles during cortical development (Aprea et al., 2013). Particularly intriguing was the fact that a subclass of those regulators was enriched in non-coding transcripts, specifically in lncRNAs. Among those, the lncRNA Miat was found to regulate neural progenitors fate, possibly via splicing (Aprea et al., 2013). Those findings opened two interesting scenarios:

1. Role of Miat during corticogenesis. To further dissect the function of Miat, I aimed at a) clarifying the effect of Miat on neural progenitors fate and b) comprehensively identifying Miat-spliced targets.

2. Small non-coding RNAs. Other classes of non-coding RNAs, like miRNAs are potent regulators of developmental processes. Hence, I pursued the assembly of a complete atlas of cortical miRNAs and the identification of new miRNAs playing a role in corticogenesis.

3.1 MIAT REGULATES NEUROGENESIS

Miat delays neural progenitors differentiation

The lncRNA Miat was shown to play a critical role in neural progenitors fate control. In fact, *in vivo* manipulation of Miat led to an increase in the generation of BPs, which remained in a proliferative state, rather than becoming DPs, consequently yielding a reduced neuronal output after 48 hours (Aprea et al., 2013). Although, it was not clarified whether those supernumerary BPs just delayed the switch from proliferation to differentiation or never underwent neurogenic divisions, thereby partially blocking neurogenesis.

In order to address that question, additional manipulations of Miat by IUE were required. To do so, a plasmid expressing Miat and an RFPnls from two identical and independent promoters was generated (construct details in Fig. 2.2). To validate Miat overexpression, Miat-RFPnls or control RFPnls plasmids were electroporated in E 13.5 embryos, followed by FAC-sorting of electroporated cells (RFP+) 24 hours later. RT-qPCR quantification revealed a significant 4.5 ± 0.9-fold increase in Miat abundance as compared to control (Fig. 3.1a). Next, when Miat was overexpressed for 48 hours in E 13.5 embryos, the percentage of cells in the CP resulted significantly reduced by more than 50%, counteracted by a 30% accumulation of progenitors in the VZ. The latter effect was mainly due to an increase in BPs generation within the VZ (Fig. 3.1b). This result was expected as it essentially recapitulated the findings of Aprea et al.
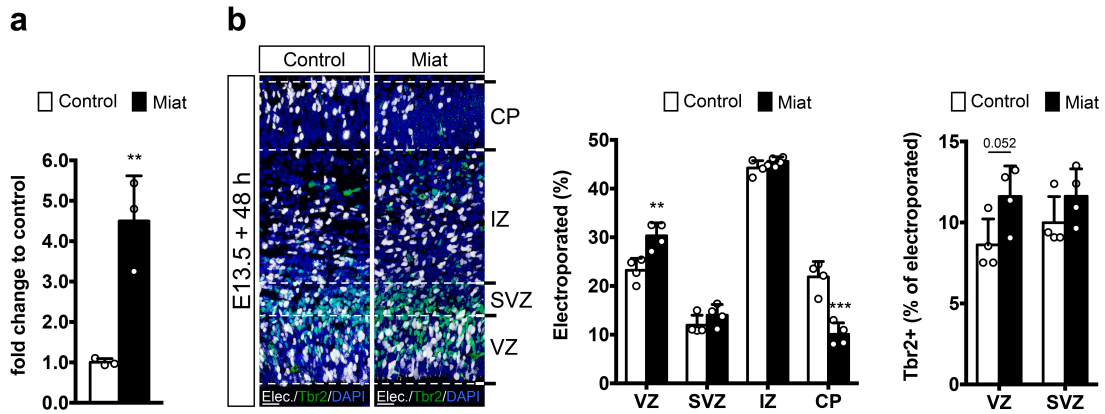
Fig. 3.1 Miat counteracts neural progenitors differentiation

a. RT-qPCR quantification of Miat abundance (black bar) compared to control (white bar) 24 hours after overexpression in E 13.5 embryos. **b.** Fluorescent pictures of mourse cortices and quantifications of the distribution of electroporated cells (RFP+, white) and electroporated BPs (RFP+Tbr2+, white/green) across cortical layers 48 hours after Miat (black bars) or control (white bars) IUE in E 13.5 embryos. Individual dots = biological replicates. Error bars = SD. ** p<0.01 ; *** p<0.001. Scale bars = 25 µm.

To investigate whether the supernumerary BPs eventually switched to neurogenic divisions or never underwent neurogenesis, a possible approach would be a later readout after Miat manipulation. The reason being that a partial block of neurogenesis would yield an even stronger reduction in neuronal output, whereas a delay would be ameliorated or even rescued. Hence, E 13.5 embryos were electroporated with Miat-RFPnls or control RFPnls plasmids and brains were collected 5 days later (E 18.5). To thoroughly analyze neuronal output, mice were also administered a single shot of BrdU at E 14.5 (Fig. 3.2a). Following injection, BrdU is incorporated in the DNA of all cells undergoing cell cycle and quickly washed out of the body. On the one hand, progenitors slowly lose BrdU positivity through consecutive cell divisions, whereas post-mitotic neurons generated at E 14.5 are permanently labeled, thereby allowing tracking their migration. Assessment of electroporated cells (RFP+) distribution revealed that Miat overexpression induced a significant increase in the percentage of cells

in the proliferative layers VZ/SVZ (here jointly considered due to the proportionally small amount of cells populating them), as compared to control (17$\pm$ 1% versus 10 $\pm$ 1%, respectively). In addition, the neuronal population of the CP was significantly reduced by 27 $\pm$ 4% in Miat-manipulated brains (56 $\pm$ 2% and 71 $\pm$ 3%, respectively). Interestingly, Miat overexpression also induced a significant increase in neurons in the IZ (from 19 $\pm$ 2% to 27$\pm$ 1% in control and Miat, respectively) (Fig. 3.2b). As the IZ is a primarily migratory layer that neurons cross on their way to the CP, an accumulation of cells in IZ might mean that neurons are either generated later and are still migrating or that their migration is impaired. To investigate the latter possibility, the distribution of BrdU+RFP+ neurons birth-dated at E 14.5 was analyzed across 8 equidistant bins covering IZ and CP. As shown in Fig. 3.2c, the scattering of those neurons was virtually identical in Miat-overexpressing and control brains, thereby excluding a migration defect.

Taken together, the observations described so far indicate that Miat gain-of-function increases the pool of BPs, which undergo additional proliferative divisions and belated neurogenesis. This conclusion is corroborated by the fact that readout 5 days after Miat manipulation showed an amelioration of the deficit in the CP as well as a wave of late-generated neurons still migrating across the IZ.
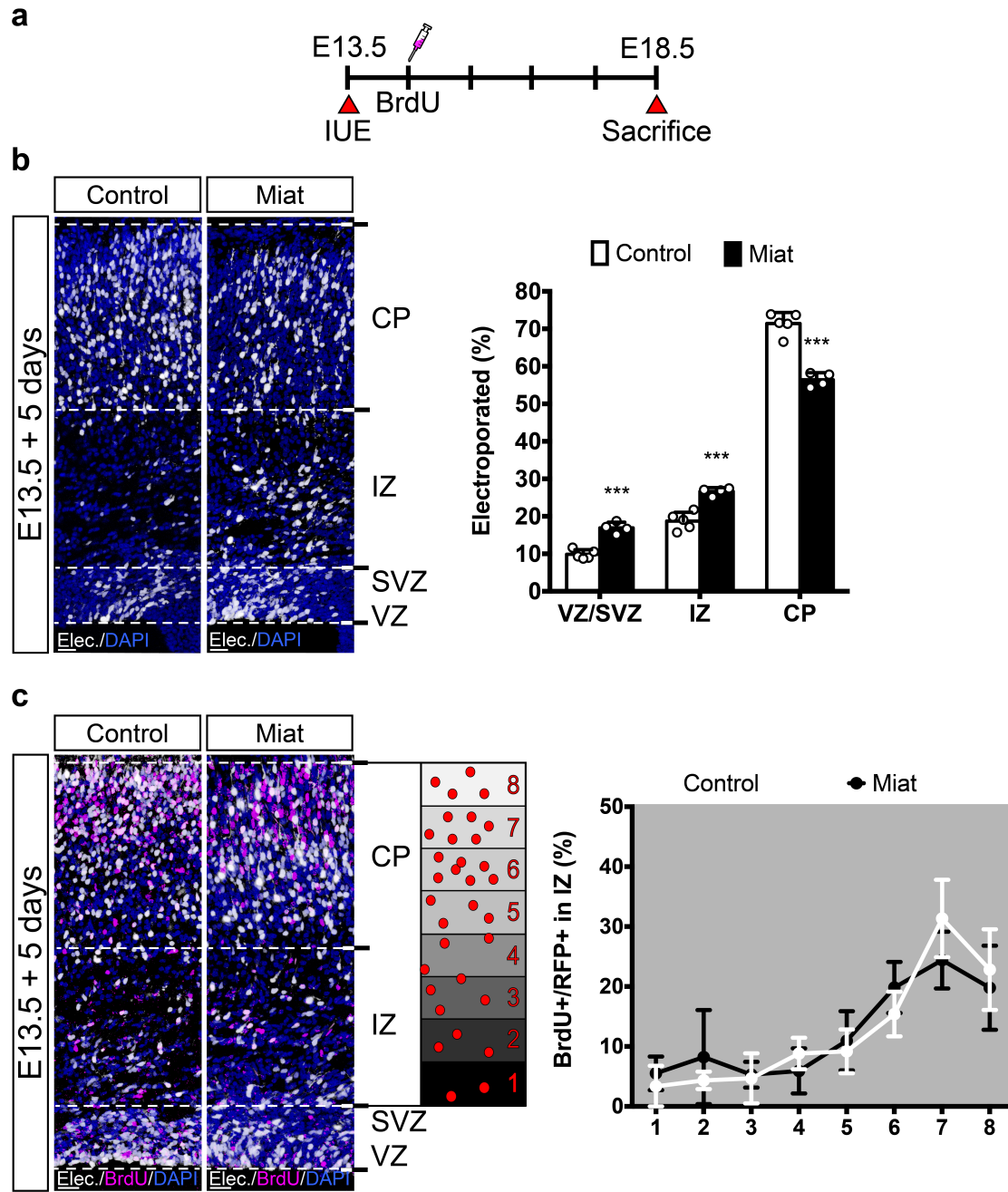
Fig. 3.2 Miat delays neurogenesis

a. Electroporation paradigm. **b-c.** Fluorescent pictures and quantifications of cell distribution (**b**) and neuronal migration (**c**) 5 days after Miat or control plasmids electroporation in E 13.5 embryos. Electroporated cells (RFP+, white) distribution was assessed across cortical layers (**b**), whereas neuronal migration by calculating the percentage of neurons (RFP+BrdU+, white/magenta), birth-dated as described in (**a**) across 8 equidistant bins in IZ and CP (**c**). Individual dots = biological replicates. Error bars = SD. *** p<0.001. Scale bars = 25 µm.

Establishment of a system to unravel Miat-spliced genes

The fact that Miat regulates cell fate of BPs opened interesting questions regarding the mechanisms mediating that function. In this regard, Miat was found to interact with splicing factors, like the SF1 and Celf3 (Ishizuka et al., 2014; Sone et al., 2007), hinting at a cross-talk between Miat and the splicing machinery. Supporting that theory, Aprea et al., showed that Miat manipulation led to a significantly different usage of Wnt7b isoforms, implying that Miat might trigger aberrant splicing of cell-fate determinants in neural progenitors. However, as Miat not only controls BP fate, but also neuronal survival (Aprea et al., 2013), Miat-spliced targets might be different in different cell types, thereby making it particularly interesting to unravel those targets at single-population level. That elegant resolution could be theoretically achieved by electroporation of $Btg2^{RFP}/Tubb3^{GFP}$ embryos with Miat and a third reporter protein, followed by analyzes of PP, DP and N transcriptomes.

To establish that system, a vector expressing a BFPnls was cloned (as described in Fig. 2.2b) and subsequently electroporated in E 13.5 $Btg2^{RFP}/Tubb3^{GFP}$ embryos. Brains were collected 48 hour later, and FACS gates were set so that all manipulated cells (BFP+) were sorted first, followed by fractioning into the three cell populations of interest: PP (BFP+/RFP−/GFP−), DP (BFP+/RFP+/GFP−) and N (BFP+/ GFP+) (Fig. 3.3). Negligible spillover was detected between channels, thus proving the feasibility of the setup.
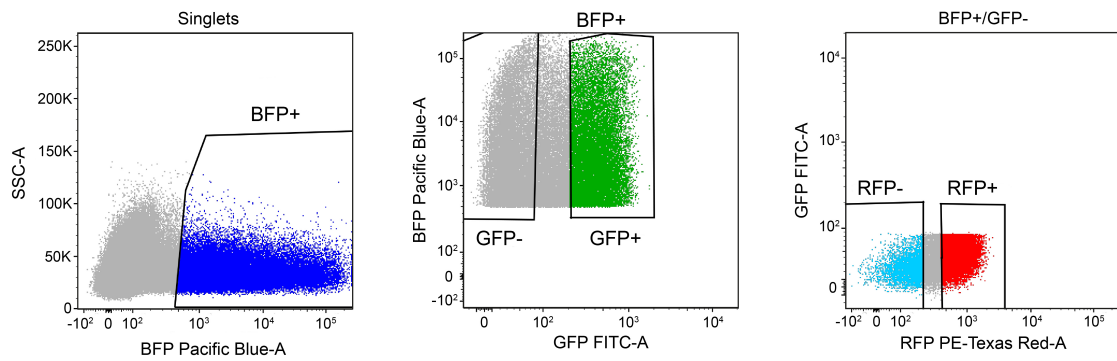
Fig. 3.3 FAC-sorting of manipulated PP, DP and N

After excluding duplets and dead cells, BFP+ cells were isolated (left, blue), followed by fractioning in GFP− and GFP+ populations (middle, grey and green, respectively). Eventually, GFP− cells were split in RFP− and RFP+ (right, light blue and red, respectively). Cells outside marked gates were discarded.

However, the amount of cells collected for each population was low, due to three limiting factors: a) The $Btg2^{RFP}/Tubb3^{GFP}$ is a double-heterozygous mouse line and only 25% of the embryos are double-positive, b) a small population of cells is targeted by IUE and c) that population is further divided into the 3 subpopulations of PP, DP and N. To overcome those hurdles, a library preparation method that amplifies the cDNA library was tested on RNA extracted from sorted cells, resulting in robust transcriptome coverage (data not shown).

Then, Miat was cloned into the BFPnls plasmid and IUE was performed in E 13.5 $Btg2^{RFP}/Tubb3^{GFP}$ using Miat-BFPnls or empty BFPnls (as a control) plasmids. Manipulated PP, DP and N were sorted in three biological replicates and total RNA was used for cDNA library preparation, followed by 75-bp paired-end deep sequencing. Bioinformatics alignments (performed by Mathias Lesche, Deep Sequencing Group) highlighted a disproportionate fraction of reads mapping onto both strands of the expression plasmid, only in Miat

manipulated samples (e.g. in PP reads on plasmid were 20.4% 4.4% and 9.3% versus 0.02% 0.02% and 0.05% in Miat and control samples, respectively). Miat plasmid partially escaped DNase treatment (or remained fragmented) and was efficiently amplified during library preparation. This technical problem, not observed during troubleshooting tests performed using the control BFPnls vector, unbalanced isoform amplification and limited the depth of Miat samples transcriptome coverage, thereby impeding solid differential splicing analyses.

Despite the intriguing biological question, collecting new RNA in biological triplicates was not feasible in a reasonable time-frame for this work of thesis due to: a) intrinsic limits of electroporating the Btg2$^{\text{RFP}}$/Tubb3$^{\text{GFP}}$ line and b) further time-consuming tests were required. The project was thereby momentarily paused and the rest of this dissertation will focus on another class of regulatory non-coding RNAs: miRNAs.

3.2 GENERATION OF A COMPLETE miRNA CATALOG OF PROGENITORS AND NEURONS

Assembling the miRNome of cortical progenitors and neurons

The Btg2^{RFP}/Tubb3^{GFP} mouse line was previously exploited to comprehensively describe the events taking place during neural progenitors lineage differentiation at both DNA (methylation and hydroxymethylation) and RNA levels (including protein-coding, long non-coding and circular RNAs) (Aprea et al., 2013; Dori et al., In revision; Noack et al., In revision). Although, other classes of regulatory non-coding RNAs such as miRNAs are fundamental fine-tuners of cortical development, (Rajman and Schratt, 2017). Importantly, no cell-specific genome-wide miRNA study during cortical development was reported to date.

In order to assemble an atlas of miRNAs expressed in cortical progenitors and neurons, a previous student in the lab (Martina Dori) FAC-sorted PP, DP and N (each in three biological replicates) from the lateral cortices of Btg2^{RFP}/Tubb3^{GFP} mouse embryos at E 14.5. Total RNA was used for cDNA library preparation and sRNAs were isolated by size selection, followed by 75-bp high-throughput sequencing. Then, reads were aligned with gsnap (Wu and Nacu, 2010) using miRBase (v.20) as reference (Kozomara and Griffiths-Jones, 2014), yielding an average of 1.5 million unique-mapped reads (51% of total), a depth sufficient to perform differential expression analysis (alignment performed by Mathias Lesche, Deep Sequencing Group)(Fig. 3.4a-b). Thereof, 1058 mature miRNAs derived from 703 pre-miRNA were detected (read count >1), corresponding to 55% and 59% of the 1908 mature and 1186 pre-miRNAs reported in the reference, respectively. Specifically, 640 mature miRNAs were

common to all 3 cell-types, whereas 49 (4.6%), 58 (5.5%), 129 (12.2%) specific to PP, DP and N, respectively (Fig. 3.4a). Notably, when compared to a previous study which reported 294 pre-miRNAs (read count >1) expressed in the whole E 15.5 mouse brain (Ling et al., 2011), these datasets included 96% of those miRNAs and further extended the list by another 421 pre-miRNAs. Next, read counts were normalized using DESeq2 (median-ratio normalization) (Love et al., 2014) to account for differences in sequencing depth. Upon normalization, principal component analysis (PCA) showed a clear separation of the three cell types, which distributed according to lineage differentiation (PP $\rightarrow$ DP $\rightarrow$ N) for the component displaying the highest variance (PC1) (Fig. 3.4c).
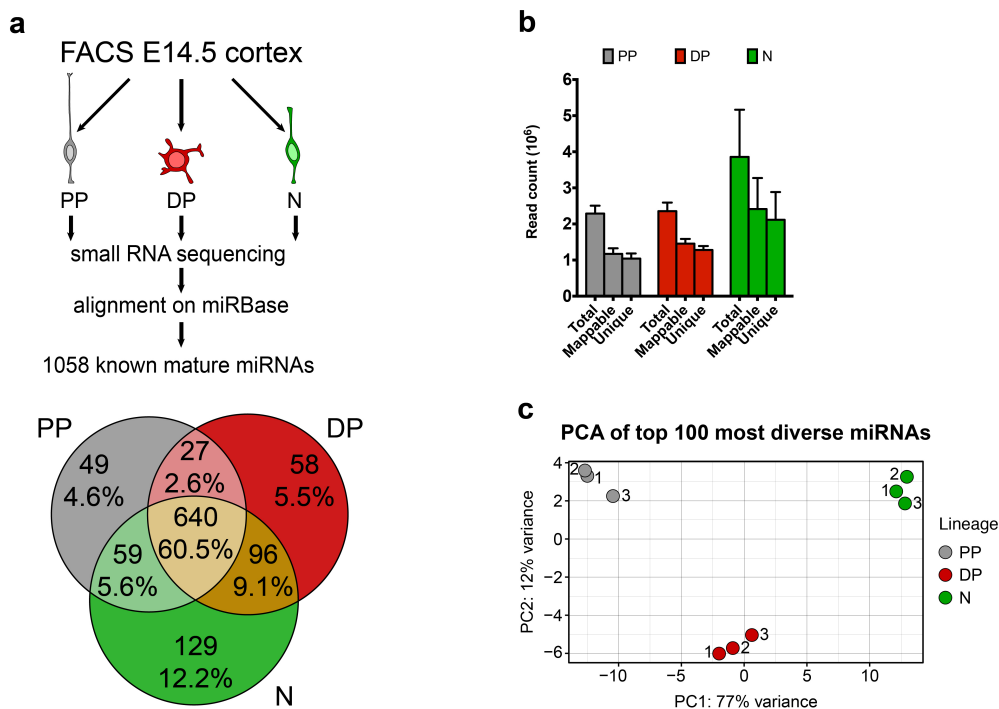
Fig. 3.4 miRNome of cortical progenitors and neurons

a. Flowchart of the steps undertaken to assemble the miRNome catalogs. PP (RFP□/GFP□), DP (RFP+/GFP□) and N (GFP+) were isolated from E 14.5 Btg2^{RFP}/Tubb3^{GFP} embryos, followed by sRNA deep sequencing and alignment on miRBase. **b.** Alignment statistics of PP (grey), DP (red) and N (green) datasets, reporting total, mappable and unique reads (x10^6). **c.** Principal component analysis of top 100 most diverse miRNA between biological replicates (numbers) and lineage populations (colors).

Validation of datasets

After assembling the miRNA catalogs of progenitors and neurons, the robustness of the datasets needed to be carefully evaluated. To do so, the normalized expression of miRNAs measured by deep sequencing was compared to their in-tissue distribution detected by ISH. For ISH, the data of six miRNAs were downloaded from Eurexpress (Diez-Roux et al., 2011), a genome-wide expression atlas of E 14.5 mouse embryos. Five of those miRNAs were known regulators of neurogenesis and one was never linked with brain functions before. Specifically, miR-9-5p and miR-17-5p, two widely known regulators of progenitors fate (Mao et al., 2014; Zhao et al., 2009), showed similar expression levels in PP, DP and N, matching their in-tissue distribution (Fig. 3.5). Conversely, miR-92b-3p and miR-92a-3p, which down-regulate Tbr2 to keep progenitors proliferating (Bian et al., 2013; Fei et al., 2014; Nowakowski et al., 2013), decreased in expression along lineage differentiation. Again, ISH displayed a strong signal in VZ and SVZ fading away in neuronal layers, overlapping the sequencing data (Fig. 3.5). Furthermore, the neuron-specific miR-124-3p (Visvanathan et al., 2007) detected only in the CP by ISH, showed a strong up-regulation in N in the deep-sequencing datasets. Similarly, miR-296-3p, a miRNA not yet connected with any brain developmental function, was detected specifically in the CP, decently matching the sequencing data and making it a potentially novel candidate regulating neuronal specification or survival. Last, to validate also a subtle expression pattern such as an on-switch in DP, ISH for let-7b-5p was performed on E 14.5 mouse brains. Tissue distribution of let-7b-5p peaked in the SVZ, with some strong signal in few cells of the VZ, probably DP that were delaminating and migrating to the SVZ (Fig. 3.5). This pattern is consistent with the biological function of let-7b, which promotes neural progenitors differentiation (Zhao et al., 2010).

All in all, tissue distribution and sequencing data matched for known regulators of neurogenesis as well as for miR-296-3p that has no link with corticogenesis. This correlation was not limited to the distribution, but also extended to the signal intensity. For instance, miR-9-5p which took >50% of the reads in all datasets displayed the strongest ISH signal. Signal intensity and expression correlated also for the other miRNAs, with miR-124-3p and miR-296-3p showing the lowest expressions and the weakest signals.
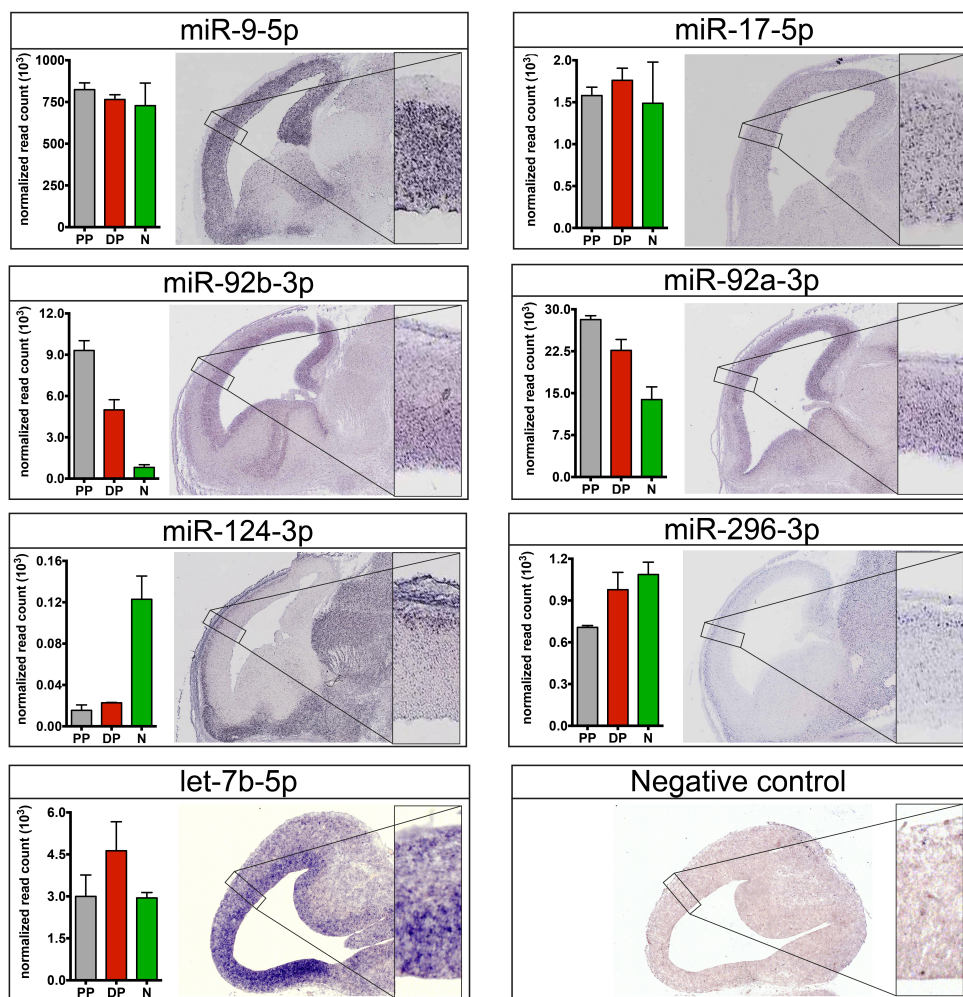
Fig. 3.5 Validation of miRNA deep sequencing datasets

In situ hybridization of E 14.5 mouse cortices: sagittal sections from Eurexpress (miR-9-5p, miR-17-5p, miR-92b-3p, miR-92a-3p, miR-124-3p, miR-296-3p) or coronal sections hybridized in house (let-7b-5p, Negative control). Magnifications of the lateral cortex are shown to appreciate the overlap with miRNA deep-sequencing data (histograms). Error bars = SD. n = 3.

Cortical miRNAs annotation is complete and comprehensive

The advent of high-throughput technologies exponentially enlarged the number of miRNAs included in miRBase in the early 2010's, before reaching a plateau in recent years. Despite that, some studies still reported the detection of few novel miRNAs in both humans and mice (de Rie et al., 2017; Li et al., 2013). Considering that the aim of this project was to assemble a complete catalog of cortical miRNAs and that 42% of the deep sequencing reads did not align to known miRNAs, it was reasonable to investigate whether some of those reads might come from actual novel miRNAs. To do so, miRDeep2 (Friedländer et al., 2008) was used to align unmapped reads on mouse genome, searching for regions that could potentially transcribe a pre-miRNA (prediction performed by Martina Dori) (Fig. 3.6a). Indeed, miRDeep2 predicted 163 novel miRNAs (read count >1), of which 21 common to all 3 cell types and 20 (12.3%), 39 (23.9%) and 57 (34.9%) specific to PP, DP and N, respectively (Fig. 3.6b).

In order to proceed with validation, the list of predicted novel miRNAs was first rank-ordered based on 2 criteria: a) consistency of detection among biological replicates (i.e. at least 2 out of 3 samples of the same cell type), and b) average read count. Hence, the 8 top-hits were selected for validation by Northern blot. To do so, total RNA was extracted from lateral cortices of wild-type E 14.5 mouse embryos and hybridized with 32P-labeled DNA probes against the predicted novel mature miRNA sequences (experiment performed by Sharof Khudayberdiev – Schratt G. group – BPC Marburg). Out of 8 putative novel miRNAs assessed, 3 were not detected and the remaining 5 showed a band in the range of 90-150 nt (Fig. 3.6c). Those bands did not correspond to the expected size of mature (20-25 nt) or pre-miRNA (~60 nt), but rather matched the length of other sRNAs such as tRNA, snRNA or snoRNA.

Despite not completely excluding that other predicted miRNA might be actual novel miRNAs, these results tag that possibility as unlikely. This conclusion is in line with the FANTOM5 project, which reported that highly expressed mouse miRNAs have already been largely annotated in nearly all tissues (de Rie et al., 2017). All in all, the results presented so far provide a complete and sophisticated catalog of miRNAs expression during mouse cortical development.
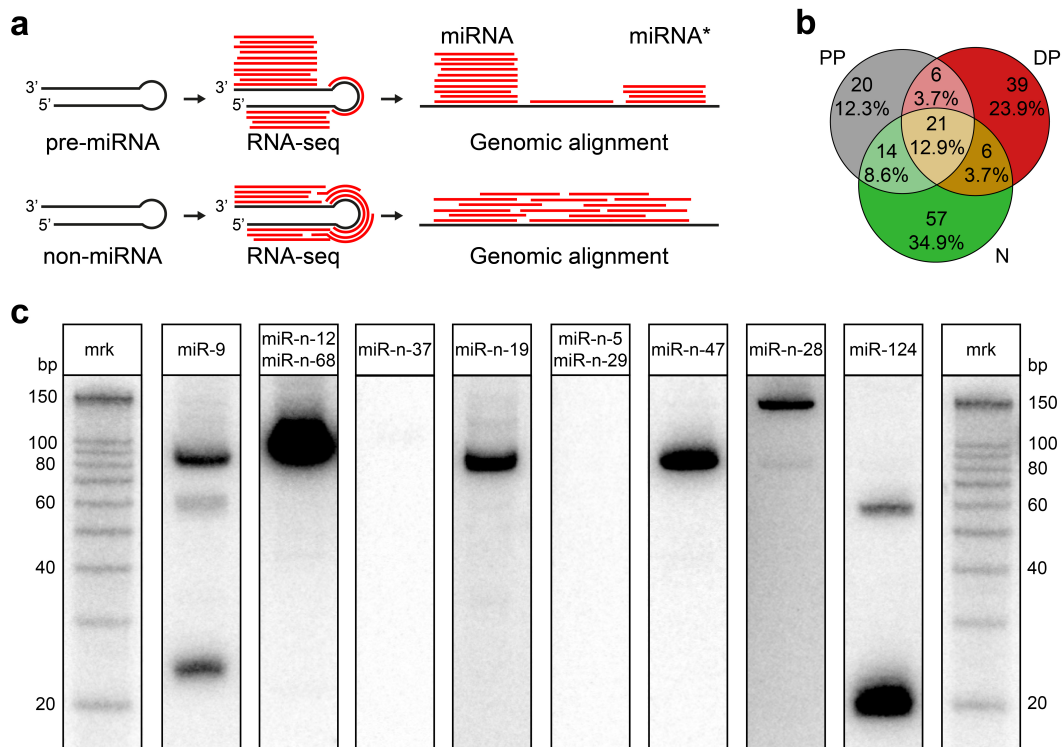
Fig. 3.6 Novel miRNAs prediction and experimental investigation

a. miRDeep2 algorithm: novel miRNAs are predicted assuming that, on the reference genome, reads from a pre-miRNA (top) would stack on the mature miRNA with smaller representations of miRNA* and stem-loop. Alignments not matching that pattern (bottom) are discarded. (Adapted from Friedländer et al., 2008). **b.** Venn diagram showing novel miRNAs predicted in PP (grey), DP (red) and N (green). **c.** Northern blots performed with 32P-labeled DNA probes on RNA from E 14.5 cortices. Radioactive markers (mrk) were used to determine fragment size. Novel miRNA names are reported in boxes (top), double names indicate identical mature sequence. miR-9-5p and miR-124-3p were used as positive controls. The 80 nt band in miR-9 is a carryover from hybridization with miR-n-19 probe (despite stripping). All blots were performed in biological triplicates.

3.3 DIFFERENTIAL miRNA EXPRESSION IS UNDERREPRESENTED AND OCCURS AT GENOMIC LOCUS LEVEL

Intergenic miRNAs are robustly expressed

The generation of comprehensive miRNomes of neural progenitors and newborn neurons allowed the analyses of global miRNA expression changes during lineage differentiation. In this regard, miRNAs might originate from various genomic locations, thereby classifying in three main categories: a) intergenic: not overlapping any gene, b) intragenic: sense-overlapping a gene and excised from the mRNAs and c) other: anti-sense overlapping a gene or displaying multiple locations in the genome. As previously mentioned, a general increase in the number of miRNAs was detected along with lineage differentiation, but the genomic distribution of those miRNAs remained proportionally unchanged. In fact, in PP, DP and N, roughly 20% of miRNAs were intergenic, 50% intragenic and the remaining 30% came from other locations (anti-sense overlapping or multi-locus) (Fig. 3.7a). This observation excluded the up-regulation of a specific subtype of miRNAs during lineage differentiation and rather pointed at a global increase in transcriptome complexity in neurons, a trend observed also for longer transcripts and splicing events (Aprea, 2014). However, when analyzing the expression level of miRNAs belonging to different categories, intergenic miRNAs showed a significantly higher median expression compared to both intragenic and other miRNAs in all three cell types (Fig. 3.7b). Notably, the spread in expression widened from PP to DP to N. This observation suggests that there might be discrepancies in precursor stability or processing efficiency of miRNAs originating from different genomic sources.

Altogether, these results provide evidences that miRNome complexity increases along lineage differentiation, with intergenic regions constituting a source of robustly expressed miRNAs.
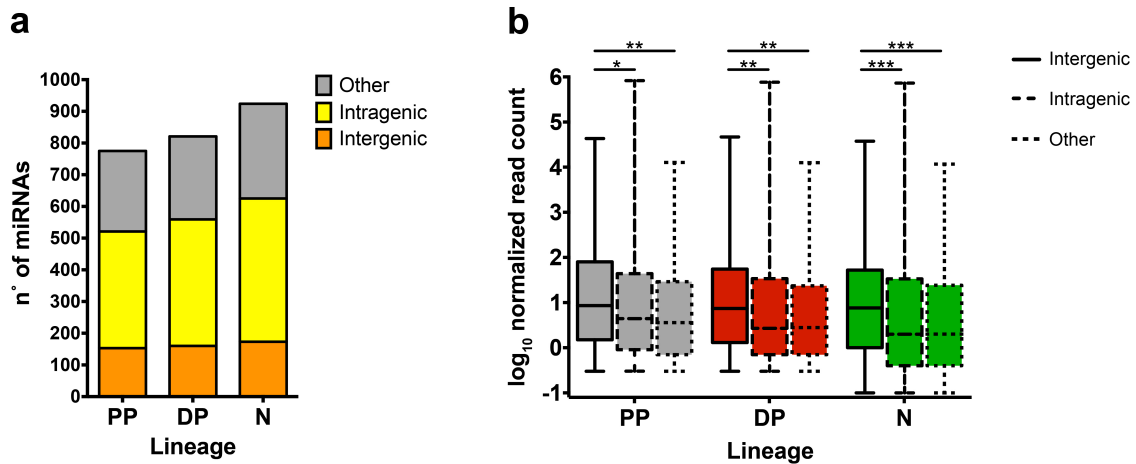
Fig. 3.7 Intergenic miRNAs are robustly expressed

a. Genomic distribution of the number (y-axis) of intergenic (orange), intragenic (sense-overlapping, yellow) and other (anti-sense overlapping or multi-locus) miRNAs in PP, DP and N. **b.** Box plots representing the expression (y-axis, $\log_{10}$ normalized read count) of intergenic (solid line), intragenic (dashed line) and other (dotted line) miRNAs in PP, DP and N. * $p < 0.05$; ** $p < 0.01$; *** $p < 0.001$.

Differential expression analysis

The versatility of the $Btg2^{RFP}/Tubb3^{GFP}$ line not only allowed the analysis of global miRNA changes, but also to perform differential miRNA expression at single-population level during corticogenesis. As lineage differentiation almost exclusively proceeds from PP → DP → N, the comparison PP-N was considered biologically irrelevant, thus only PP-DP and DP-N were confronted. To define up- or down-regulation, a threshold of >50% change in expression (i.e. $\log_2$ fold change ≥0.58 or ≤-0.58 for up- and down-regulation, respectively) and FDR <5% were set. As a result, the vast majority (80%) of miRNAs were constantly expressed throughout lineage differentiation and only 7% and 17% showed a

significant change between PP-DP and DP-N, respectively (Fig. 3.8a-b). Notably, the number of differentially expressed miRNAs increased by 2.5-fold between DP-N as compared to PP-DP. In this regard, miRNAs seemed not to be an exception to a general increase in differential expression during lineage commitment, as a remarkably similar trend was observed for protein-coding, long non-coding and circular transcripts (Aprea et al., 2013; Dori et al., In revision). Another remarkable analogy between miRNAs and the aforementioned transcripts was that >90% of the miRNAs up- or down-regulated between PP-DP continued to follow the same trend between DP-N or remained constant (Fig. 3.8b). Interestingly, newborn neurons not only expressed a higher number of miRNAs compared to progenitors but also seemed to favor up- over down-regulation, which may hint towards a more critical role of miRNAs in neurons than in progenitors.

Given that miRNAs are short molecules, often excised from longer transcripts, it was tempting to speculate that differential miRNA expression might occur mainly as a consequence of a regulatory process happening at genomic locus level, rather being a feature intrinsic to the single miRNAs. To investigate that hypothesis, the miRNAs significantly up- or down-regulated in at least one of the two lineage transitions (PP-DP or DP-N) were extracted. Then, for each of those miRNAs, the overlapping or closest gene (regardless of strand specificity) was located and the expression data of those genes were retrieved from the transcriptome sequencing of the very same cell types performed by Aprea et al., 2013. Finally, the $\log_2$ fold change from PP-DP or DP-N of the differentially expressed miRNAs was correlated with their overlapping/closest gene. As a result, significantly positive correlations were observed in both transitions: in particular, from PP-DP the correlation value was moderate (Spearman r_s=0.45,

n=142, p<1.46×10^{-8}) and it became substantially stronger from DP-N (Spearman r_s=0.70, n=142, p<7.59×10^{-22}) (Fig. 3.8c). These positive correlation values confirm that miRNAs and genes transcribed from the same genomic locus display similar differential expression magnitudes during lineage differentiation.

Taken together, these results indicate that, during corticogenesis, differential miRNA expression is an underrepresented event that occurs mostly as a consequence of regulatory processes of the genomic locus, rather than at single-miRNA level.
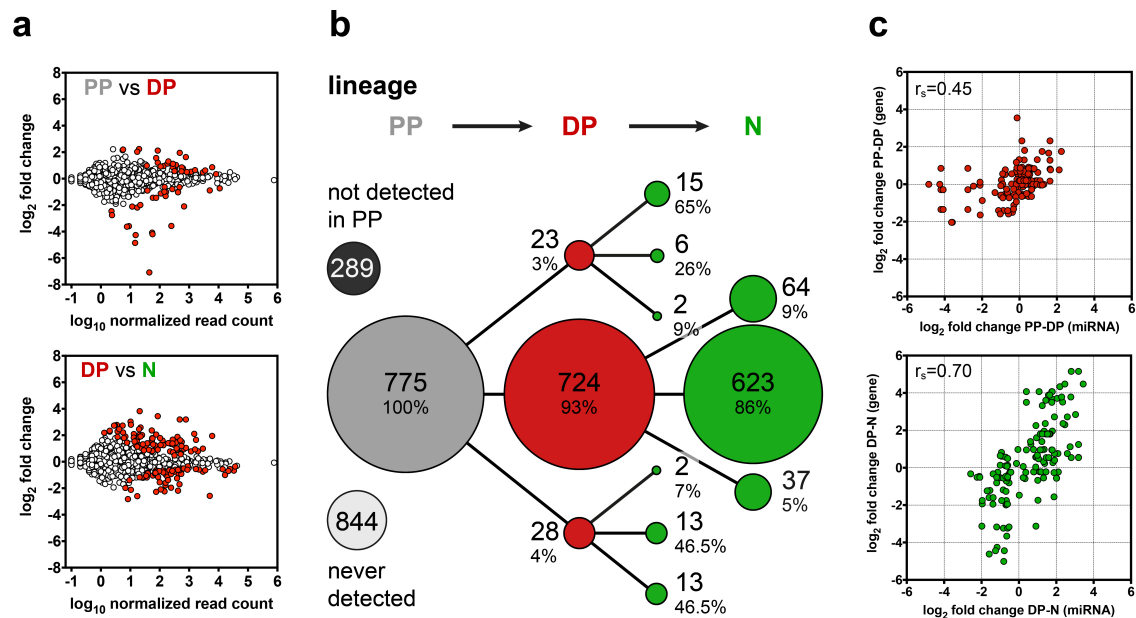
Fig. 3.8 Differential expression analysis of cortical miRNAs

a. MA plot of differential miRNA expression between PP-DP (top) and DP-N (bottom). DESeq2-normalized read count (x-axis; $\log_{10}$ scale) and fold change (y-axis; $\log_2$ scale) are indicated for differentially expressed (red) and unchanged (white) miRNAs (FDR <5%). **b.** Differentially expressed miRNAs between PP (grey), DP (red) and N (green). The number of miRNA in each group is reported and percentages are calculated over the parental population. miRNAs not detected in PP or never detected in any cell type are depicted. Oblique lines represent a >50% change and FDR <5%, whereas horizontal lines a <50% change or FDR >5%. **c.** Representation of Spearman correlation between $\log_2$ fold change of miRNAs (x-axis) and host/closest genes (y-axis) between PP-DP (top) and DP-N (bottom).

Switch miRNAs are rare and enriched in regulators of neurogenesis

Previous studies from Calegari's group identified a class of genes up- or down-regulated only in DP, as compared to both PP and N. Those switch transcripts, being specific of the transient population of DP, constitute the signature of neurogenic commitment (Aprea et al., 2013; Dori et al., In revision). Strikingly, *in vivo* manipulation of essentially all tested switch genes resulted in abnormal neurogenesis, highlighting their critical role in regulating progenitors proliferation versus differentiation (Aprea et al., 2013; Artegiani et al., 2015). Intriguingly, the subset of miRNAs displaying such a switch expression pattern was strongly underrepresented, accounting for only 4 miRNAs (0.5% of the total) (Fig. 3.8b). Peculiarly symmetrically distributed, 2 on-switch (let-7b-5p and miR-135a-2-3p) and 2 off-switch (miR-486a-5p and miR-486b-5p) miRNAs were found (Fig. 3.9a-b). Among them, let-7b is a well-known inductor of progenitors commitment by targeting pro-proliferative genes such as Tlx nuclear-receptor and cyclin D1 (Zhao et al., 2010). Analogously, miR-135a-2 gain-of-function was shown to reduce cortical size, possibly by targeting members of the Wnt/β-catenin pathway (Caronia-Brown et al., 2016). On the contrary, no neurogenesis-related function was reported to date for miR-486a and miR-486b. Collectively, despite the strong underrepresentation, switch miRNAs are enriched in regulators of progenitors proliferation and target several members of critical signaling pathways.

When analyzing the genomic locations, all switch miRNAs were found to be intragenic. In particular, the on-switch let-7b-5p and miR-135a-2-3p are processed, respectively, from lncRNAs AC162302.2 and Rmst, whereas the off-switch miR-486a-5p and miR-486b-5p from Ankirin1 (Ank1) and the predicted gene Gm15816, respectively (Fig. 3.9a-b). Ank1 and Gm15816 are transcribed

from different strands of the same genomic locus on Chr8 and one of their introns gives rise to pre-miR-486a and pre-miR-486b, respectively. Interestingly, the processing of those two pre-miRNAs eventually results in the generation of two identical mature sequences: miR-486a-5p and miR-486b-5p (from now on jointly referred to as miR-486-5p) (Fig. 3.9b). Unsurprisingly, when assessing the expression patterns of the host genes of switch miRNAs (retrieved from Aprea et al., 2013), a remarkable overlap was observed in 3 out of 4 cases (Fig. 3.9a-b), once again confirming that differential expression occurs mainly at genomic locus level. Last, in the case of miR-135a-2 and Rmst, not only they share the genomic locus and the expression pattern, but also they are involved in the same biological process. In fact, they both regulate neural progenitors proliferation by mediating Wnt/β-catenin pathway and Sox2 functions, respectively (Caronia-Brown et al., 2016; Ng et al., 2013). This observation opens intriguing questions regarding the roles of the other switch miRNA host genes, as none of them has been studied in the context of cortical development yet.
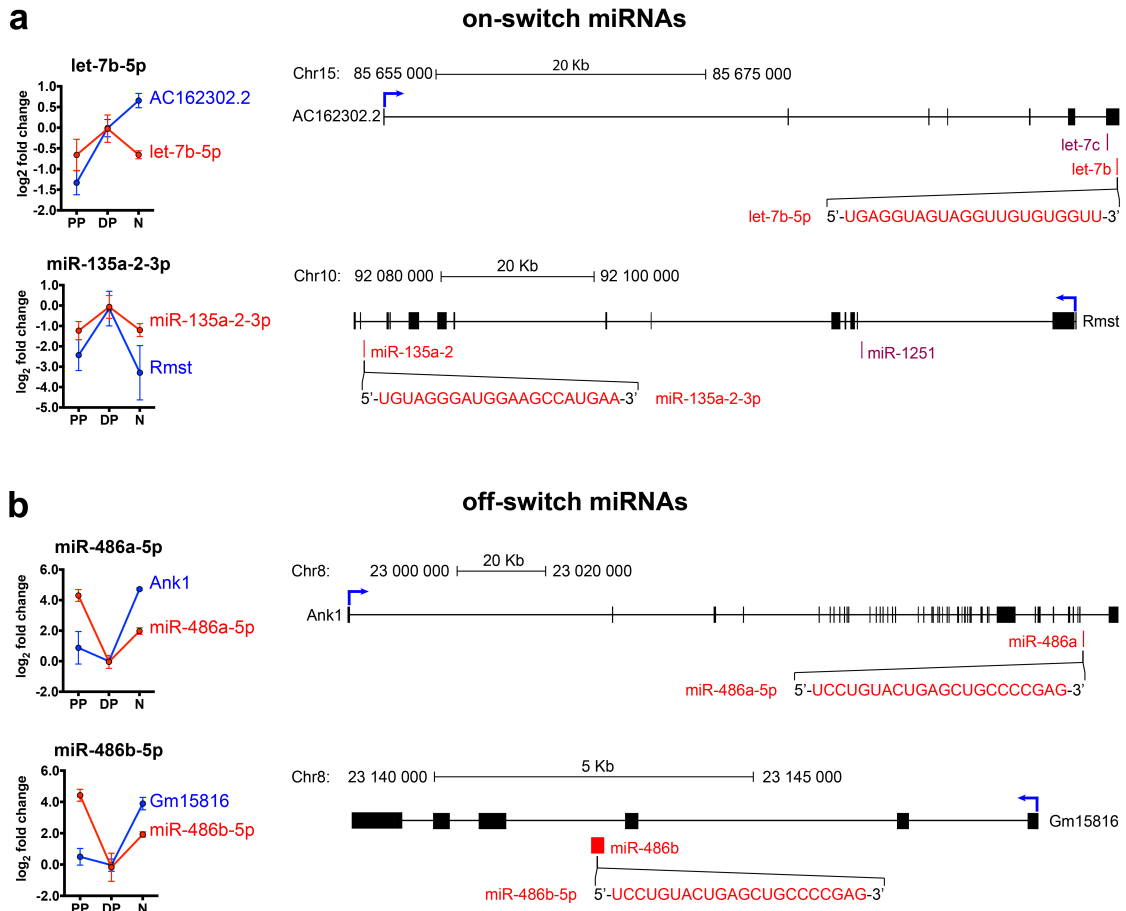
Fig. 3.9 Switch miRNAs genomic locus

Genomic loci of switch miRNAs: host genes are depicted (black), blue arrows represent the direction of transcription, whereas black boxes and lines constitute exons and introns, respectively. Position and mature sequence of switch miRNAs are indicated in red. Expression patterns in PP, DP and N of miRNAs (red line) and host genes (blue line) are reported (graphs) on the left.

3.4 miR-486-5p IS A NOVEL REGULATOR OF NEUROGENESIS

miR-486-5p inhibition increases neural progenitors pool

miR-486-5p was initially studied in the process of myogenic lineage development, where it promotes myoblasts differentiation by targeting the proliferation factor Pax7 (Dey et al., 2011). Then, other reports linked it with regulatory functions in ectodermal-derived tissues such as the olfactory epithelium and spinal cord motor-neurons (Jee et al., 2012; Kurtenbach et al., 2017). The absence of corticogenesis-related reports together with the intriguing switch in expression, made miR-486-5p an interesting candidate to further investigate whether it was involved in regulating neural progenitors fate. To do so, inhibition of miR-486-5p was pursued using locked nucleic acids (LNA).

First, in order to confirm the efficacy of the LNA in inhibiting miR-486-5p (LNA-486), the 3'-UTRs of two validated targets of miR-486-5p, namely Pten and Foxo1 (Small et al., 2010; Wang et al., 2015), were cloned downstream of the Renilla luciferase coding sequence (constructs details in Fig. 2.2c-e) and luciferase assays were performed in N2a cells. An effective LNA is supposed to prevent the miRNA-mediated destabilization of Renilla mRNA, thereby yielding an increase in luminescence. Indeed, knockdown of miR-486-5p by LNA-486 significantly increased luciferase activity compared to LNA-Control for both constructs, thus validating its targeting efficacy (Fig. 3.10a-b). To further test the specificity of LNA-486, both constructs were subjected to a 3-nt-mutation in miR-486-5p binding site, hence disrupting it (constructs details in Fig. 2.2c-e). If the effect of LNA-486 was specific for miR-486-5p, mutated constructs should

also increase Renilla luciferase activity. Indeed, mutated vectors co-transfected with LNA-Control or LNA-486 significantly increased luminescence, as compared to their respective wild-type construct co-transfected with LNA-Control (Fig. 3.10a-b). The extent of that increase was similar to the one induced by LNA-486 for Pten (Fig. 3.10a), but significantly higher for Foxo1 (Fig. 3.10b), indicating that the latter disruption was more efficient than LNA-486 alone in inhibiting miR-486-5p binding.
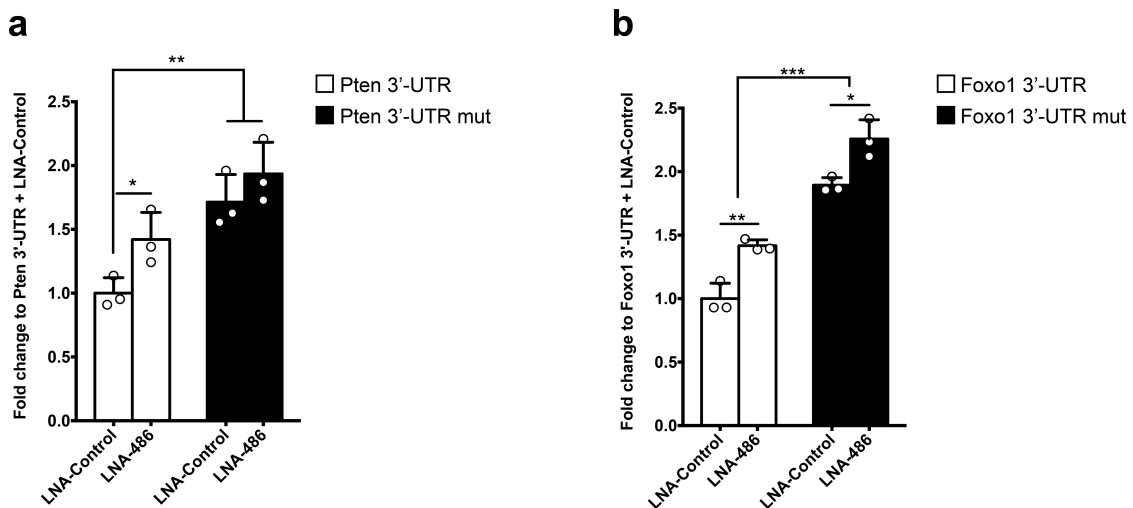
Fig. 3.10 Validation of LNA-486 efficacy and specificity

Luciferase assay showing that miR-486-5p inhibition by LNA-486 increased Renilla luciferase signal for both Pten (**a**) and Foxo1 (**b**) constructs (white bars). Mutagenesis of miR-486-5p binding sites on Pten (**a**) and Foxo1 (**b**) 3'-UTRs (black bars) also increased Renilla activity. Individual dots = biological replicates. Error bars = SD. * $p < 0.05$; ** $p < 0.01$; *** $p < 0.001$.

As a next step, to investigate the effect of miR-486-5p inhibition on cortical progenitors, IUE was performed using LNA-486 or LNA-Control together with the RFPnls reporter plasmid to mark electroprated cells. Embryos were electroporated at E 13.5 and brains were collected 48 hours later. Mice were also administered a single shot of EdU 3 hours before sacrifice (Fig. 3.11a). EdU is incorporated into all cells that go through the S phase of the cell cycle, thereby

allowing the estimation of the fraction of progenitors actively cycling. Assessment of electroporated cells (RFP+) distribution revealed significant alterations in all cortical layers induced by LNA-486. As visually noticeable, cells accumulated in progenitors layers (VZ and SVZ) and were deficient in neuronal layers (IZ and CP) in LNA-486-electroporated brains (Fig. 3.11b). Particularly affected were the SVZ which showed an increase from 12 ± 1 % to 20 ± 2 % and the CP that displayed a decrease from 20 ± 3 % to 12 ± 2 % in LNA-486- as compared to LNA-Control-electroporated brains. Given that at E 15.5 the SVZ is composed almost exclusively by BPs, a higher proportion of cells in SVZ means, by definition, an expansion of BPs. However, the VZ is populated by both AP and BP, therefore the increase in VZ might be due to expansion of either APs or BPs or both. To distinguish between those possibilities, immmunostaining for Tbr2, the main marker of BPs (Englund et al., 2005), was carried out. As a result, both AP (RFP+Tbr2□ in VZ) and BP (RFP+Tbr2+ in VZ and SVZ) were significantly increased and, consequently, neurons (Tbr2□ in IZ and CP) were reduced in LNA-486 electroporated brains (Fig. 3.11c). An expansion of progenitors pools might be an indication of an effect on neural progenitors cell cycle. To investigate whether that was the case, the distribution of electroporated progenitors, which underwent S phase during the 3 hours before sacrifice (RFP+EdU+) was assessed. The scattering of those progenitors in VZ and SVZ was nearly identical in LNA-486- and LNA-Control-electroporated brains, implying that the fraction of progenitors actively cycling was physiological (Fig. 3.11c).
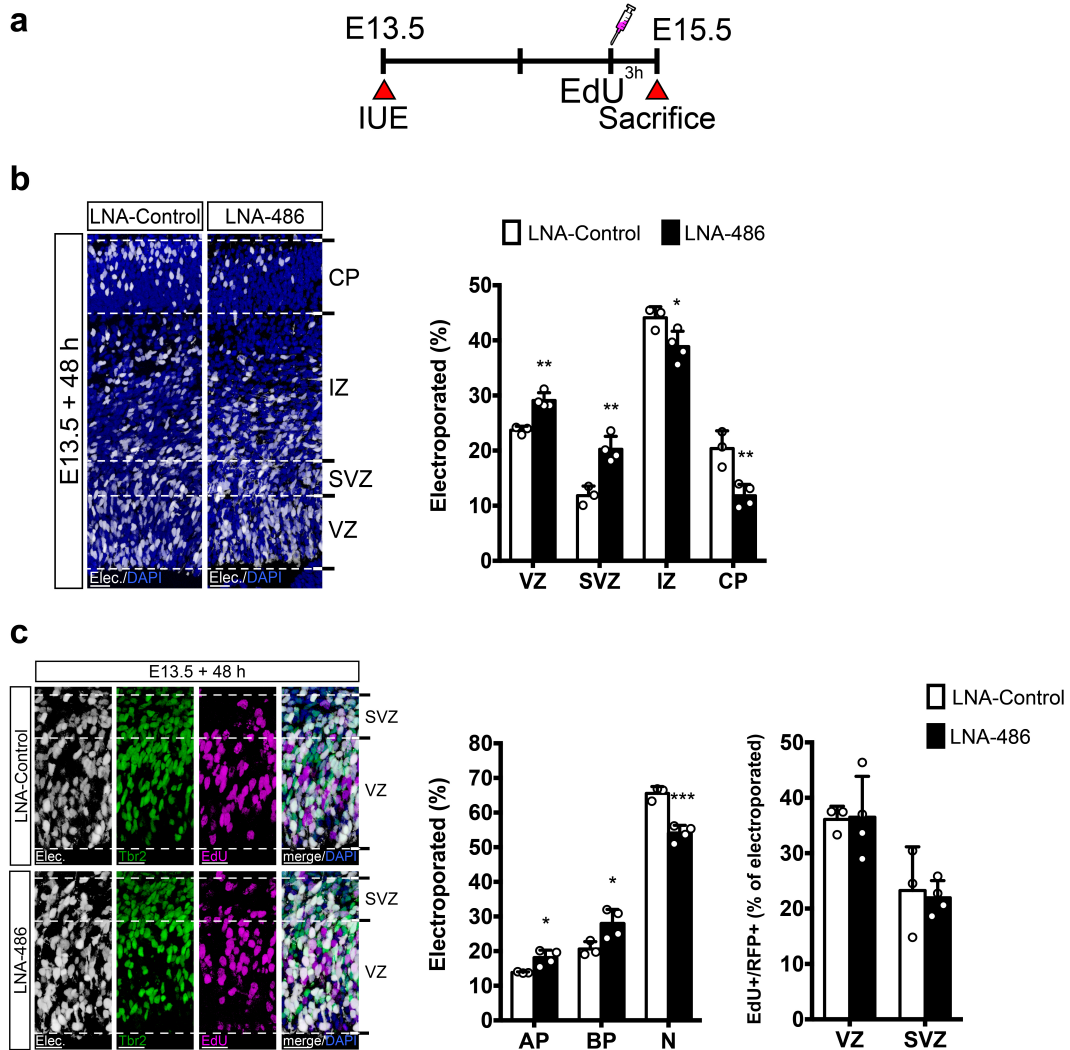
Fig. 3.11 miR-486-5p inhibition increases neural progenitors pools

a. Electroporation paradigm. **b-c.** Fluorescent pictures and quantifications of the distribution of electroporated cells (RFP+, white) (**b**) or AP (RFP+Tbr2–, white, in VZ), BP (RFP+Tbr2+, white/green, in VZ and SVZ) and N (RFP+Tbr2–, white, in SVZ, IZ and CP) (**c**) or cycling cells (RFP+EdU+, white/magenta, in VZ or SVZ) (**c**) 48 hours after LNA-486 (black bars) or LNA-Control (white bars) electroporation. Individual dots = biological replicates. Error bars = SD. * p<0.05 ; ** p<0.01 ; *** p<0.001. Scale bars = 25 µm.

Progenitors expanions may be the cause or the consequence of neuronal deficit. In fact, neural progenitors fate change could delay/prevent neurogenesis or abnormal neuronal apoptosis coupled with defective migration could prevent neurons from reaching the CP and, in turn, increase progenitors pools. To investigate whether the effect of miR-486-5p inhibition was restricted to

newborn neurons, LNA-486 or LNA-Control were co-electroporated with the RFPnls vector in E 13.5 embryos. Neurons generated at E 14.5 were labeled by a single ip-injection of BrdU and brains were collected at E 15.5 (Fig. 3.12a). First, in order to check if LNA-486 induced abnormal neuronal apoptosis, the number of cells reactive for active caspase3 (marker of programmed cell death) was quantified. Caspase3+ cells per area (regardless of whether electroporated or not) were slightly but significantly reduced in LNA-486-electroporated brains, excluding an apoptotic phenotype (data not shown). Next, the distribution of neurons birth-dated at E 14.5 was assessed across 5 equidistant bins spanning the IZ, as readout of neuronal migration. The migration rate of those electroporated neurons (BrdU+RFP+) resulted essentially identical in LNA486- and LNA-Control-electroporated brains, thus concluding that miR-486-5p inhibition did not affect the capacity of neurons to reach the CP (Fig. 3.12b).
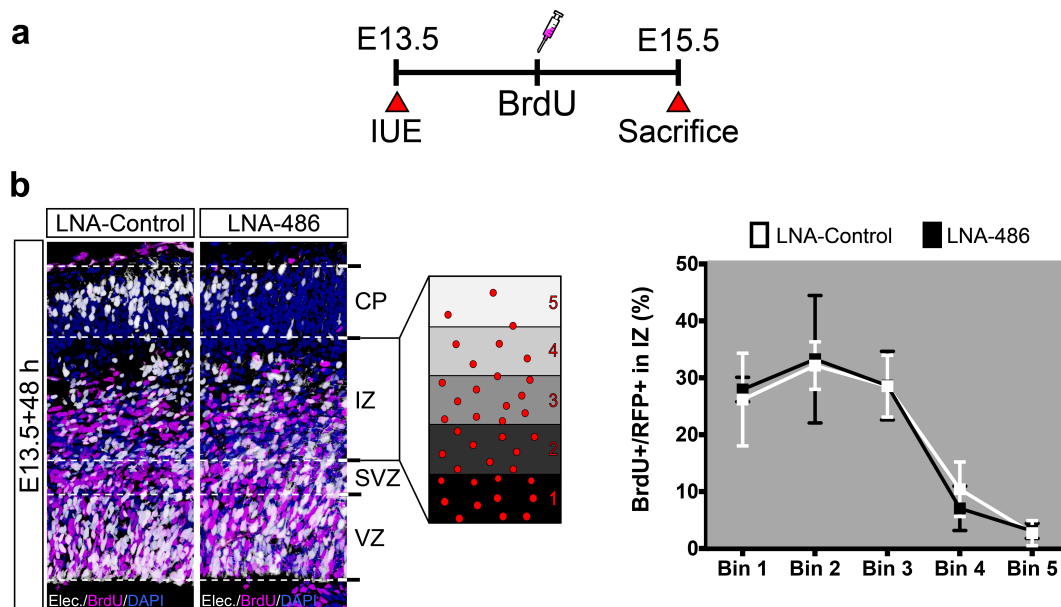

Fig. 3.12 miR-486-5p inhibition does not affect neuronal migration

a. Electroporation paradigm. **b.** Fluorescent pictures and quantification of electroporated neurons (RFP+/BrdU+, white/magenta) birth-dated as in (**a**) across 5 equidistant bins in the IZ (as depicted in **b**) 48 hours after LNA-486 or LNA-Control electroporation in E 13.5 embryos. n=3. Error bars = SD. Scale bars = 25 µm.

Taken together, these results showed a functional involvement of miR-486-5p in the regulation of cortical progenitors differentiation. In particular, miR-486-5p inhibition increased the pool of neural progenitors and counteracted their differentiation, without affecting neuronal migration. These findings suggest that miR-486-5p inhibition alters neural progenitors fate and open interesting questions regarding the targets and pathways responsible for that phenotypic effect.

miR-486-5p predicted targets include on-switch signaling molecules

In order to dig deeper into the biological effect observed upon miR-486-5p inhibition, an efficient way to identify the genes mediating that phenotype would be required. In this regard, in the last two decades many tools that perform miRNA target prediction were developed (recently reviewed by Riffo-Campos et al., 2016). Despite being based on different algorithms, all predictions generally yield hundreds or thousands of putative targets with a high rate of false positives. One way to limit that consists in taking advantage of miRWalk 2.0 (Dweep et al., 2011; Dweep and Gretz, 2015), which allows the combination of miRWalk algorithm with several others, thereby increasing the prediction power. Thereon, miR-486-5p target prediction was performed by combining 6 different algorithms: miRWalk, miRanda, TargetScan, PITA, RNA hybrid and RNA22 (minimum seed length: 7 nt ; p-value < 0.01). This combined prediction yielded 427 genes (Fig. 3.13a), whose GO term analysis (Enrichr, v.2017, Chen et al., 2013) highlighted significant enrichment in biological processes such as cell morphogenesis, learning, regulation of neurotransmitter secretion, brain development and cognition (Fig. 3.13b).
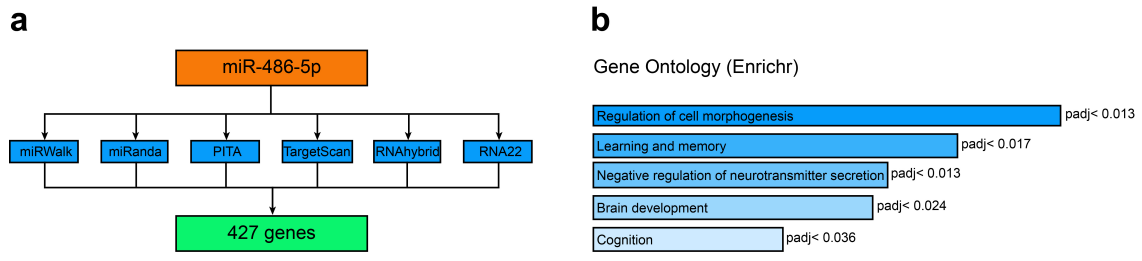
Fig. 3.13 miR-486-5p target prediction

a. Flowchart of miR-486-5p target prediction on miRWalk 2.0 website combining six different algorithms. **b.** GO term analysis of miR-486-5p predicted targets on Enrichr.

Given that during lineage differentiation miR-486-5p displayed an off-switch expression pattern, an ideal target gene, whose mRNA is subjected to miR-486-5p-mediated degradation, should show an on-switch expression in DP. To investigate whether any of the predicted targets displayed such ideal pattern, the expressions of all those targets was retrieved once again from Aprea's transcriptome sequencing of PP, DP and N. Among the predicted targets, there were six on-switch genes: the signaling molecules Itga4, Dll4 and Bmp6, the transcription factors Insm1 and Sp5 and the actin-binding protein Afap1. These findings provide an intriguing list of high-confidence predicted targets of miR-486-5p to be validated experimentally. Should any of those be revealed as a true target, it would be a remarkable indication of the role exerted by miR-486-5p in the regulation of neural progenitors fate decision.

CHAPTER 4

DISCUSSION

The timely regulation of neural progenitors switch from proliferative to differentiative divisions is a key mechanism for proper formation of the mammalian cortex. This study investigated the contribution of non-coding RNAs such as lncRNAs and miRNAs in regulating that process and set the ground for further advancements.

4.1 MIAT DELAYS NEUROGENESIS

The lncRNA Miat is expressed throughout the developing mouse central nervous system (Sone et al., 2007) and, at the peak of neurogenesis in the dorsal telencephalon, it shows an on-switch pattern with a specific up-regulation in DP (Aprea et al., 2013). Miat manipulation in the developing cortex increased the pool of BPs, which remained proliferative rather undergoing neurogenic divisions (Aprea et al., 2013). The present study showed that Miat overexpression did not prevent BPs from becoming neurogenic, but delayed the switch from proliferation to differentiation. Consequently, neurogenesis was lagged, as demonstrated by the detection of a substantial wave of neurons still migrating across the IZ at E 18.5. Since BPs were increased but not prevented from differentiating, it is reasonable to assume that neuronal output should

ultimately be increased as well. However, after 5 days of Miat manipulation, the neuronal population was still lower than in control brains. Therefore it would be interesting to assess a) whether cortical layering is affected by the delay in neurogenesis and b) if an even longer manipulation of Miat finally leads to an increase in neurons postnatally.

Mechanistically, Miat was hypothesized to influence the kinetic of splicing via sequence-specific sequestration of a fraction of the splicing factors SF1 and Celf3 (Ishizuka et al., 2014; Tsuiji et al., 2011). Notably, Miat manipulation in the developing cortex was shown to affect isoform usage of the cell-fate determinant Wnt7b (Aprea et al., 2013). Since Miat plays different roles in different cell types (i.e. regulation of neural progenitors fate and neuronal survival (Aprea et al., 2013)), a system to comprehensively unravel Miat-spliced targets at single-population level in the developing cortex was established here. This system consists in overexpressing Miat together with a BFP in $Btg2^{RFP}/Tubb3^{GFP}$ mouse embryos, followed by FAC-sorting of electroporated cell types of interest: PP (BFP+/RFP–/GFP–), DP (BFP+/RFP+/GFP–) and N (BFP+/GFP+). Despite technically challenging, this method would allow a complete investigation of the crosstalk between Miat and the splicing machinery at single-population level during cortical development. This set up was successfully applied to control brains, but encountered a technical problem with Miat samples. Despite equimolar dosage, the huge size of Miat plasmid (13Kb versus 5Kb of control) might have prevented complete degradation by DNase treatment. Plasmid fragments were efficiently amplified during library preparation, impairing transcriptome sequencing depth. Despite further tests are needed, this problem can surely be overcome by recent advancements in library preparation methods for low input material allowing poly(A) selection and

strand specificity. Moreover, third generation sequencers such as the MinION^{TM} from Oxford Nanopore Technologies, which allows long-read RNA sequencing, might drastically improve splicing analysis (Clark et al., 2018; Weirather et al., 2017), provided that kits for low-input RNA will be developed.

4.2 miRNA EXPRESSION ATLAS OF CORTICAL PROGENITORS AND NEURONS

Ever since the discovery that miRNAs are fundamental gene expression regulators (Bartel, 2004), great efforts were made to assemble an atlas of miRNAs expressed during brain development. The number of miRNAs detected in the developing mouse brain steadily increased during the microarray era (Krichevsky et al., 2003; Miska et al., 2004; Nielsen et al., 2009; Sempere et al., 2004) and even more with the advent of next-generation sequencing (Derrien et al., 2012; Ling et al., 2011). However, all those studies were performed on whole brain lysates or large brain portions, thus lacking cell-type specificity. Here, the Btg2^{RFP}/Tubb3^{GFP} mouse line, which allows efficient separation of PP, DP and N during cortical development, was used to generate an accurate catalogue of cortical miRNAs at single-population level. Considering that single-cell sequencing of small RNAs is currently hindered by two major technical limitations a) drop-seq is applicable only for poly(A)-RNAs and b) library preparations with <1000 cells display poor coverage (Faridani et al., 2016), the datasets presented in this work of thesis represent a state-of-the-art resource for cortical miRNAs studies. In addition to that, novel miRNA prediction did not result in the experimental detection of any mature miRNA, thus implying that

the atlas is complete. This conclusion is in line with other reports suggesting that the very vast majority of mouse miRNAs was already cataloged (de Rie et al., 2017).

General analyses revealed an increase in the number of miRNAs expressed along with lineage differentiation. Interestingly, in all three cell types, intergenic miRNAs showed a significantly higher median expression compared to intragenic and multi-locus miRNAs. Among the possibilities explaining this observation there are a) different regulation at genomic locus level, b) higher stability of intergenic pri-miRNA and c) higher processing efficiency of intergenic miRNAs precursors. The latter two options are relatively likely scenarios considering that transcription of intergenic miRNAs is mainly carried out by RNA polymerase II, resulting in stable 5'-capped and 3'-poly(A) pri-miRNAs. On the contrary, intragenic miRNAs are processed from introns/exons of longer transcripts that are spliced out and (partially) escape degradation by folding into atypical pre-miRNAs. Moreover, those pre-miRNAs are often processed in a Drosha-independent fashion, which might result in the lack of the staggered cut and, consequently, in suboptimal Dicer recognition efficiency.

Cell-type specific comparisons revealed that differential miRNA expression is a belittled event during lineage differentiation, with only 20% of miRNAs showing a significant up- or down-regulation in either transition PP-DP or DP-N. This relatively low percentage of differentially expressed miRNAs is not entirely surprising as also only 34% of longer transcripts were reported to be differentially expressed during lineage differentiation (Aprea et al., 2013). Moreover, the magnitude (i.e. $\log_2$ fold change) of miRNA differential expression between one population and the parental one positively correlated with the

magnitude of the host or closest gene (for intragenic and intergenic miRNA, respectively). This positive correlation suggests that differential expression is regulated at genomic locus, rather than for every single transcript. This hypothesis is supported by the fact that also circular RNAs positively correlate with their host gene (Dori et al., In revision) and so do lncRNAs, even when located 100 Kb far away from the closest gene (Aprea et al., 2015, 2013).

That positive correlation was observed also for the most underrepresented group of differentially expressed miRNAs: switch miRNAs. Those miRNAs showed a specific up- or down-regulation in the population of DP, a pattern previously linked with functional roles in neural progenitors fate decision for protein-coding and long non-coding transcripts (Aprea et al., 2013; Artegiani et al., 2015). Two of the four switch miRNAs detected here, let-7b and miR-135a-2 were reported to play roles in neural progenitors commitment by targeting the Tlx and Wnt/ß-catenin pathway, respectively (Caronia-Brown et al., 2016; Zhao et al., 2010). Interestingly, miR-135a-2 and its host gene, the lncRNA Rmst, not only share genomic locus and expression pattern, but also they are involved in the same biological process. In fact, they both regulate neural progenitors proliferation by mediating Wnt/β-catenin pathway and Sox2 functions, respectively (Caronia-Brown et al., 2016; Ng et al., 2013). Consequently, it would be interesting to assess whether AC162302.2, the predicted lncRNA hosting let-7b, also plays a role in the regulation of neural progenitors fate decision.

4.3 miR-486 AS A NOVEL REGULATORS OF CORTICOGENESIS

Other two switch miRNAs were detected here: miR-486a-5p and miR-486b-5p. Those miRNAs are transcribed as two independent precursors on different strands of the same locus on chromosome 8 and are eventually processed into the same mature sequence (here referred to as miR-486-5p). miR-486-5p was initially regarded as a master regulator of myoblast differentiation (Dey et al., 2011) and only recently appointed as counteracting olfactory epithelium neurogenesis (Kurtenbach et al., 2017) and spinal cord regeneration after injury (Jee et al., 2012). Here, a novel role of miR-486-5p as a regulator of neural progenitors fate during cortical development was described through its inhibition by a specific antisense oligonucleotide (LNA-486). *In vitro*, LNA-486 showed a 40% silencing efficacy, a decent effect considering that a) miR-486-5p was artificially overexpressed in N2a cells and b) a similar efficacy was reported for other LNAs (Ghosh et al., 2014). *In vivo*, miR-486-5p inhibition increased the pool of neural progenitors at the expense of newborn neurons. The lack of neurons reaching the CP was neither due to apoptosis nor to defects in migration. Moreover, the fraction of progenitors actively cycling was unchanged upon LNA-486 electroporation. These observations point against an effect on cell cycle and rather suggest that miR-486-5p plays an important role in neural progenitors fate decision. To investigate that, it would be interesting to silence miR-486-5p in Btg2^{RFP} embryos and assess the proportion of electroporated progenitors that "switch on" the pro-differentiation factor Btg2. Ultimately, considering that cell fate determinants such as Itga4, Dll4, Bmp6, Insm1 and Sp5 are among high-confidence miR-486-5p predicted targets, *in vitro* validation

by luciferase assays, combined with *in vivo* manipulation by IUE of some of those targets might clarify which genes and pathways miR-486-5p fine-tunes.

4.4 FUTURE OUTLOOK

Non-coding RNAs started to be considered critical players in neural progenitors fate decision only in the last two decades. In this context, this study extended previous knowledge of the lncRNA Miat as a regulator of neural progenitors proliferation versus differentiation. In the next years it will be possible to dissect the crosstalk between Miat and the splicing machinery at single-population level in the developing cortex, finally clarifying Miat developmental role.

Moreover, the catalog of cortical miRNAs generated here provides the field with an accurate resource for the detection of new miRNAs playing a role during corticogenesis. Importantly, the transcriptome of PP, DP and N is also publicly available to facilitate the identification and validation of miRNA targets.

REFERENCES

Aaku-Saraste, E., Hellwig, A., Huttner, W.B., 1996. Loss of occludin and functional tight junctions, but not ZO-1, during neural tube closure--remodeling of the neuroepithelium prior to neurogenesis. Dev. Biol. 180, 664–679. https://doi.org/10.1006/dbio.1996.0336

Alberts, B., Johnson, A., Lewis, J., Morgan, D., Raff, M., Roberts, K., Walter, P., 2014. Molecular Biology of the Cell, 6th ed. Garland Science.

Ambros, V., Bartel, B., Bartel, D.P., Burge, C.B., Carrington, J.C., Chen, X., Dreyfuss, G., Eddy, S.R., Griffiths-Jones, S., Marshall, M., Matzke, M., Ruvkun, G., Tuschl, T., 2003. A uniform system for microRNA annotation. RNA N. Y. N 9, 277–279.

Aprea, J., 2014. Novel factors regulating progenitor cells fate in the developing mouse cerebral cortex.

Aprea, J., Calegari, F., 2015. Long non-coding RNAs in corticogenesis: deciphering the non-coding code of the brain. EMBO J. 34, 2865–2884. https://doi.org/10.15252/embj.201592655

Aprea, J., Lesche, M., Massalini, S., Prenninger, S., Alexopoulou, D., Dahl, A., Hiller, M., Calegari, F., 2015. Identification and expression patterns of novel long non-coding RNAs in neural progenitors of the developing mammalian cortex. Neurogenesis Austin Tex 2, e995524. https://doi.org/10.1080/23262133.2014.995524

Aprea, J., Prenninger, S., Dori, M., Ghosh, T., Monasor, L.S., Wessendorf, E., Zocher, S., Massalini, S., Alexopoulou, D., Lesche, M., Dahl, A., Groszer, M., Hiller, M., Calegari, F., 2013. Transcriptome sequencing during mouse brain development identifies long non-coding RNAs functionally involved in neurogenic commitment. EMBO J. 32, 3145–3160. https://doi.org/10.1038/emboj.2013.245

Arslan, S., Berkan, Ö., Lalem, T., Özbilüm, N., Göksel, S., Korkmaz, Ö., Çetin, N., Devaux, Y., Cardiolinc[TM] network, 2017. Long non-coding RNAs in the atherosclerotic plaque. Atherosclerosis 266, 176–181. https://doi.org/10.1016/j.atherosclerosis.2017.10.012

Artegiani, B., de Jesus Domingues, A.M., Bragado Alonso, S., Brandl, E., Massalini, S., Dahl, A., Calegari, F., 2015. Tox: a multifunctional

transcription factor and novel regulator of mammalian corticogenesis. EMBO J. 34, 896–910. https://doi.org/10.15252/embj.201490061

Artegiani, B., Lange, C., Calegari, F., 2012. Expansion of embryonic and adult neural stem cells by in utero electroporation or viral stereotaxic injection. J. Vis. Exp. JoVE. https://doi.org/10.3791/4093

Attardo, A., Calegari, F., Haubensak, W., Wilsch-Bräuninger, M., Huttner, W.B., 2008. Live imaging at the onset of cortical neurogenesis reveals differential appearance of the neuronal phenotype in apical versus basal progenitor progeny. PloS One 3, e2388. https://doi.org/10.1371/journal.pone.0002388

Babiarz, J.E., Hsu, R., Melton, C., Thomas, M., Ullian, E.M., Blelloch, R., 2011. A role for noncanonical microRNAs in the mammalian brain revealed by phenotypic differences in Dgcr8 versus Dicer1 knockouts and small RNA sequencing. RNA N. Y. N 17, 1489–1501. https://doi.org/10.1261/rna.2442211

Bagga, S., Bracht, J., Hunter, S., Massirer, K., Holtz, J., Eachus, R., Pasquinelli, A.E., 2005. Regulation by let-7 and lin-4 miRNAs results in target mRNA degradation. Cell 122, 553–563. https://doi.org/10.1016/j.cell.2005.07.031

Barca-Mayo, O., De Pietri Tonelli, D., 2014. Convergent microRNA actions coordinate neocortical development. Cell. Mol. Life Sci. CMLS 71, 2975–2995. https://doi.org/10.1007/s00018-014-1576-5

Barry, G., Briggs, J.A., Vanichkina, D.P., Poth, E.M., Beveridge, N.J., Ratnu, V.S., Nayler, S.P., Nones, K., Hu, J., Bredy, T.W., Nakagawa, S., Rigo, F., Taft, R.J., Cairns, M.J., Blackshaw, S., Wolvetang, E.J., Mattick, J.S., 2014. The long non-coding RNA Gomafu is acutely regulated in response to neuronal activation and involved in schizophrenia-associated alternative splicing. Mol. Psychiatry 19, 486–494. https://doi.org/10.1038/mp.2013.45

Bartel, D.P., 2004. MicroRNAs: genomics, biogenesis, mechanism, and function. Cell 116, 281–297.

Behm-Ansmant, I., Rehwinkel, J., Doerks, T., Stark, A., Bork, P., Izaurralde, E., 2006. mRNA degradation by miRNAs and GW182 requires both CCR4:NOT deadenylase and DCP1:DCP2 decapping complexes. Genes Dev. 20, 1885–1898. https://doi.org/10.1101/gad.1424106

Berezikov, E., Chung, W.-J., Willis, J., Cuppen, E., Lai, E.C., 2007. Mammalian mirtron genes. Mol. Cell 28, 328–336. https://doi.org/10.1016/j.molcel.2007.09.028

Bernstein, E., Kim, S.Y., Carmell, M.A., Murchison, E.P., Alcorn, H., Li, M.Z., Mills, A.A., Elledge, S.J., Anderson, K.V., Hannon, G.J., 2003. Dicer is

essential for mouse development. Nat. Genet. 35, 215–217. https://doi.org/10.1038/ng1253

Bian, S., Hong, J., Li, Q., Schebelle, L., Pollock, A., Knauss, J.L., Garg, V., Sun, T., 2013. MicroRNA cluster miR-17-92 regulates neural stem cell expansion and transition to intermediate progenitors in the developing mouse neocortex. Cell Rep. 3, 1398–1406. https://doi.org/10.1016/j.celrep.2013.03.037

Blackshaw, S., Harpavat, S., Trimarchi, J., Cai, L., Huang, H., Kuo, W.P., Weber, G., Lee, K., Fraioli, R.E., Cho, S.-H., Yung, R., Asch, E., Ohno-Machado, L., Wong, W.H., Cepko, C.L., 2004. Genomic analysis of mouse retinal development. PLoS Biol. 2, E247. https://doi.org/10.1371/journal.pbio.0020247

Boulder Committee, 1970. Embryonic vertebrate central nervous system: revised terminology. Anat. Rec. 166, 257–261. https://doi.org/10.1002/ar.1091660214

Cabili, M.N., Dunagin, M.C., McClanahan, P.D., Biaesch, A., Padovan-Merhar, O., Regev, A., Rinn, J.L., Raj, A., 2015. Localization and abundance analysis of human lncRNAs at single-cell and single-molecule resolution. Genome Biol. 16, 20. https://doi.org/10.1186/s13059-015-0586-4

Cabili, M.N., Trapnell, C., Goff, L., Koziol, M., Tazon-Vega, B., Regev, A., Rinn, J.L., 2011. Integrative annotation of human large intergenic noncoding RNAs reveals global properties and specific subclasses. Genes Dev. 25, 1915–1927. https://doi.org/10.1101/gad.17446611

Cai, X., Hagedorn, C.H., Cullen, B.R., 2004. Human microRNAs are processed from capped, polyadenylated transcripts that can also function as mRNAs. RNA N. Y. N 10, 1957–1966. https://doi.org/10.1261/rna.7135204

Caronia-Brown, G., Anderegg, A., Awatramani, R., 2016. Expression and functional analysis of the Wnt/beta-catenin induced mir-135a-2 locus in embryonic forebrain development. Neural Develop. 11, 9. https://doi.org/10.1186/s13064-016-0065-y

Carthew, R.W., Sontheimer, E.J., 2009. Origins and Mechanisms of miRNAs and siRNAs. Cell 136, 642–655. https://doi.org/10.1016/j.cell.2009.01.035

Cheloufi, S., Dos Santos, C.O., Chong, M.M.W., Hannon, G.J., 2010. A dicer-independent miRNA biogenesis pathway that requires Ago catalysis. Nature 465, 584–589. https://doi.org/10.1038/nature09092

Chendrimada, T.P., Finn, K.J., Ji, X., Baillat, D., Gregory, R.I., Liebhaber, S.A., Pasquinelli, A.E., Shiekhattar, R., 2007. MicroRNA silencing through RISC recruitment of eIF6. Nature 447, 823–828. https://doi.org/10.1038/nature05841

REFERENCES

Chen, E.Y., Tan, C.M., Kou, Y., Duan, Q., Wang, Z., Meirelles, G.V., Clark, N.R., Ma'ayan, A., 2013. Enrichr: interactive and collaborative HTML5 gene list enrichment analysis tool. BMC Bioinformatics 14, 128. https://doi.org/10.1186/1471-2105-14-128

Chong, M.M.W., Rasmussen, J.P., Rudensky, A.Y., Rundensky, A.Y., Littman, D.R., 2008. The RNAseIII enzyme Drosha is critical in T cells for preventing lethal inflammatory disease. J. Exp. Med. 205, 2005–2017. https://doi.org/10.1084/jem.20081219

Church, D.M., Goodstadt, L., Hillier, L.W., Zody, M.C., Goldstein, S., She, X., Bult, C.J., Agarwala, R., Cherry, J.L., DiCuccio, M., Hlavina, W., Kapustin, Y., Meric, P., Maglott, D., Birtle, Z., Marques, A.C., Graves, T., Zhou, S., Teague, B., Potamousis, K., Churas, C., Place, M., Herschleb, J., Runnheim, R., Forrest, D., Amos-Landgraf, J., Schwartz, D.C., Cheng, Z., Lindblad-Toh, K., Eichler, E.E., Ponting, C.P., Mouse Genome Sequencing Consortium, 2009. Lineage-specific biology revealed by a finished genome assembly of the mouse. PLoS Biol. 7, e1000112. https://doi.org/10.1371/journal.pbio.1000112

Cifuentes, D., Xue, H., Taylor, D.W., Patnode, H., Mishima, Y., Cheloufi, S., Ma, E., Mane, S., Hannon, G.J., Lawson, N.D., Wolfe, S.A., Giraldez, A.J., 2010. A novel miRNA processing pathway independent of Dicer requires Argonaute2 catalytic activity. Science 328, 1694–1698. https://doi.org/10.1126/science.1190809

Clark, M., Wrzesinski, T., Garcia-Bea, A., Kleinman, J., Hyde, T., Weinberger, D., Haerty, W., Tunbridge, E., 2018. Long-read sequencing reveals the splicing profile of the calcium channel gene CACNA1C in human brain. bioRxiv 260562. https://doi.org/10.1101/260562

Conaco, C., Otto, S., Han, J.-J., Mandel, G., 2006. Reciprocal actions of REST and a microRNA promote neuronal identity. Proc. Natl. Acad. Sci. U. S. A. 103, 2422–2427. https://doi.org/10.1073/pnas.0511041103

Custo Greig, L.F., Woodworth, M.B., Galazo, M.J., Padmanabhan, H., Macklis, J.D., 2013. Molecular logic of neocortical projection neuron specification, development and diversity. Nat. Rev. Neurosci. 14, 755–769. https://doi.org/10.1038/nrn3586

Davis, T.H., Cuellar, T.L., Koch, S.M., Barker, A.J., Harfe, B.D., McManus, M.T., Ullian, E.M., 2008. Conditional loss of Dicer disrupts cellular and tissue morphogenesis in the cortex and hippocampus. J. Neurosci. Off. J. Soc. Neurosci. 28, 4322–4330. https://doi.org/10.1523/JNEUROSCI.4815-07.2008

Del Bene, F., Wehman, A.M., Link, B.A., Baier, H., 2008. Regulation of neurogenesis by interkinetic nuclear migration through an apical-basal

notch gradient. Cell 134, 1055–1065. https://doi.org/10.1016/j.cell.2008.07.017

De Rie, D., Abugessaisa, I., Alam, T., Arner, E., Arner, P., Ashoor, H., Åström, G., Babina, M., Bertin, N., Burroughs, A.M., Carlisle, A.J., Daub, C.O., Detmar, M., Deviatiiarov, R., Fort, A., Gebhard, C., Goldowitz, D., Guhl, S., Ha, T.J., Harshbarger, J., Hasegawa, A., Hashimoto, K., Herlyn, M., Heutink, P., Hitchens, K.J., Hon, C.C., Huang, E., Ishizu, Y., Kai, C., Kasukawa, T., Klinken, P., Lassmann, T., Lecellier, C.-H., Lee, W., Lizio, M., Makeev, V., Mathelier, A., Medvedeva, Y.A., Mejhert, N., Mungall, C.J., Noma, S., Ohshima, M., Okada-Hatakeyama, M., Persson, H., Rizzu, P., Roudnicky, F., Sætrom, P., Sato, H., Severin, J., Shin, J.W., Swoboda, R.K., Tarui, H., Toyoda, H., Vitting-Seerup, K., Winteringham, L., Yamaguchi, Y., Yasuzawa, K., Yoneda, M., Yumoto, N., Zabierowski, S., Zhang, P.G., Wells, C.A., Summers, K.M., Kawaji, H., Sandelin, A., Rehli, M., Hayashizaki, Y., Carninci, P., Forrest, A.R.R., de Hoon, M.J.L., 2017. An integrated expression atlas of miRNAs and their promoters in human and mouse. Nat. Biotechnol. 35, 872–878. https://doi.org/10.1038/nbt.3947

Derrien, T., Johnson, R., Bussotti, G., Tanzer, A., Djebali, S., Tilgner, H., Guernec, G., Martin, D., Merkel, A., Knowles, D.G., Lagarde, J., Veeravalli, L., Ruan, X., Ruan, Y., Lassmann, T., Carninci, P., Brown, J.B., Lipovich, L., Gonzalez, J.M., Thomas, M., Davis, C.A., Shiekhattar, R., Gingeras, T.R., Hubbard, T.J., Notredame, C., Harrow, J., Guigó, R., 2012. The GENCODE v7 catalog of human long noncoding RNAs: analysis of their gene structure, evolution, and expression. Genome Res. 22, 1775–1789. https://doi.org/10.1101/gr.132159.111

Dey, B.K., Gagan, J., Dutta, A., 2011. miR-206 and -486 Induce Myoblast Differentiation by Downregulating Pax7. Mol. Cell. Biol. 31, 203–214. https://doi.org/10.1128/MCB.01009-10

Diez-Roux, G., Banfi, S., Sultan, M., Geffers, L., Anand, S., Rozado, D., Magen, A., Canidio, E., Pagani, M., Peluso, I., Lin-Marq, N., Koch, M., Bilio, M., Cantiello, I., Verde, R., De Masi, C., Bianchi, S.A., Cicchini, J., Perroud, E., Mehmeti, S., Dagand, E., Schrinner, S., Nürnberger, A., Schmidt, K., Metz, K., Zwingmann, C., Brieske, N., Springer, C., Hernandez, A.M., Herzog, S., Grabbe, F., Sieverding, C., Fischer, B., Schrader, K., Brockmeyer, M., Dettmer, S., Helbig, C., Alunni, V., Battaini, M.-A., Mura, C., Henrichsen, C.N., Garcia-Lopez, R., Echevarria, D., Puelles, E., Garcia-Calero, E., Kruse, S., Uhr, M., Kauck, C., Feng, G., Milyaev, N., Ong, C.K., Kumar, L., Lam, M., Semple, C.A., Gyenesei, A., Mundlos, S., Radelof, U., Lehrach, H., Sarmientos,

P., Reymond, A., Davidson, D.R., Dollé, P., Antonarakis, S.E., Yaspo, M.-L., Martinez, S., Baldock, R.A., Eichele, G., Ballabio, A., 2011. A high-resolution anatomical atlas of the transcriptome in the mouse embryo. PLoS Biol. 9, e1000582. https://doi.org/10.1371/journal.pbio.1000582

Djebali, S., Davis, C.A., Merkel, A., Dobin, A., Lassmann, T., Mortazavi, A., Tanzer, A., Lagarde, J., Lin, W., Schlesinger, F., Xue, C., Marinov, G.K., Khatun, J., Williams, B.A., Zaleski, C., Rozowsky, J., Röder, M., Kokocinski, F., Abdelhamid, R.F., Alioto, T., Antoshechkin, I., Baer, M.T., Bar, N.S., Batut, P., Bell, K., Bell, I., Chakrabortty, S., Chen, X., Chrast, J., Curado, J., Derrien, T., Drenkow, J., Dumais, E., Dumais, J., Duttagupta, R., Falconnet, E., Fastuca, M., Fejes-Toth, K., Ferreira, P., Foissac, S., Fullwood, M.J., Gao, H., Gonzalez, D., Gordon, A., Gunawardena, H., Howald, C., Jha, S., Johnson, R., Kapranov, P., King, B., Kingswood, C., Luo, O.J., Park, E., Persaud, K., Preall, J.B., Ribeca, P., Risk, B., Robyr, D., Sammeth, M., Schaffer, L., See, L.-H., Shahab, A., Skancke, J., Suzuki, A.M., Takahashi, H., Tilgner, H., Trout, D., Walters, N., Wang, H., Wrobel, J., Yu, Y., Ruan, X., Hayashizaki, Y., Harrow, J., Gerstein, M., Hubbard, T., Reymond, A., Antonarakis, S.E., Hannon, G., Giddings, M.C., Ruan, Y., Wold, B., Carninci, P., Guigó, R., Gingeras, T.R., 2012. Landscape of transcription in human cells. Nature 489, 101–108. https://doi.org/10.1038/nature11233

Dori, M., Abdullah Alieh, L.H., Cavalli, D., Massalini, S., Lesche, M., Dahl, A., Calegari, F., In revision. Comprehensive Assessment of Sequence and Expression of Circular-RNAs in Progenitor Cell Types of the Developing Mammalian Cortex.

Dweep, H., Gretz, N., 2015. miRWalk2.0: a comprehensive atlas of microRNA-target interactions. Nat. Methods 12, 697. https://doi.org/10.1038/nmeth.3485

Dweep, H., Sticht, C., Pandey, P., Gretz, N., 2011. miRWalk--database: prediction of possible miRNA binding sites by "walking" the genes of three genomes. J. Biomed. Inform. 44, 839–847. https://doi.org/10.1016/j.jbi.2011.05.002

Ebisuya, M., Yamamoto, T., Nakajima, M., Nishida, E., 2008. Ripples from neighbouring transcription. Nat. Cell Biol. 10, 1106–1113. https://doi.org/10.1038/ncb1771

ENCODE Project Consortium, 2012. An integrated encyclopedia of DNA elements in the human genome. Nature 489, 54–74. https://doi.org/10.1038/nature11247

Englund, C., Fink, A., Lau, C., Pham, D., Daza, R.A.M., Bulfone, A., Kowalczyk, T., Hevner, R.F., 2005. Pax6, Tbr2, and Tbr1 are expressed sequentially by radial glia, intermediate progenitor cells, and postmitotic neurons in developing neocortex. J. Neurosci. Off. J. Soc. Neurosci. 25, 247–251. https://doi.org/10.1523/JNEUROSCI.2899-04.2005

Erickson, C.A., Weston, J.A., 1983. An SEM analysis of neural crest migration in the mouse. J. Embryol. Exp. Morphol. 74, 97–118.

Faridani, O.R., Abdullayev, I., Hagemann-Jensen, M., Schell, J.P., Lanner, F., Sandberg, R., 2016. Single-cell sequencing of the small-RNA transcriptome. Nat. Biotechnol. 34, 1264–1266. https://doi.org/10.1038/nbt.3701

Fei, J.-F., Haffner, C., Huttner, W.B., 2014. 3' UTR-dependent, miR-92-mediated restriction of Tis21 expression maintains asymmetric neural stem cell division to ensure proper neocortex size. Cell Rep. 7, 398–411. https://doi.org/10.1016/j.celrep.2014.03.033

Feng, L., Hatten, M.E., Heintz, N., 1994. Brain lipid-binding protein (BLBP): a novel signaling system in the developing mammalian CNS. Neuron 12, 895–908.

Fietz, S.A., Lachmann, R., Brandl, H., Kircher, M., Samusik, N., Schröder, R., Lakshmanaperumal, N., Henry, I., Vogt, J., Riehn, A., Distler, W., Nitsch, R., Enard, W., Pääbo, S., Huttner, W.B., 2012. Transcriptomes of germinal zones of human and mouse fetal neocortex suggest a role of extracellular matrix in progenitor self-renewal. Proc. Natl. Acad. Sci. U. S. A. 109, 11836–11841. https://doi.org/10.1073/pnas.1209647109

Forman, J.J., Legesse-Miller, A., Coller, H.A., 2008. A search for conserved sequences in coding regions reveals that the let-7 microRNA targets Dicer within its coding sequence. Proc. Natl. Acad. Sci. U. S. A. 105, 14879–14884. https://doi.org/10.1073/pnas.0803230105

Friedländer, M.R., Chen, W., Adamidi, C., Maaskola, J., Einspanier, R., Knespel, S., Rajewsky, N., 2008. Discovering microRNAs from deep sequencing data using miRDeep. Nat. Biotechnol. 26, 407–415. https://doi.org/10.1038/nbt1394

Friedländer, M.R., Lizano, E., Houben, A.J.S., Bezdan, D., Báñez-Coronel, M., Kudla, G., Mateu-Huertas, E., Kagerbauer, B., González, J., Chen, K.C., LeProust, E.M., Martí, E., Estivill, X., 2014. Evidence for the biogenesis of more than 1,000 novel human microRNAs. Genome Biol. 15, R57. https://doi.org/10.1186/gb-2014-15-4-r57

Gadisseux, J.F., Evrard, P., 1985. Glial-neuronal relationship in the developing central nervous system. A histochemical-electron microscope study of

REFERENCES

radial glial cell particulate glycogen in normal and reeler mice and the human fetus. Dev. Neurosci. 7, 12–32. https://doi.org/10.1159/000112273

Geisler, S., Coller, J., 2013. RNA in unexpected places: long non-coding RNA functions in diverse cellular contexts. Nat. Rev. Mol. Cell Biol. 14, 699–712. https://doi.org/10.1038/nrm3679

Ghosh, T., Aprea, J., Nardelli, J., Engel, H., Selinger, C., Mombereau, C., Lemonnier, T., Moutkine, I., Schwendimann, L., Dori, M., Irinopoulou, T., Henrion-Caude, A., Benecke, A.G., Arnold, S.J., Gressens, P., Calegari, F., Groszer, M., 2014. MicroRNAs establish robustness and adaptability of a critical gene network to regulate progenitor fate decisions during cortical neurogenesis. Cell Rep. 7, 1779–1788. https://doi.org/10.1016/j.celrep.2014.05.029

Gilbert, S.F., 2000. Developmental Biology, 6th ed. Sinauer Associates.

Giraldez, A.J., Mishima, Y., Rihel, J., Grocock, R.J., Van Dongen, S., Inoue, K., Enright, A.J., Schier, A.F., 2006. Zebrafish MiR-430 promotes deadenylation and clearance of maternal mRNAs. Science 312, 75–79. https://doi.org/10.1126/science.1122689

Golden, J.A., Chernoff, G.F., 1993. Intermittent pattern of neural tube closure in two strains of mice. Teratology 47, 73–80. https://doi.org/10.1002/tera.1420470112

Götz, M., Huttner, W.B., 2005. The cell biology of neurogenesis. Nat. Rev. Mol. Cell Biol. 6, 777–788. https://doi.org/10.1038/nrm1739

Grewal, S.I.S., Elgin, S.C.R., 2007. Transcription and RNA interference in the formation of heterochromatin. Nature 447, 399–406. https://doi.org/10.1038/nature05914

Han, J., Lee, Y., Yeom, K.-H., Nam, J.-W., Heo, I., Rhee, J.-K., Sohn, S.Y., Cho, Y., Zhang, B.-T., Kim, V.N., 2006. Molecular basis for the recognition of primary microRNAs by the Drosha-DGCR8 complex. Cell 125, 887–901. https://doi.org/10.1016/j.cell.2006.03.043

Haubensak, W., Attardo, A., Denk, W., Huttner, W.B., 2004. Neurons arise in the basal neuroepithelium of the early mammalian telencephalon: a major site of neurogenesis. Proc. Natl. Acad. Sci. U. S. A. 101, 3196–3201. https://doi.org/10.1073/pnas.0308600100

Hirabayashi, Y., Gotoh, Y., 2010. Epigenetic control of neural precursor cell fate during development. Nat. Rev. Neurosci. 11, 377–388. https://doi.org/10.1038/nrn2810

His W., 1889. Die Neuroblasten und deren Entstehung im embryonalen Mark. Abh Kgl Sachs Ges Wissensch Math Phys Kl 15, 313–372.

Humphreys, D.T., Westman, B.J., Martin, D.I.K., Preiss, T., 2005. MicroRNAs control translation initiation by inhibiting eukaryotic initiation factor

4E/cap and poly(A) tail function. Proc. Natl. Acad. Sci. U. S. A. 102, 16961–16966. https://doi.org/10.1073/pnas.0506482102

Iacopetti, P., Michelini, M., Stuckmann, I., Oback, B., Aaku-Saraste, E., Huttner, W.B., 1999. Expression of the antiproliferative gene TIS21 at the onset of neurogenesis identifies single neuroepithelial cells that switch from proliferative to neuron-generating division. Proc. Natl. Acad. Sci. U. S. A. 96, 4639–4644.

Ilott, N.E., Ponting, C.P., 2013. Predicting long non-coding RNAs using RNA sequencing. Methods San Diego Calif 63, 50–59. https://doi.org/10.1016/j.ymeth.2013.03.019

Ishii, N., Ozaki, K., Sato, H., Mizuno, H., Saito, S., Takahashi, A., Miyamoto, Y., Ikegawa, S., Kamatani, N., Hori, M., Saito, S., Nakamura, Y., Tanaka, T., 2006. Identification of a novel non-coding RNA, MIAT, that confers risk of myocardial infarction. J. Hum. Genet. 51, 1087–1099. https://doi.org/10.1007/s10038-006-0070-9

Ishizuka, A., Hasegawa, Y., Ishida, K., Yanaka, K., Nakagawa, S., 2014. Formation of nuclear bodies by the lncRNA Gomafu-associating proteins Celf3 and SF1. Genes Cells Devoted Mol. Cell. Mech. 19, 704–721. https://doi.org/10.1111/gtc.12169

Jee, M.K., Jung, J.S., Choi, J.I., Jang, J.A., Kang, K.S., Im, Y.B., Kang, S.K., 2012. MicroRNA 486 is a potentially novel target for the treatment of spinal cord injury. Brain J. Neurol. 135, 1237–1252. https://doi.org/10.1093/brain/aws047

Jiang, Q., Shan, K., Qun-Wang, X., Zhou, R.-M., Yang, H., Liu, C., Li, Y.-J., Yao, J., Li, X.-M., Shen, Y., Cheng, H., Yuan, J., Zhang, Y.-Y., Yan, B., 2016. Long non-coding RNA-MIAT promotes neurovascular remodeling in the eye and brain. Oncotarget 7, 49688–49698. https://doi.org/10.18632/oncotarget.10434

Kamei, Y., Inagaki, N., Nishizawa, M., Tsutsumi, O., Taketani, Y., Inagaki, M., 1998. Visualization of mitotic radial glial lineage cells in the developing rat brain by Cdc2 kinase-phosphorylated vimentin. Glia 23, 191–199.

Kawase-Koga, Y., Otaegi, G., Sun, T., 2009. Different timings of Dicer deletion affect neurogenesis and gliogenesis in the developing mouse central nervous system. Dev. Dyn. Off. Publ. Am. Assoc. Anat. 238, 2800–2812. https://doi.org/10.1002/dvdy.22109

Kim, V.N., 2005. MicroRNA biogenesis: coordinated cropping and dicing. Nat. Rev. Mol. Cell Biol. 6, 376–385. https://doi.org/10.1038/nrm1644

Kiriakidou, M., Tan, G.S., Lamprinaki, S., De Planell-Saguer, M., Nelson, P.T., Mourelatos, Z., 2007. An mRNA m7G cap binding-like motif within

human Ago2 represses translation. Cell 129, 1141–1151. https://doi.org/10.1016/j.cell.2007.05.016

Kowalczyk, M.S., Higgs, D.R., Gingeras, T.R., 2012. Molecular biology: RNA discrimination. Nature 482, 310–311. https://doi.org/10.1038/482310a

Kozomara, A., Griffiths-Jones, S., 2014. miRBase: annotating high confidence microRNAs using deep sequencing data. Nucleic Acids Res. 42, D68–73. https://doi.org/10.1093/nar/gkt1181

Krichevsky, A.M., King, K.S., Donahue, C.P., Khrapko, K., Kosik, K.S., 2003. A microRNA array reveals extensive regulation of microRNAs during brain development. RNA N. Y. N 9, 1274–1281.

Kriegstein, A., Alvarez-Buylla, A., 2009. The glial nature of embryonic and adult neural stem cells. Annu. Rev. Neurosci. 32, 149–184. https://doi.org/10.1146/annurev.neuro.051508.135600

Kriegstein, A., Noctor, S., Martínez-Cerdeño, V., 2006. Patterns of neural stem and progenitor cell division may underlie evolutionary cortical expansion. Nat. Rev. Neurosci. 7, 883–890. https://doi.org/10.1038/nrn2008

Kurtenbach, S., Ding, W., Goss, G.M., Hare, J.M., Goldstein, B.J., Shehadeh, L.A., 2017. Differential expression of microRNAs among cell populations in the regenerating adult mouse olfactory epithelium. PLoS ONE 12. https://doi.org/10.1371/journal.pone.0187576

Kwon, G.S., Hadjantonakis, A.-K., 2007. Eomes::GFP-a tool for live imaging cells of the trophoblast, primitive streak, and telencephalon in the mouse embryo. Genes. N. Y. N 2000 45, 208–217. https://doi.org/10.1002/dvg.20293

Lagos-Quintana, M., Rauhut, R., Lendeckel, W., Tuschl, T., 2001. Identification of novel genes coding for small expressed RNAs. Science 294, 853–858. https://doi.org/10.1126/science.1064921

Lagos-Quintana, M., Rauhut, R., Meyer, J., Borkhardt, A., Tuschl, T., 2003. New microRNAs from mouse and human. RNA N. Y. N 9, 175–179.

Lagos-Quintana, M., Rauhut, R., Yalcin, A., Meyer, J., Lendeckel, W., Tuschl, T., 2002. Identification of tissue-specific microRNAs from mouse. Curr. Biol. CB 12, 735–739.

Laguesse, S., Creppe, C., Nedialkova, D.D., Prévot, P.-P., Borgs, L., Huysseune, S., Franco, B., Duysens, G., Krusy, N., Lee, G., Thelen, N., Thiry, M., Close, P., Chariot, A., Malgrange, B., Leidel, S.A., Godin, J.D., Nguyen, L., 2015. A Dynamic Unfolded Protein Response Contributes to the Control of Cortical Neurogenesis. Dev. Cell 35, 553–567. https://doi.org/10.1016/j.devcel.2015.11.005

REFERENCES

LaMonica, B.E., Lui, J.H., Hansen, D.V., Kriegstein, A.R., 2013. Mitotic spindle orientation predicts outer radial glial cell generation in human neocortex. Nat. Commun. 4, 1665. https://doi.org/10.1038/ncomms2647

Laneve, P., Gioia, U., Andriotto, A., Moretti, F., Bozzoni, I., Caffarelli, E., 2010. A minicircuitry involving REST and CREB controls miR-9-2 expression during human neuronal differentiation. Nucleic Acids Res. 38, 6895–6905. https://doi.org/10.1093/nar/gkq604

Lange, C., Huttner, W.B., Calegari, F., 2009. Cdk4/cyclinD1 overexpression in neural stem cells shortens G1, delays neurogenesis, and promotes the generation and expansion of basal progenitors. Cell Stem Cell 5, 320–331. https://doi.org/10.1016/j.stem.2009.05.026

Langford, C.J., Klinz, F.J., Donath, C., Gallwitz, D., 1984. Point mutations identify the conserved, intron-contained TACTAAC box as an essential splicing signal sequence in yeast. Cell 36, 645–653.

Lau, N.C., Lim, L.P., Weinstein, E.G., Bartel, D.P., 2001. An abundant class of tiny RNAs with probable regulatory roles in Caenorhabditis elegans. Science 294, 858–862. https://doi.org/10.1126/science.1065062

Lee, R.C., Ambros, V., 2001. An extensive class of small RNAs in Caenorhabditis elegans. Science 294, 862–864. https://doi.org/10.1126/science.1065329

Lee, R.C., Feinbaum, R.L., Ambros, V., 1993. The C. elegans heterochronic gene lin-4 encodes small RNAs with antisense complementarity to lin-14. Cell 75, 843–854.

Lee, Y., Kim, M., Han, J., Yeom, K.-H., Lee, S., Baek, S.H., Kim, V.N., 2004. MicroRNA genes are transcribed by RNA polymerase II. EMBO J. 23, 4051–4060. https://doi.org/10.1038/sj.emboj.7600385

Levitt, P., Cooper, M.L., Rakic, P., 1981. Coexistence of neuronal and glial precursor cells in the cerebral ventricular zone of the fetal monkey: an ultrastructural immunoperoxidase analysis. J. Neurosci. Off. J. Soc. Neurosci. 1, 27–39.

Liao, Y., Smyth, G.K., Shi, W., 2014. featureCounts: an efficient general purpose program for assigning sequence reads to genomic features. Bioinforma. Oxf. Engl. 30, 923–930. https://doi.org/10.1093/bioinformatics/btt656

Liem, K.F., Tremml, G., Roelink, H., Jessell, T.M., 1995. Dorsal differentiation of neural plate cells induced by BMP-mediated signals from epidermal ectoderm. Cell 82, 969–979.

Lim, L.P., Lau, N.C., Garrett-Engele, P., Grimson, A., Schelter, J.M., Castle, J., Bartel, D.P., Linsley, P.S., Johnson, J.M., 2005. Microarray analysis

shows that some microRNAs downregulate large numbers of target mRNAs. Nature 433, 769–773. https://doi.org/10.1038/nature03315

Ling, K.-H., Brautigan, P.J., Hahn, C.N., Daish, T., Rayner, J.R., Cheah, P.-S., Raison, J.M., Piltz, S., Mann, J.R., Mattiske, D.M., Thomas, P.Q., Adelson, D.L., Scott, H.S., 2011. Deep sequencing analysis of the developing mouse brain reveals a novel microRNA. BMC Genomics 12, 176. https://doi.org/10.1186/1471-2164-12-176

Li, N., You, X., Chen, T., Mackowiak, S.D., Friedländer, M.R., Weigt, M., Du, H., Gogol-Döring, A., Chang, Z., Dieterich, C., Hu, Y., Chen, W., 2013. Global profiling of miRNAs and the hairpin precursors: insights into miRNA processing and novel miRNA discovery. Nucleic Acids Res. 41, 3619–3634. https://doi.org/10.1093/nar/gkt072

Li, Q., Lee, J.-A., Black, D.L., 2007. Neuronal regulation of alternative pre-mRNA splicing. Nat. Rev. Neurosci. 8, 819–831. https://doi.org/10.1038/nrn2237

Liu, A., Niswander, L.A., 2005. Bone morphogenetic protein signalling and vertebrate nervous system development. Nat. Rev. Neurosci. 6, 945–954. https://doi.org/10.1038/nrn1805

Liu, J., Rivas, F.V., Wohlschlegel, J., Yates, J.R., Parker, R., Hannon, G.J., 2005. A role for the P-body component GW182 in microRNA function. Nat. Cell Biol. 7, 1261–1266. https://doi.org/10.1038/ncb1333

Livak, K.J., Schmittgen, T.D., 2001. Analysis of relative gene expression data using real-time quantitative PCR and the 2(-Delta Delta C(T)) Method. Methods San Diego Calif 25, 402–408. https://doi.org/10.1006/meth.2001.1262

Love, M.I., Huber, W., Anders, S., 2014. Moderated estimation of fold change and dispersion for RNA-seq data with DESeq2. Genome Biol. 15, 550. https://doi.org/10.1186/s13059-014-0550-8

Lytle, J.R., Yario, T.A., Steitz, J.A., 2007. Target mRNAs are repressed as efficiently by microRNA-binding sites in the 5' UTR as in the 3' UTR. Proc. Natl. Acad. Sci. U. S. A. 104, 9667–9672. https://doi.org/10.1073/pnas.0703820104

Magini J., 1888. Nouvelles recherches histologiques sur le cerveau du foetus. Arch Ital Biol 10, 384–387.

Makeyev, E.V., Zhang, J., Carrasco, M.A., Maniatis, T., 2007. The MicroRNA miR-124 promotes neuronal differentiation by triggering brain-specific alternative pre-mRNA splicing. Mol. Cell 27, 435–448. https://doi.org/10.1016/j.molcel.2007.07.015

REFERENCES

Malone, C.D., Hannon, G.J., 2009. Molecular evolution of piRNA and transposon control pathways in Drosophila. Cold Spring Harb. Symp. Quant. Biol. 74, 225–234. https://doi.org/10.1101/sqb.2009.74.052

Manabe, N., Hirai, S.-I., Imai, F., Nakanishi, H., Takai, Y., Ohno, S., 2002. Association of ASIP/mPAR-3 with adherens junctions of mouse neuroepithelial cells. Dev. Dyn. Off. Publ. Am. Assoc. Anat. 225, 61–69. https://doi.org/10.1002/dvdy.10139

Mao, S., Li, H., Sun, Q., Zen, K., Zhang, C.-Y., Li, L., 2014. miR-17 regulates the proliferation and differentiation of the neural precursor cells during mouse corticogenesis. FEBS J. 281, 1144–1158. https://doi.org/10.1111/febs.12680

Marinaro, F., Marzi, M.J., Hoffmann, N., Amin, H., Pelizzoli, R., Niola, F., Nicassio, F., De Pietri Tonelli, D., 2017. MicroRNA-independent functions of DGCR8 are essential for neocortical development and TBR1 expression. EMBO Rep. 18, 603–618. https://doi.org/10.15252/embr.201642800

Maroney, P.A., Yu, Y., Fisher, J., Nilsen, T.W., 2006. Evidence that microRNAs are associated with translating messenger RNAs in human cells. Nat. Struct. Mol. Biol. 13, 1102–1107. https://doi.org/10.1038/nsmb1174

Martynoga, B., Drechsel, D., Guillemot, F., 2012. Molecular control of neurogenesis: a view from the mammalian cerebral cortex. Cold Spring Harb. Perspect. Biol. 4. https://doi.org/10.1101/cshperspect.a008359

Mathonnet, G., Fabian, M.R., Svitkin, Y.V., Parsyan, A., Huck, L., Murata, T., Biffo, S., Merrick, W.C., Darzynkiewicz, E., Pillai, R.S., Filipowicz, W., Duchaine, T.F., Sonenberg, N., 2007. MicroRNA inhibition of translation initiation in vitro by targeting the cap-binding complex eIF4F. Science 317, 1764–1767. https://doi.org/10.1126/science.1146067

Meister, G., Landthaler, M., Peters, L., Chen, P.Y., Urlaub, H., Lührmann, R., Tuschl, T., 2005. Identification of novel argonaute-associated proteins. Curr. Biol. CB 15, 2149–2155. https://doi.org/10.1016/j.cub.2005.10.048

Memczak, S., Jens, M., Elefsinioti, A., Torti, F., Krueger, J., Rybak, A., Maier, L., Mackowiak, S.D., Gregersen, L.H., Munschauer, M., Loewer, A., Ziebold, U., Landthaler, M., Kocks, C., le Noble, F., Rajewsky, N., 2013. Circular RNAs are a large class of animal RNAs with regulatory potency. Nature 495, 333–338. https://doi.org/10.1038/nature11928

Miska, E.A., Alvarez-Saavedra, E., Townsend, M., Yoshii, A., Sestan, N., Rakic, P., Constantine-Paton, M., Horvitz, H.R., 2004. Microarray analysis of microRNA expression in the developing mammalian brain. Genome Biol. 5, R68. https://doi.org/10.1186/gb-2004-5-9-r68

REFERENCES

Misson, J.P., Edwards, M.A., Yamamoto, M., Caviness, V.S., 1988. Identification of radial glial cells within the developing murine central nervous system: studies based upon a new immunohistochemical marker. Brain Res. Dev. Brain Res. 44, 95–108.

Miyata, T., Kawaguchi, A., Okano, H., Ogawa, M., 2001. Asymmetric inheritance of radial glial fibers by cortical neurons. Neuron 31, 727–741.

Miyata, T., Kawaguchi, A., Saito, K., Kawano, M., Muto, T., Ogawa, M., 2004. Asymmetric production of surface-dividing and non-surface-dividing cortical progenitor cells. Dev. Camb. Engl. 131, 3133–3145. https://doi.org/10.1242/dev.01173

Moazed, D., 2009. Small RNAs in transcriptional gene silencing and genome defence. Nature 457, 413–420. https://doi.org/10.1038/nature07756

Morita, S., Horii, T., Kimura, M., Goto, Y., Ochiya, T., Hatada, I., 2007. One Argonaute family member, Eif2c2 (Ago2), is essential for development and appears not to be involved in DNA methylation. Genomics 89, 687–696. https://doi.org/10.1016/j.ygeno.2007.01.004

Ng, S.-Y., Bogu, G.K., Soh, B.S., Stanton, L.W., 2013. The long noncoding RNA RMST interacts with SOX2 to regulate neurogenesis. Mol. Cell 51, 349–359. https://doi.org/10.1016/j.molcel.2013.07.017

Nielsen, J.A., Lau, P., Maric, D., Barker, J.L., Hudson, L.D., 2009. Integrating microRNA and mRNA expression profiles of neuronal progenitors to identify regulatory networks underlying the onset of cortical neurogenesis. BMC Neurosci. 10, 98. https://doi.org/10.1186/1471-2202-10-98

Nievelstein, R.A., Hartwig, N.G., Vermeij-Keers, C., Valk, J., 1993. Embryonic development of the mammalian caudal neural tube. Teratology 48, 21–31. https://doi.org/10.1002/tera.1420480106

Noack, F., Pataskar, A., Schneider, M., Buchholz, F., Tiwari, V.K., Calegari, F., In revision. Assessment and Locus Specific Manipulation of DNA (Hydroxy-)Methylation Reveals the Dynamics of Cytosine Modifications During Neurogenic Commitment.

Noctor, S.C., Flint, A.C., Weissman, T.A., Wong, W.S., Clinton, B.K., Kriegstein, A.R., 2002. Dividing precursor cells of the embryonic cortical ventricular zone have morphological and molecular characteristics of radial glia. J. Neurosci. Off. J. Soc. Neurosci. 22, 3161–3173. https://doi.org/20026299

Noctor, S.C., Martínez-Cerdeño, V., Ivic, L., Kriegstein, A.R., 2004. Cortical neurons arise in symmetric and asymmetric division zones and migrate through specific phases. Nat. Neurosci. 7, 136–144. https://doi.org/10.1038/nn1172

REFERENCES

Noctor, S.C., Martínez-Cerdeño, V., Kriegstein, A.R., 2007. Contribution of intermediate progenitor cells to cortical histogenesis. Arch. Neurol. 64, 639–642. https://doi.org/10.1001/archneur.64.5.639

Nonaka-Kinoshita, M., Reillo, I., Artegiani, B., Martínez-Martínez, M.Á., Nelson, M., Borrell, V., Calegari, F., 2013. Regulation of cerebral cortex size and folding by expansion of basal progenitors. EMBO J. 32, 1817–1828. https://doi.org/10.1038/emboj.2013.96

Norris, A.D., Calarco, J.A., 2012. Emerging Roles of Alternative Pre-mRNA Splicing Regulation in Neuronal Development and Function. Front. Neurosci. 6, 122. https://doi.org/10.3389/fnins.2012.00122

Nowakowski, T.J., Fotaki, V., Pollock, A., Sun, T., Pratt, T., Price, D.J., 2013. MicroRNA-92b regulates the development of intermediate cortical progenitors in embryonic mouse brain. Proc. Natl. Acad. Sci. U. S. A. 110, 7056–7061. https://doi.org/10.1073/pnas.1219385110

Nowakowski, T.J., Mysiak, K.S., Pratt, T., Price, D.J., 2011. Functional dicer is necessary for appropriate specification of radial glia during early development of mouse telencephalon. PloS One 6, e23013. https://doi.org/10.1371/journal.pone.0023013

Okamura, K., Hagen, J.W., Duan, H., Tyler, D.M., Lai, E.C., 2007. The mirtron pathway generates microRNA-class regulatory RNAs in Drosophila. Cell 130, 89–100. https://doi.org/10.1016/j.cell.2007.06.028

O'Leary, D.D.M., Chou, S.-J., Sahara, S., 2007. Area patterning of the mammalian cortex. Neuron 56, 252–269. https://doi.org/10.1016/j.neuron.2007.10.010

OpenStax, 2013. Anatomy and Physiology.

Paridaen, J.T.M.L., Huttner, W.B., 2014. Neurogenesis during development of the vertebrate central nervous system. EMBO Rep. 15, 351–364. https://doi.org/10.1002/embr.201438447

Pauli, A., Rinn, J.L., Schier, A.F., 2011. Non-coding RNAs as regulators of embryogenesis. Nat. Rev. Genet. 12, 136–149. https://doi.org/10.1038/nrg2904

Pauli, A., Valen, E., Lin, M.F., Garber, M., Vastenhouw, N.L., Levin, J.Z., Fan, L., Sandelin, A., Rinn, J.L., Regev, A., Schier, A.F., 2012. Systematic identification of long noncoding RNAs expressed during zebrafish embryogenesis. Genome Res. 22, 577–591. https://doi.org/10.1101/gr.133009.111

Petersen, C.P., Bordeleau, M.-E., Pelletier, J., Sharp, P.A., 2006. Short RNAs repress translation after initiation in mammalian cells. Mol. Cell 21, 533–542. https://doi.org/10.1016/j.molcel.2006.01.031

Pinzón, N., Li, B., Martinez, L., Sergeeva, A., Presumey, J., Apparailly, F., Seitz, H., 2016. The number of biologically relevant microRNA targets has been largely overestimated. Genome Res. https://doi.org/10.1101/gr.205146.116

Raj, B., Blencowe, B.J., 2015. Alternative Splicing in the Mammalian Nervous System: Recent Insights into Mechanisms and Functional Roles. Neuron 87, 14–27. https://doi.org/10.1016/j.neuron.2015.05.004

Rajman, M., Schratt, G., 2017. MicroRNAs in neural development: from master regulators to fine-tuners. Dev. Camb. Engl. 144, 2310–2322. https://doi.org/10.1242/dev.144337

Rakic, P., 1974. Neurons in rhesus monkey visual cortex: systematic relation between time of origin and eventual disposition. Science 183, 425–427.

Rakic, P., 1972. Mode of cell migration to the superficial layers of fetal monkey neocortex. J. Comp. Neurol. 145, 61–83. https://doi.org/10.1002/cne.901450105

Rakic, P., 1971. Guidance of neurons migrating to the fetal monkey neocortex. Brain Res. 33, 471–476.

Rapicavoli, N.A., Poth, E.M., Blackshaw, S., 2010. The long noncoding RNA RNCR2 directs mouse retinal cell specification. BMC Dev. Biol. 10, 49. https://doi.org/10.1186/1471-213X-10-49

Reinhart, B.J., Slack, F.J., Basson, M., Pasquinelli, A.E., Bettinger, J.C., Rougvie, A.E., Horvitz, H.R., Ruvkun, G., 2000. The 21-nucleotide let-7 RNA regulates developmental timing in Caenorhabditis elegans. Nature 403, 901–906. https://doi.org/10.1038/35002607

Riffo-Campos, Á.L., Riquelme, I., Brebi-Mieville, P., 2016. Tools for Sequence-Based miRNA Target Prediction: What to Choose? Int. J. Mol. Sci. 17. https://doi.org/10.3390/ijms17121987

Rinn, J.L., Chang, H.Y., 2012. Genome regulation by long noncoding RNAs. Annu. Rev. Biochem. 81, 145–166. https://doi.org/10.1146/annurev-biochem-051410-092902

Roelink, H., Porter, J.A., Chiang, C., Tanabe, Y., Chang, D.T., Beachy, P.A., Jessell, T.M., 1995. Floor plate and motor neuron induction by different concentrations of the amino-terminal cleavage product of sonic hedgehog autoproteolysis. Cell 81, 445–455.

Romero-Barrios, N., Legascue, M.F., Benhamed, M., Ariel, F., Crespi, M., 2018. Splicing regulation by long noncoding RNAs. Nucleic Acids Res. 46, 2169–2184. https://doi.org/10.1093/nar/gky095

Sattari, A., Siddiqui, H., Moshiri, F., Ngankeu, A., Nakamura, T., Kipps, T.J., Croce, C.M., 2016. Upregulation of long noncoding RNA MIAT in

aggressive form of chronic lymphocytic leukemias. Oncotarget 7, 54174–54182. https://doi.org/10.18632/oncotarget.11099

Sauer, F.C., 1935. Mitosis in the neural tube. J. Comp. Neurol. 62, 377–405. https://doi.org/10.1002/cne.900620207

Sauer, M.E., Walker, B.E., 1959. Radioautographic study of interkinetic nuclear migration in the neural tube. Proc. Soc. Exp. Biol. Med. Soc. Exp. Biol. Med. N. Y. N 101, 557–560.

Saurat, N., Andersson, T., Vasistha, N.A., Molnár, Z., Livesey, F.J., 2013. Dicer is required for neural stem cell multipotency and lineage progression during cerebral cortex development. Neural Develop. 8, 14. https://doi.org/10.1186/1749-8104-8-14

Sayed, D., Abdellatif, M., 2011. MicroRNAs in development and disease. Physiol. Rev. 91, 827–887. https://doi.org/10.1152/physrev.00006.2010

Schnall-Levin, M., Zhao, Y., Perrimon, N., Berger, B., 2010. Conserved microRNA targeting in Drosophila is as widespread in coding regions as in 3'UTRs. Proc. Natl. Acad. Sci. U. S. A. 107, 15751–15756. https://doi.org/10.1073/pnas.1006172107

Sempere, L.F., Freemantle, S., Pitha-Rowe, I., Moss, E., Dmitrovsky, E., Ambros, V., 2004. Expression profiling of mammalian microRNAs uncovers a subset of brain-expressed microRNAs with possible roles in murine and human neuronal differentiation. Genome Biol. 5, R13. https://doi.org/10.1186/gb-2004-5-3-r13

Sheik Mohamed, J., Gaughwin, P.M., Lim, B., Robson, P., Lipovich, L., 2010. Conserved long noncoding RNAs transcriptionally regulated by Oct4 and Nanog modulate pluripotency in mouse embryonic stem cells. RNA N. Y. N 16, 324–337. https://doi.org/10.1261/rna.1441510

Shitamukai, A., Konno, D., Matsuzaki, F., 2011. Oblique radial glial divisions in the developing mouse neocortex induce self-renewing progenitors outside the germinal zone that resemble primate outer subventricular zone progenitors. J. Neurosci. Off. J. Soc. Neurosci. 31, 3683–3695. https://doi.org/10.1523/JNEUROSCI.4773-10.2011

Shoemaker, C.J., Green, R., 2012. Translation drives mRNA quality control. Nat. Struct. Mol. Biol. 19, 594–601. https://doi.org/10.1038/nsmb.2301

Slack, F.J., Basson, M., Liu, Z., Ambros, V., Horvitz, H.R., Ruvkun, G., 2000. The lin-41 RBCC gene acts in the C. elegans heterochronic pathway between the let-7 regulatory RNA and the LIN-29 transcription factor. Mol. Cell 5, 659–669.

Small, E.M., O'Rourke, J.R., Moresi, V., Sutherland, L.B., McAnally, J., Gerard, R.D., Richardson, J.A., Olson, E.N., 2010. Regulation of PI3-kinase/Akt signaling by muscle-enriched microRNA-486. Proc. Natl.

Acad. Sci. U. S. A. 107, 4218–4223. https://doi.org/10.1073/pnas.1000300107

Smart, I.H., 1973. Proliferative characteristics of the ependymal layer during the early development of the mouse neocortex: a pilot study based on recording the number, location and plane of cleavage of mitotic figures. J. Anat. 116, 67–91.

Smart, I.H.M., Dehay, C., Giroud, P., Berland, M., Kennedy, H., 2002. Unique morphological features of the proliferative zones and postmitotic compartments of the neural epithelium giving rise to striate and extrastriate cortex in the monkey. Cereb. Cortex N. Y. N 1991 12, 37–53.

Smith, J.L., Schoenwolf, G.C., 1989. Notochordal induction of cell wedging in the chick neural plate and its role in neural tube formation. J. Exp. Zool. 250, 49–62. https://doi.org/10.1002/jez.1402500107

Sone, M., Hayashi, T., Tarui, H., Agata, K., Takeichi, M., Nakagawa, S., 2007. The mRNA-like noncoding RNA Gomafu constitutes a novel nuclear domain in a subset of neurons. J. Cell Sci. 120, 2498–2506. https://doi.org/10.1242/jcs.009357

Stahl, R., Walcher, T., De Juan Romero, C., Pilz, G.A., Cappello, S., Irmler, M., Sanz-Aquela, J.M., Beckers, J., Blum, R., Borrell, V., Götz, M., 2013. Trnp1 regulates expansion and folding of the mammalian cerebral cortex by control of radial glial fate. Cell 153, 535–549. https://doi.org/10.1016/j.cell.2013.03.027

Struhl, K., 2007. Transcriptional noise and the fidelity of initiation by RNA polymerase II. Nat. Struct. Mol. Biol. 14, 103–105. https://doi.org/10.1038/nsmb0207-103

Takahashi, T., Misson, J.P., Caviness, V.S., 1990. Glial process elongation and branching in the developing murine neocortex: a qualitative and quantitative immunohistochemical analysis. J. Comp. Neurol. 302, 15–28. https://doi.org/10.1002/cne.903020103

Tan, S.-L., Ohtsuka, T., González, A., Kageyama, R., 2012. MicroRNA9 regulates neural stem cell differentiation by controlling Hes1 expression dynamics in the developing brain. Genes Cells Devoted Mol. Cell. Mech. 17, 952–961. https://doi.org/10.1111/gtc.12009

Thermann, R., Hentze, M.W., 2007. Drosophila miR2 induces pseudo-polysomes and inhibits translation initiation. Nature 447, 875–878. https://doi.org/10.1038/nature05878

Tsuiji, H., Yoshimoto, R., Hasegawa, Y., Furuno, M., Yoshida, M., Nakagawa, S., 2011. Competition between a noncoding exon and introns: Gomafu contains tandem UACUAAC repeats and associates with splicing factor-

1. Genes Cells Devoted Mol. Cell. Mech. 16, 479–490. https://doi.org/10.1111/j.1365-2443.2011.01502.x

Ulitsky, I., Bartel, D.P., 2013. lincRNAs: genomics, evolution, and mechanisms. Cell 154, 26–46. https://doi.org/10.1016/j.cell.2013.06.020

Vance, K.W., Sansom, S.N., Lee, S., Chalei, V., Kong, L., Cooper, S.E., Oliver, P.L., Ponting, C.P., 2014. The long non-coding RNA Paupar regulates the expression of both local and distal genes. EMBO J. 33, 296–311. https://doi.org/10.1002/embj.201386225

Van Straaten, H.W., Hekking, J.W., Wiertz-Hoessels, E.J., Thors, F., Drukker, J., 1988. Effect of the notochord on the differentiation of a floor plate area in the neural tube of the chick embryo. Anat. Embryol. (Berl.) 177, 317–324.

Visvanathan, J., Lee, S., Lee, B., Lee, J.W., Lee, S.-K., 2007. The microRNA miR-124 antagonizes the anti-neural REST/SCP1 pathway during embryonic CNS development. Genes Dev. 21, 744–749. https://doi.org/10.1101/gad.1519107

Vuong, C.K., Black, D.L., Zheng, S., 2016. The neurogenetics of alternative splicing. Nat. Rev. Neurosci. 17, 265–281. https://doi.org/10.1038/nrn.2016.27

Wang, B., Yanez, A., Novina, C.D., 2008. MicroRNA-repressed mRNAs contain 40S but not 60S components. Proc. Natl. Acad. Sci. U. S. A. 105, 5343–5348. https://doi.org/10.1073/pnas.0801102105

Wang, L.-S., Li, L., Li, L., Chu, S., Shiang, K.-D., Li, M., Sun, H.-Y., Xu, J., Xiao, F.-J., Sun, G., Rossi, J.J., Ho, Y., Bhatia, R., 2015. MicroRNA-486 regulates normal erythropoiesis and enhances growth and modulates drug response in CML progenitors. Blood 125, 1302–1313. https://doi.org/10.1182/blood-2014-06-581926

Wang, Y., Medvid, R., Melton, C., Jaenisch, R., Blelloch, R., 2007. DGCR8 is essential for microRNA biogenesis and silencing of embryonic stem cell self-renewal. Nat. Genet. 39, 380–385. https://doi.org/10.1038/ng1969

Watson, J.D., 1965. Molecular Biology of the Gene, 1st ed. W. A. Benjamin, New York.

Weirather, J.L., de Cesare, M., Wang, Y., Piazza, P., Sebastiano, V., Wang, X.-J., Buck, D., Au, K.F., 2017. Comprehensive comparison of Pacific Biosciences and Oxford Nanopore Technologies and their applications to transcriptome analysis. F1000Research 6, 100. https://doi.org/10.12688/f1000research.10571.2

Wightman, B., Ha, I., Ruvkun, G., 1993. Posttranscriptional regulation of the heterochronic gene lin-14 by lin-4 mediates temporal pattern formation in C. elegans. Cell 75, 855–862.

REFERENCES

Winter, J., Jung, S., Keller, S., Gregory, R.I., Diederichs, S., 2009. Many roads to maturity: microRNA biogenesis pathways and their regulation. Nat. Cell Biol. 11, 228–234. https://doi.org/10.1038/ncb0309-228

Wu, L., Fan, J., Belasco, J.G., 2006. MicroRNAs direct rapid deadenylation of mRNA. Proc. Natl. Acad. Sci. U. S. A. 103, 4034–4039. https://doi.org/10.1073/pnas.0510928103

Wu, T.D., Nacu, S., 2010. Fast and SNP-tolerant detection of complex variants and splicing in short reads. Bioinforma. Oxf. Engl. 26, 873–881. https://doi.org/10.1093/bioinformatics/btq057

Wutz, A., 2011. Gene silencing in X-chromosome inactivation: advances in understanding facultative heterochromatin formation. Nat. Rev. Genet. 12, 542–553. https://doi.org/10.1038/nrg3035

Yan, B., Yao, J., Liu, J.-Y., Li, X.-M., Wang, X.-Q., Li, Y.-J., Tao, Z.-F., Song, Y.-C., Chen, Q., Jiang, Q., 2015. lncRNA-MIAT regulates microvascular dysfunction by functioning as a competing endogenous RNA. Circ. Res. 116, 1143–1156. https://doi.org/10.1161/CIRCRESAHA.116.305510

Yang, J.-S., Maurin, T., Robine, N., Rasmussen, K.D., Jeffrey, K.L., Chandwani, R., Papapetrou, E.P., Sadelain, M., O'Carroll, D., Lai, E.C., 2010. Conserved vertebrate mir-451 provides a platform for Dicer-independent, Ago2-mediated microRNA biogenesis. Proc. Natl. Acad. Sci. U. S. A. 107, 15163–15168. https://doi.org/10.1073/pnas.1006432107

Zhadanov, A.B., Provance, D.W., Speer, C.A., Coffin, J.D., Goss, D., Blixt, J.A., Reichert, C.M., Mercer, J.A., 1999. Absence of the tight junctional protein AF-6 disrupts epithelial cell-cell junctions and cell polarity during mouse development. Curr. Biol. CB 9, 880–888.

Zhao, C., Sun, G., Li, S., Lang, M.-F., Yang, S., Li, W., Shi, Y., 2010. MicroRNA let-7b regulates neural stem cell proliferation and differentiation by targeting nuclear receptor TLX signaling. Proc. Natl. Acad. Sci. U. S. A. 107, 1876–1881. https://doi.org/10.1073/pnas.0908750107

Zhao, C., Sun, G., Li, S., Shi, Y., 2009. A feedback regulatory loop involving microRNA-9 and nuclear receptor TLX in neural stem cell fate determination. Nat. Struct. Mol. Biol. 16, 365–371. https://doi.org/10.1038/nsmb.1576

Zhong, X., Ma, X., Zhang, L., Li, Y., Li, Y., He, R., 2018. MIAT promotes proliferation and hinders apoptosis by modulating miR-181b/STAT3 axis in ox-LDL-induced atherosclerosis cell models. Biomed. Pharmacother. Biomedecine Pharmacother. 97, 1078–1085. https://doi.org/10.1016/j.biopha.2017.11.052

ACKNOLEDGMENTS

Thanks to...

...Federico, for mentoring and guiding me through these projects, for his invaluable skills that I had the chance to appreciate and make partially mine.

...My TAC members, Caghan Kizil and Pavel Tomancak, for providing me with support and feedback throughout my PhD.

...All the labmates for helping me every day and for the amazing memories collected inside and outside the lab. Special thanks to Martina for kick-starting the miRNA project and to Simone for bearing me in the lab and at the gym.

...To all the people involved in the projects: Sharof, the BMS, VTH and all CRTD facilities. Special thanks to the Deep Sequencing Group that took care of all my bioinformatics requests. Mathias, without you I would not have written this thesis.

...To all the people I met along this journey. You guys are amazing, you helped me take my mind off and enjoy these years so much.

...To my family, that has always been by my side and will always be there.

...To "the PhD". I started this journey as a boy and I finish it as a grown up. It has been a fulfilling experience and now it is time to move on.

APPENDIX I

Technische Universität Dresden

Medizinische Fakultät Carl Gustav Carus

Promotionsordnung vom 24. Juli 2011

Erklärungen zur Eröffnung des Promotionsverfahrens

1. Hiermit versichere ich, dass ich die vorliegende Arbeit ohne unzulässige Hilfe Dritter und ohne Benutzung anderer als der angegebenen Hilfsmittel angefertigt habe; die aus fremden Quellen direkt oder indirekt übernommenen Gedanken sind als solche kenntlich gemacht.

2. Bei der Auswahl und Auswertung des Materials sowie bei der Herstellung des Manuskripts habe ich Unterstützungsleistungen von folgenden Personen erhalten: nicht zutreffend.

3. Weitere Personen waren an der geistigen Herstellung der vorliegenden Arbeit nicht beteiligt. Insbesondere habe ich nicht die Hilfe eines kommerziellen Promotionsberaters in Anspruch genommen. Dritte haben von mir weder unmittelbar noch mittelbar geldwerte Leistungen für Arbeiten erhalten, die im Zusammenhang mit dem Inhalt der vorgelegten Dissertation stehen.

4. Die Arbeit wurde bisher weder im Inland noch im Ausland in gleicher oder ähnlicher Form einer anderen Prüfungsbehörde vorgelegt.

5. Die Inhalte dieser Dissertation wurden in folgender Form veröffentlicht: nicht zutreffend

6. Ich bestätige, dass es keine zurückliegenden erfolglosen Promotionsverfahren gab.

7. Ich bestätige, dass ich die Promotionsordnung der Medizinischen Fakultät der Technischen Universität Dresden anerkenne.

8. Ich habe die Zitierrichtlinien für Dissertationen an der Medizinischen Fakultät der Technischen Universität Dresden zur Kenntnis genommen und befolgt.

Dresden, den 29.10.2018   Daniel Cavalli

APPENDIX II

Hiermit bestätige ich die Einhaltung der folgenden aktuellen gesetzlichen Vorgaben im Rahmen meiner Dissertation

- das zustimmende Votum der Ethikkommission bei Klinischen Studien, epidemiologischen Untersuchungen mit Personenbezug oder Sachverhalten, die das Medizinproduktegesetz betreffen

  Aktenzeichen der zuständigen Ethikkommission

  DD 24-9168.11-1/2011-11, HD 35-9185.81/G-61/15

- die Einhaltung der Bestimmungen des Tierschutzgesetzes

  Aktenzeichen der Genehmigungsbehörde zum Vorhaben/zur Mitwirkung

  LDS Achtenzeichen: 11-1-2011-41, TVV 16-2018

- die Einhaltung des Gentechnikgesetzes

  Projektnummer

  LDS Achtenzeichen: 55-8811.71/210

- die Einhaltung von Datenschutzbestimmungen der Medizinischen Fakultät und des Universitätsklinikums Carl Gustav Carus.

Dresden, den 29.10.2018   Daniel Cavalli